

**Studies on the Interaction between the Molecular Chaperone
DnaK and Nucleotide Exchange Factor GrpE from
*Thermus thermophilus***

A Dissertation

Submitted to the Chemistry Department
of the University of Dortmund, Germany
for the Degree of *Doctor Rerum Naturalium*

by
Alena Akhrymuk
born in Brest/BY

Heidelberg 2004

The work described in this thesis was performed in the period October 2000 to December 2003 at Max Planck Institute for Molecular Physiology, Dortmund under the supervision of PD Dr. Joachim Reinstein in the department of Physical Biochemistry headed by Prof. Dr. Roger S. Goody.

1. Referee: Prof. Dr. Roger S. Goody
2. Referee: Prof. Dr. Christof M. Niemeyer

Heidelberg, May 2004

Contents

1. Introduction	1
1.1. Protein folding in the cell.....	1
1.2. Molecular chaperones.....	3
1.2.1. Hsp60.....	4
1.2.2. Hsp100.....	8
1.2.3. Hsp70.....	11
1.2.3.1. Structure and function of DnaK.....	12
1.2.3.2. Structure and function of DnaJ.....	14
1.2.3.3. Structure and function of GrpE.....	16
1.3. Scope of this thesis.....	18
2. Materials and Methods.....	19
2.1. Enzymes and chemicals.....	19
2.2. Microbiological methods.....	20
2.2.1. Site-directed mutagenesis.....	20
2.2.2. Agarose gel electrophoresis of DNA.....	22
2.2.3. Growth of <i>E.coli</i> cells.....	23
2.3. Fluorescent labeling of single cysteine mutants.....	23
2.4. Protein methods.....	24
2.4.1. Protein purification.....	24
2.4.1.1. Proteins without His-Tag.....	24
2.4.1.2. Purification of 6xHis-tagged protein.....	26
2.4.2. SDS-Polyacrylamide gel electrophoresis (SDS-PAGE).....	27
2.4.3. Determination of nucleotides in protein solution.....	28
2.4.4. Protein affinity chromatography.....	29
2.4.4.1. Ni-NTA affinity chromatography.....	29
2.4.4.2. Co-elution experiment with DnaK and ATP-Agarose.....	29
2.5. Spectroscopic methods.....	30
2.5.1. Determination of protein concentration.....	30
2.5.2. Chaperone-assisted reactivation of Lactate dehydrogenase.....	30

2.5.3. Circular dichroism (CD).....	32
2.5.4. Fluorescence spectroscopy.....	33
2.5.4.1. Equilibrium fluorescence measurements.....	33
2.5.4.1.1. Tryptophan fluorescence.....	33
2.5.4.1.2. IANBD fluorescence.....	33
2.5.4.2. Fluorescence correlation spectroscopy (FCS).....	34
2.6. Differential scanning calorimetry (DSC).....	35
3. Results.....	36
3.1. Establishing new substrates for the DnaK-ClpB chaperone system from <i>T.thermophilus</i>	36
3.1.1. Lactate dehydrogenase from <i>S.scrofa</i> muscle (LDH _{Ssc}).....	36
3.1.1.1. Chemical (urea, GdnHCl) and temperature denaturation of LDH _{Ssc}	37
3.1.1.2. Refolding of urea-, GdnHCl- and thermally denatured LDH _{Ssc} mediated by the DnaK _{Tth} -ClpB _{Tth} chaperone system.....	40
3.1.2. Lactate dehydrogenase from <i>B.stearothermophilus</i> (LDH _{Bst}).....	45
3.1.2.1. Refolding of thermally denatured LDH _{Bst} mediated by the DnaK _{Tth} - ClpB _{Tth} chaperone system.....	47
3.2. Investigation of the interactions between DnaK and GrpE.....	48
3.2.1. Protein affinity chromatography.....	48
3.2.1.1. Interaction between GrpE(Δ C) and DnaK _{Chis} in the absence of nucleotides.....	50
3.2.1.2. Interaction of DnaK _{Chis} with protein substrate (LDH _{Ssc}).....	52
3.2.1.3. Effect of Mg ²⁺ /ADP and Mg ²⁺ /ATP on the GrpE(Δ C)-DnaK _{Chis} complex.....	54
3.2.2. Differential scanning calorimetry.....	58
3.2.2.1. Thermal stability of DnaK and GrpE(Δ C).....	58
3.2.2.2. Study of the interactions between DnaK and GrpE(Δ C).....	60
3.2.2.3. Influence of Mg ²⁺ /ADP on the thermal stability of DnaK, GrpE(Δ C) and DnaK-GrpE(Δ C) complex.....	62
3.2.2.4. Temperature dependence of the DnaK-GrpE(Δ C) interactions.....	66
3.2.3. Fluorescence spectroscopy.....	69

3.2.3.1. Site specific DnaK-GrpE interactions.....	69
3.2.4. Fluorescence correlation spectroscopy (FCS).....	77
3.2.4.1. Use of the Alexa488 and IANBD (amide) fluorophores coupled to GrpE(V17C) for the FCS measurements.....	77
3.2.4.2. Conformational stability of the nucleotide binding and peptide binding domains of DnaK.....	79
3.2.4.3. Interactions between GrpE(V17C)Alexa488 and DnaK.....	83
4. Discussion.....	86
4.1. LDH from <i>S.scrofa</i> muscle and LDH from <i>B.stearothermophilus</i> as model substrates for the DnaK _{Tth} -ClpB _{Tth} system.....	86
4.2. Interaction between DnaK and GrpE.....	91
4.3. Structural features of GrpE, implications for functions.....	94
4.4. Regulation of the DnaK _{Tth} chaperone cycle on the level of the DnaK _{Tth} -GrpE _{Tth} interactions.....	98
4.5. Outlook.....	101
5. Summary.....	103
6. List of abbreviations.....	105
7. Literature.....	107

1. Introduction

1.1. Protein Folding in the Cell

Proteins are involved in virtually every biological process in all living cells. They are synthesized on ribosomes from activated amino acids as linear chains in a specific order according to the information encoded within the cellular DNA. To become functionally active, it is necessary for the synthesized polypeptide chains to adopt the unique, native, three-dimensional structures that are characteristic of the individual proteins. It is known that in addition to biological activity, precisely folded protein structures exhibit increased resistance to proteases, decreased aggregation, and, also show increased thermal stability. In the cellular environment, the native state of a particular protein, which corresponds to the minimum free energy conformation is attained within a time scale ranging from milliseconds to few minutes. For decades scientists have been intrigued by a better understanding of how a newly synthesized protein chain is navigated to its unique, active conformation. Structural and biochemical investigations of the protein folding process have scientific importance, providing insights into accurate expression of a particular gene sequence to the 3D structure of a protein.

Within the cell, protein folding takes place in a complex, highly crowded molecular environment. Living cells are densely packed with proteins and other molecules that occupy 20% to 30% of the total volume (Kinjo and Takada, 2002). More than 95 percent of the proteins present within cells have been shown to be in their native conformation. The concentration of total protein inside cells is in the range 200-300 mg/ml (Zimmerman and Trach, 1991). When the total concentration of macromolecules inside cells is so high that a significant proportion of the volume is physically occupied, the effective concentration, or thermodynamic activity, of each macromolecular species inside cells is increased. In addition, in such crowded environments the diffusion coefficient of the molecule is considerably

reduced and the configurational entropy of each macromolecular species becomes smaller (Hartl, 1996). Thus, effects of macromolecular crowding in the cell, as well as high local concentration of nascent polypeptide chains on ribosomes are expected to cause an increase in macromolecular association constants over those on dilute solution by several orders of magnitude, resulting in binding of non-native polypeptides to one another. Aggregates mostly form when folding or unfolding intermediates become trapped in partially misfolded states and then successively associate with one another through hydrophobic interactions to become increasingly larger and more stable (Jaenicke, 1998). This aggregation process irreversibly removes proteins from their productive folding pathways. Especially under heat shock or other stress conditions, the excluded volume effect is aggravated resulting in collapse of newly synthesized polypeptide chains, unfolding and aggregation of proteins (Ellis, 2001a). In the aggregated state, proteins are functionally inactive and enriched in antiparallel β -strands as compared with the native state (Turnell and Finch, 1992). They are observed as amorphous structures, such as inclusion bodies and heat shock granules, or highly ordered fiber structures, such as amyloid plaques and prions (Hartl and Hayer-Hartl, 2002; Horwich and Weissman, 1997).

To enable folding under crowded conditions a whole range of helper proteins exist in the cell. These folding catalysts include protein disulfide isomerase (PDI, EC 5.3.4.1) accelerating the formation and rearrangement of disulfide bonds; peptidyl prolyl *cis-trans* isomerases (PPIs, EC 5.2.1.8) increasing the rates of isomerization of peptidyl proline bonds. These enzymes are abundant in all organisms, suggesting that disulfide shuffling and proline isomerization are catalysed both in eu- and prokaryotes (Webb et al., 2001). About 10 to 20% of newly synthesized polypeptides are found associated with naturally occurring stabilizing molecules so called molecular chaperones (Ewalt et al., 1997; Teter et al., 1999). Molecular chaperones are described as a class of proteins whose physiological role is to assist in the correct transport, folding and assembly of other polypeptide chains whilst not themselves being part of the final structure (Burston et al., 1995). They are found in all organisms from bacteria to humans. Chaperones are located in every cellular compartment and act in preventing off-pathway reactions during folding that leads to aggregation and may be part of a general protein-folding mechanism. Over the last decade it has been revealed that the protection afforded by molecular chaperones is due to their ability to recognize and bind protein regions composed of clusters of hydrophobic residues flanked by basic residues that are commonly found on a wide range of non-native polypeptides but not accessible in folded proteins. This

binding is non-covalent and reversible, and serves to reduce the chance that such exposed regions will aggregate with one another or trigger premature proteolytic degradation (Hartl, 1996). Thus, molecular chaperones are a key part of the cellular defense mechanism to protect the cell from this inner danger. Due to chaperones the newly synthesized polypeptides can be maintained in a folding-competent state.

1.2. Molecular Chaperones

In the last decade a complicated and sophisticated machinery of proteins has emerged that assists protein folding and allows the functional state of proteins to be maintained under conditions, in which they would normally unfold and aggregate. Mutant forms of some proteins and, under conditions not yet understood, even some wild type proteins, can form ordered aggregates called amyloid fibrils, protease-resistant structures characterized by a high content of β -sheets. Because of the role of chaperones in refolding of stress-damaged proteins as well as de novo protein folding, chaperone function is closely linked with a number of disease states. To date 15 or 20 proteins have been found to form amyloids, which are associated with Creutzfeld-Jakob, Alzheimer's, Huntington's, and Parkinson's diseases as well as systemic amyloidoses (Bonifacino et al., 1990;Stevens et al., 1994). One of the important biological properties of molecular chaperones is their ability to recognize and dissociate protein aggregates once they form. It has been shown that overexpression of chaperones reduces aggregate formation and suppresses apoptosis in several polyglutamine diseases models including spinal and bulbar muscular atrophy (Kobayashi and Sobue, 2001). These facts suggest that increasing expression level or enhancing the function of chaperones will provide a possible medical application of molecular chaperones.

There are several major families of chaperones that interact with large numbers of non-native proteins and assist in protein folding. Some members of these families are also known to be stress proteins (heat shock proteins, Hsp), they increase in amount when the organism experiences abnormal conditions, such as elevated temperatures. The major criteria of proteins acting as molecular chaperones are: they assist the noncovalent assembly of protein-containing structures *in vivo*, but are not permanent components of these structures when the

latter are performing their normal biological functions (Ellis, 1997). There are three general families of chaperones, including the Hsp60 or GroEL family (chaperonins), the Hsp70 or DnaK family, and the Clp or Hsp100 family. These chaperones are highly conserved and are present in all cells.

1.2.1. Hsp60

Hsp60 molecular chaperones, also known as chaperonins, have an essential function in promoting the ATP-dependent folding of proteins, both under normal growth conditions and under stress. Chaperonins can be divided into two groups: members of the GroEL (or Hsp60) family are found in eubacteria, mitochondria and chloroplasts, and the cochaperonins of the TriC family are found in archaeobacteria and the eukaryotic cytosol (Cowan and Lewis, 2001;Frydman et al., 1992;Hartl, 1996).

All chaperonins, irrespective of their cellular or subcellular origin, were observed as double toroids in the electron microscope (Braig et al., 1993;Chen et al., 1994;Langer et al., 1992a). In addition to, the high-resolution X-ray structure of GroEL was determined (Braig et al., 1994;Chen and Sigler, 1999;Xu et al., 1997). The crystal structure of *E.coli* GroEL is shown in Fig. 1.1.

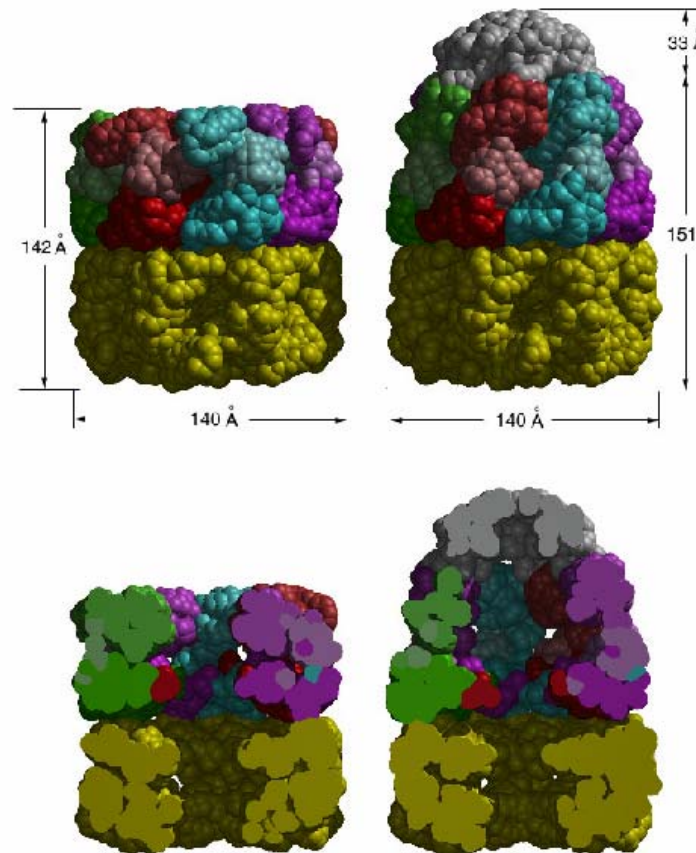


Figure 1.1: Overall architecture and dimensions of GroEL and GroEL-GroES-(ADP)₇ (Sigler et al., 1998). Van der Waals space-filling models (6Å spheres around Xa) of GroEL (*left*) and GroEL-GroES-(ADP)₇ (*right*). *Upper panels* are outside views, showing outer dimensions; *lower panels* show the insides of the assemblies and were generated by slicing off the front half with a vertical plane that contains the cylindrical axis. Various colors are used to distinguish the subunits of GroEL in the upper ring. The domains are indicated by shading: equatorial, *dark hue*; apical, *medium hue*; intermediate, *light hue*. The lower GroEL ring is *uniformly yellow*. GroES is *uniformly gray*.

The chaperonin GroEL functions as an oligomer of 14 identical subunits of 58 kDa each that are organized into two heptameric rings stacked back-to-back with 7-fold rotational symmetry and a central cavity (Chen and Sigler, 1999; Langer et al., 1992b). The GroEL cavity is thought to provide a protected folding environment for the polypeptide chain. The dimension of each cavity is measured in the crystal structure to be $\sim 80 \times 85$ Å, just large enough to accommodate proteins up to ~ 60 kDa (Hartl, 1996; Sigler et al., 1998; Weber et al., 1998). GroEL folds into three distinctive domains in each subunit: a well-ordered, highly α -helical, “equatorial” domain; an “apical” domain and an “intermediate” domain (Braig et al., 1994).

GroEL-mediated folding also requires the cochaperonin GroES controlling the entrance of proteins to the GroEL chamber (Xu et al., 1997). The crystal structure of isolated GroES (a heptamer of 10 kDa subunits) at 2.8 Å shows a sevenfold rotationally symmetric, dome-shaped architecture, about 75 Å in diameter and 30 Å high (Hunt et al., 1996). GroES binds to the apical domains of one ring of GroEL in the presence of Mg^{2+} -ATP and Mg^{2+} -ADP (Chen et al., 1994; Saibil et al., 1991) or under certain non-physiological conditions to both rings of GroEL (Burston et al., 1995).

During cycles of ATP binding and hydrolysis, changes in the conformation of the GroEL chamber result in binding and release of folded or partially folded substrate (Sigler et al., 1998). Distantly related homologs in the eukaryotic cytosol also form barrel-like structures and may exhibit similar function.

The chaperonin reaction consists of the cyclic binding and release of target polypeptides. It has been shown that during cycles of ATP binding and hydrolysis, conformational changes in the GroEL chamber result in binding and release of protein ligands (Langer et al., 1992b; Sigler et al., 1998; Yifrach and Horovitz, 1994).

GroEL is functionally asymmetrical. Each ring is an allosteric unit that is often found to bind and hydrolyze ATP with positive intra-ring cooperatively (Horovitz et al., 2001). The binding and hydrolysis of ATP in one subunit enhances these events in neighboring subunits at the level of the individual GroEL rings. The two rings are coupled by negative allostery and do not occur at the same nucleotide-bound state (Hartl and Hayer-Hartl, 2002; Horovitz et al., 2001; Yifrach and Horovitz, 1994). The two levels of allostery in GroEL correspond, therefore, to its hierarchical double-ring structure.

The basic reaction scheme is shown in Fig. 1.2 and includes the following steps:

- 1) The acceptor state for the unfolded protein substrate is the asymmetrical GroEL:ADP₁₄:GroES complex. Substrate protein, with hydrophobic amino-acid residues exposed, binds to the central cavity of the cylinder, engaging the hydrophobic surfaces exposed by the apical GroEL domains (Houry et al., 1999). The substrate binds to the GroEL ring that is not occupied by GroEL (Chen et al., 1994; Engel et al., 1995; Martin et al., 1993).

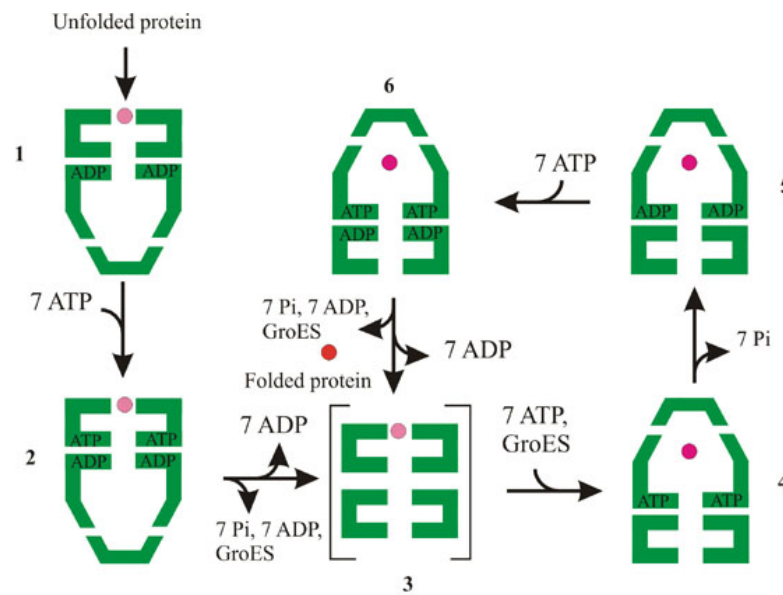


Figure 1.2: Model of the GroEL-GroES reaction cycle in folding. Nucleotide free GroEL in step (3) is thought to occur only transiently and is shown for simplicity. In step (4), GroES may either associate with the polypeptide-containing ring of GroEL or with the free ring (not shown). Rosa and red spheres represent unfolded and folded substrate protein, respectively, and the magenta sphere indicates the presence of a mixture of folded and unfolded substrate in the population of GroEL molecules. Unfolded protein can be retained in steps (6) to (3).

2-3) This step is closely followed by the binding of seven ATP molecules. ATP binding and hydrolysis in this ring as well as polypeptide binding itself result in dissociation of GroES and 14 ADP molecules.

4) Subsequently, 7 ATP molecules and GroES bind to the GroEL:protein substrate complex. Upon binding to GroES, the apical domains undergo a massive rotation and upward movement, resulting in an enlargement of the cavity and a shift in its surface properties from hydrophobic to hydrophilic (Richardson et al., 1998; Xu et al., 1997). The enclosed non-native proteins are free to fold in the resulting GroEL-GroES cage (also termed “Anfinsen cage”) (Ellis, 2001b; Weissman et al., 1996).

4-5) ATP binding and ATP hydrolysis in the GroES-bound tightens the interaction with GroES.

6) ATP binding and hydrolysis in the opposite ring then triggers the opening of the GroEL-GroES cage (Mayhew et al., 1996). At this point, the folded polypeptide leaves, whereas folding intermediates that still expose extensive hydrophobic surfaces are rapidly recaptured and folding cycles are repeated until the protein reaches to its

native state. Oligomeric assembly occurs in solution after subunit folding inside the cage (Hartl and Hayer-Hartl, 2002).

In *E.coli* 10-15% of newly synthesized polypeptides, comprising about 300 protein species, interact posttranslationally with GroEL (Bukau et al., 2000; Houry et al., 1999).

1.2.2. Hsp100

Hsp100/Clp proteins comprise an evolutionary conserved family of heat shock proteins, possessing ATP-dependent chaperone activity. They are thought to mediate protein unfolding as well as the disassembly of protein aggregates and oligomers. While some Hsp100 family acts only as molecular chaperone proteins and confer cellular thermotolerance, others can function both as chaperone proteins and subunits of ATP-dependent proteases.

Clp family is very universal. Four types of Clp proteins were found in *E.coli*: ClpA (Gottesman et al., 1990), ClpB (Squires et al., 1991), ClpX (Gottesman et al., 1993) and HslU (Chuang et al., 1993; Rohrwild et al., 1997). Other examples of this highly conserved family have been identified in the true bacteria, archaeobacteria, plants, yeast and insects (Squires et al., 1991). The first member with discernible biochemical function was the ClpA protein of *Escherichia coli*. This protein was discovered as a component of an ATP-dependent protease and was named for its capacity to promote the proteolysis of casein (caseinolytic protease, Clp) *in vitro* when complexed with the unrelated ClpP (Ti) protease (Hwang et al., 1988; Teter et al., 1999).

Clp proteins are divided into two major classes. Members of the first class contain two nucleotide-binding domains (NBDs) flanked by amino-terminal, middle and carboxy-terminal regions (Fig. 1.3A) (Guo et al., 2002; Schirmer et al., 1996).

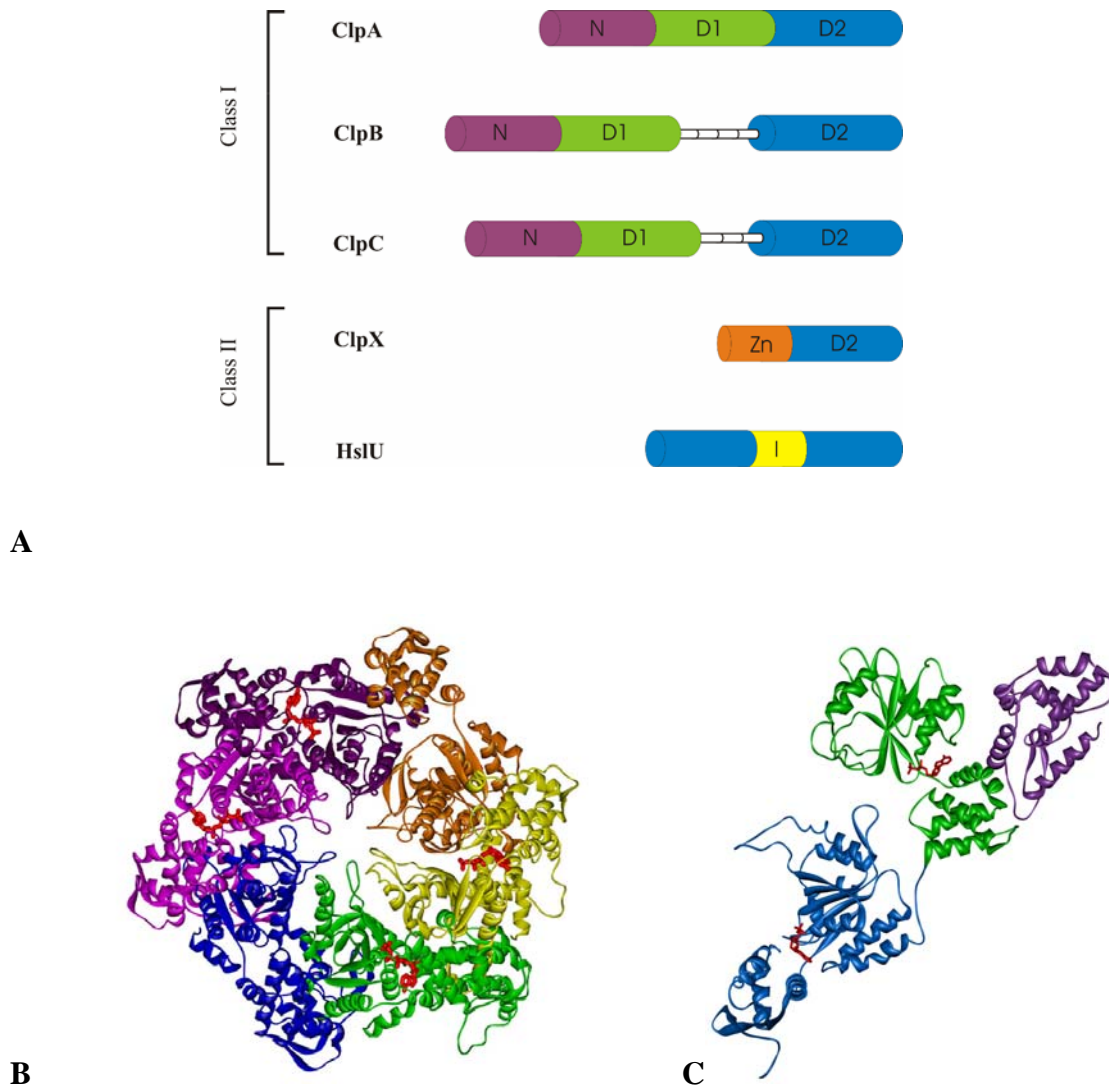


Figure 1.3: Structure of the Hsp100 proteins.

A. Structural features of the Hsp100 family. Members of the first class contain two nucleotide-binding domains (NBD: D1 (*green*), D2 (*blue*)) flanked by amino-terminal (N) (*violet*) and/or spacer (*white*) region. Members of the second class are shorter in length, containing only a single NBD. Zn^{2+} binding region in ClpX (*orange*) and intermediate domain (I) (*yellow*) in HslU are thought to play a significant role in substrate recognition.

B. The ring like hexameric structure of HslU from *E.coli* (Bochtler et al., 2000). Six subunits are shown in different color; four of those are complexed with nucleotide (ATP, *red*).

C. The structure of the ClpA monomer from *E.coli* (Guo et al., 2002). In ribbon representation, the three structural domains of ClpA monomers are colored; the N-domain, *violet*; the D1 domain, *green*, the D2 domain, *blue*. Two ADP molecules are shown in *red*.

The two NBDs are highly conserved in all members of this class and contain a Walker A motif (e.g. GX₂GXGKT, where X is any amino acid). Mutations within the first but not the second Walker A motif of ClpA or ClpB affects their oligomerization. In contrast, mutations within the second ATP-binding site influence hexamerisation of Hsp100 (Gallie et al., 2002). Members of the second class are shorter in length, containing only a single NBD (which more closely resembles the second NBD class of 1 Hsp100s) and the carboxy-terminal region.

As predicted from their sequences, all Hsp100 proteins that have been tested are ATPases. Each has a moderate basal rate of ATP hydrolysis, which is stimulated by specific proteins or peptides (Maurizi, 1992;Woo et al., 1992). In addition to, ClpA, ClpB, ClpX and ClpY belong to the AAA⁺ protein superfamily of ATPases associated with a variety of cellular activities, an ubiquitous family of ATP-dependent molecular machines with one or two 230-250 residue AAA⁺ modules containing well conserved sequence and structural motifs (Neuwald et al., 1999;Patel and Latterich, 1998). Despite their different cellular functions AAA⁺ proteins employ a general mechanism. They play essential roles in cellular housekeeping, cell division and differentiation and have been identified in prokaryotes and eukaryotes.

Another common characteristic, at least of class 1 members, is assembly into higher-order oligomers. Clp chaperones are structurally similar to GroEL in having an interior chamber formed by one or two stacked rings of six or seven protomers (Wickner and Maurizi, 1999). Electron microscopy reveals that Hsp100 proteins assemble into a ring-like structure (Schirmer et al., 1996) (Fig. 1.3B). In the absence of nucleotides, Hsp100 proteins migrate variously as monomers (Fig. 1.3C), dimers and trimers according to a variety of analytical sizing techniques. However, in the presence of either ATP or ADP, these proteins assemble into hexamers.

E.coli representatives of the Hsp100 family, notably ClpA and ClpX confer ATP-dependent turnover of their substrates through a physical association with an unrelated oligomeric protease ClpP. The role of these Clp proteins is the unfolding of substrates and the delivery of unfolded polypeptides to the protease subunit (Glover and Lindquist, 1998). In contrast ClpB from *E.coli* and *T.thermophilus* and the *Saccharomyces cerevisiae* homologue Hsp104 have no detectable role in protein degradation. They have the ability to solubilize denatured proteins from previously formed high-molecular weight aggregates by specific interactions with additional chaperones – Hsp70. Together, these proteins comprise refolding machine with novel activities (Glover and Lindquist, 1998;Mogk et al., 1999;Motohashi et al., 1999).

1.2.3. Hsp70

The ubiquitous Hsp70 molecular chaperones have a molecular mass of around 70 kDa, and assist a broad spectrum of folding processes. Representatives of this group have been found in eubacteria (DnaK from *E.coli*), some archaea, as well as within eukaryotic organelles, such as mitochondria, chloroplast and endoplasmic reticulum (Flaherty et al., 1990; Hartl and Hayer-Hartl, 2002; Palleros et al., 1992).

The DnaK system plays essential roles in many cellular functions, including stabilization of polypeptide chains in an unfolded state for translocation across organelle membranes (Wild et al., 1992); prevention of protein aggregation under stress conditions and assistance of refolding of denatured proteins (Schröder et al., 1993; Szabo et al., 1994); disassembly of protein oligomers (Zylicz et al., 1989); degradation of unstable proteins (Sherman and Goldberg, 1996).

Functionally, the best-characterized DnaK system is the *E.coli* system. For folding of newly synthesized proteins, DnaK is not strictly required (Hesterkamp and Bukau, 1998); DnaK, however, is essential for *E.coli* to survive environmental stress, including exposure to elevated temperature. The *E.coli* DnaK's reaction cycle is fueled by the binding and hydrolysis of ATP and is regulated by the two cochaperones, DnaJ and GrpE (Fig. 1.4). DnaK shuttles between an ATP-bound form, which has low affinity for peptide substrates, and an ADP-bound form, which has relatively high affinity for protein substrates. DnaJ promotes substrate binding to the ATP-bound state and also stimulates ATP hydrolysis. The nucleotide exchange factor GrpE promotes ADP dissociation. The DnaK/DnaJ/GrpE reaction cycle, defined by repeated substrate binding and release, coupled to DnaK-mediated ATP hydrolysis, probably produces a conformational change in the substrate protein that increases the probability of proper folding (Chesnokova et al., 2003).

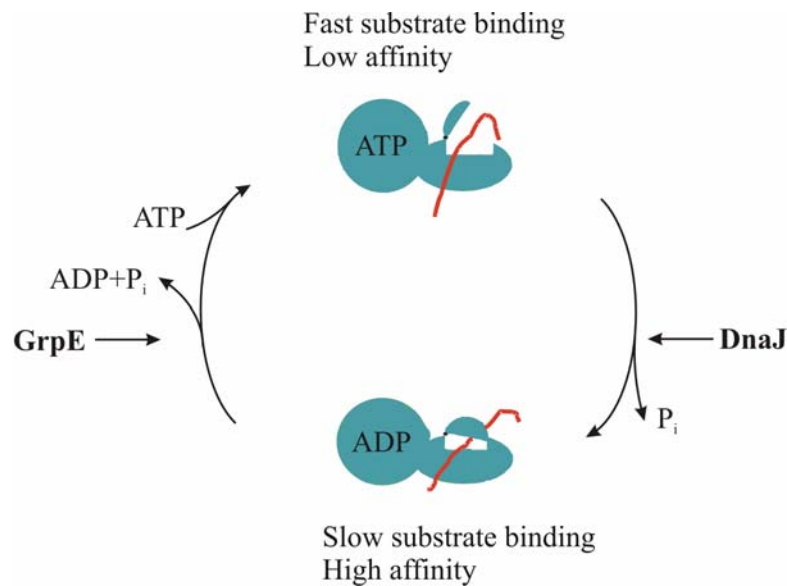


Figure 1.4: Model for the regulated chaperone cycle of DnaK_{Eco}. Under GrpE and DnaJ control, DnaK (shown in blue) alternates between the low-affinity ATP-liganded state and the high-affinity ADP-liganded state. The affinity of ATP-bound form for polypeptide and protein substrates is low, and both binding and release of substrates are fast. DnaJ stimulates ATP hydrolysis resulting to the substrate to be locked to the DnaK substrate binding domain and the rates of binding and release of substrates are too slow to be of physiological significance. GrpE mediates dissociation of DnaK-bound nucleotides.

1.2.3.1. Structure and Function of DnaK

The cellular concentration of DnaK (~50 μM) exceeds that of ribosomes (~30 μM) (Hartl, 1996), assuming an even cytosolic distribution. Substrate binding and ATP hydrolysis occur in two discrete functional domains of DnaK. The overall structure of DnaK consists of N-terminal ATPase domain and a C-terminal peptide binding domain. The NH₂-terminal, highly conserved 45-kD ATPase domain, binds ADP and ATP very tightly (in the presence of Mg²⁺ and K⁺) and hydrolyses ATP, whereas the 25-kD carboxy-terminal domain is required for polypeptide binding (Fig. 1.5).

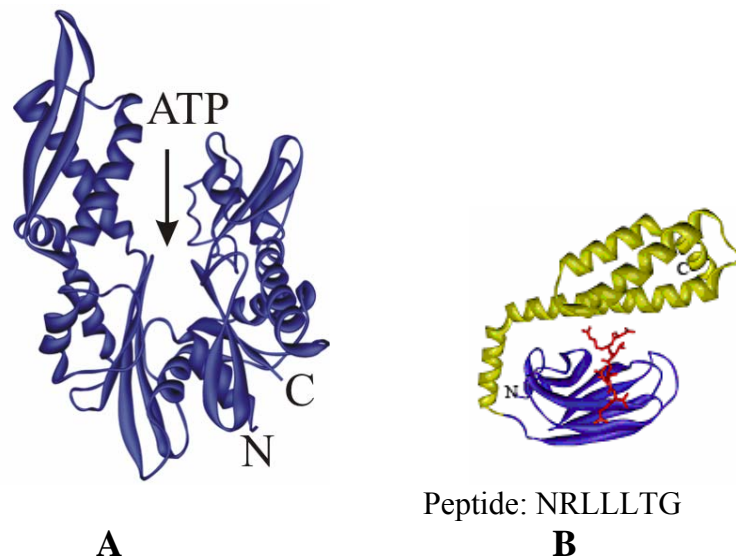


Figure 1.5: Structure of DnaK from *E. coli*. (A) Structure of the ATPase domain of DnaK (Harrison et al., 1997) (PDB-ID: 1DKG). ATP indicates the position of the nucleotide binding site. (B) Structure of the peptide binding domain of DnaK in complex with a peptide substrate (Zhu et al., 1996) (PDB-ID: 1DKX). The N-terminal β -sandwich subdomain is shown in *blue*, the α -helical latch, in *yellow* and the exchanged peptide substrate, in *red*.

Cooperation of both domains is needed for protein folding. Part of the overall tertiary structure of the ATP-ase domain from different organisms (Hsc from Bovine, DnaK from *E. coli* and human's Hsp70) (Flaherty et al., 1990; Harrison et al., 1997; Sriram et al., 1997) shares high similarity with the structure of yeast metabolic enzyme hexokinase and structure of a well-known muscle and cell skeleton protein, actin (Flaherty et al., 1990; Holmes et al., 1993). It consists of two subdomains that are separated by a deep central cleft, at the bottom of which nucleotide and Mg^{2+} are bound. On the basis of analogy to the 'induced-fit' movement in hexokinase, it has been predicted that Hsc70 ATPase domain also undergo a structural transition between two states, namely a fully closed structure with ADP bound and an open form without nucleotide (Holmes et al., 1993). In addition, comparison of the crystal structure of GrpE_{Eco}-bound, nucleotide-free ATPase domain DnaK_{Eco} with that of nucleotide-bound bovine brain Hsc70 showed that the co-factor GrpE_{Eco} stimulates mechanical opening of the DnaK_{Eco} structure (Harrison et al., 1997).

Zhu and co-workers solved the structure of the peptide-binding domain of DnaK in complex with substrate (Zhu et al., 1996). This domain is divided into a β -sandwich subdomain with a peptide-binding cleft and an α -helical latchlike segment (Fig. 1.5B) which closes the substrate binding cavity but does not contact directly the bound peptide.

DnaK recognizes substrate binding motif of extended peptides strands composed of up to seven residues long with consecutive hydrophobic residues in the central region (leucine and isoleucine residues being preferred by DnaK) and positively charged residues outside the substrate binding cavity (Rüdiger et al., 1997). The binding of polypeptide to the substrate-binding domain of DnaK is regulated by the nucleotide state of the ATPase domain (Laufen et al., 1997;McCarty et al., 1995).

1.2.3.2. Structure and Function of DnaJ

Central to the Hsp70 chaperones activities is the regulation of Hsp70 by DnaJ co-chaperone. DnaJ homologs (also referred to as Hsp40) have been identified in a large variety of prokaryotic and eukaryotic cells and viruses with an exception of specific archaebacteria lacking entire DnaK chaperone system (Laufen et al., 1997).

DnaJ proteins are multidomain proteins that share and are identified by an evolutionary highly conserved J-domain of approximately 78 amino acids (Buchberger et al., 1997;Laufen et al., 1997). In the full length *E.coli* DnaJ protein there are four domains formed by the 367-amino acid sequence (Pellecchia et al., 1996). The NMR structure of a fragment of DnaJ (residues 2-108) comprising the J domain and the Gly/Phe rich region has been solved (Pellecchia et al., 1996). The amino-terminal J domain consists of four helices (Fig. 1.6), of which amphipathic antiparallel helices 2 and 3 form a coiled coil connected by a flexible turn and helices 1 and 4 are oriented perpendicular to it. The loop connecting helices 2 and 3 is highly mobile which may be important for the association of DnaJ with DnaK.

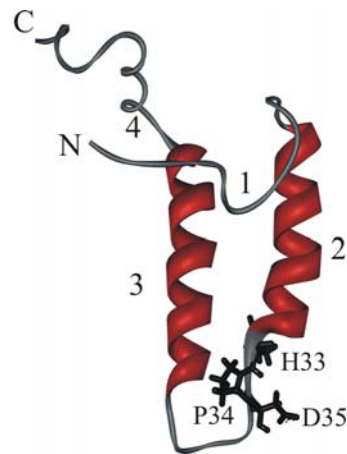


Figure 1.6: NMR-structure of the J domain of DnaJ (Pellecchia et al., 1996) (PDB-ID: 1XBL). Helices are numbered according to (Pellecchia et al., 1996). The conserved HPD motif is shown in black.

This loop contains the entirely conserved sequence motif His33-Pro34-Asp35, referred to as HPD motif, which plays a key role in the interaction DnaJ with DnaK leading to stimulation of ATPase activity (Buchberger et al., 1997; Greene et al., 1998). The adjoining Gly/Phe-rich region, comprising residues 77 to 108, contains a large number of glycyl and phenylalanyl residues. It was found that the Gly/Phe-rich region binds to DnaK mimicking a peptide substrate (Karzai and McMacken, 1996; Wall et al., 1994). Furthermore, Laufen and co-workers (1999) have also shown that DnaJ and protein substrates act synergistically to provide the signals required for stimulation of ATP hydrolysis by DnaK. Carboxy-terminal to these modules, there are a “zinc-binding” and a “low homology” region, which are also present in many other DnaJ-like proteins (Pellecchia et al., 1996).

The ATPase activity of the DnaK protein is very low (15 nmol of ATP hydrolyzed per min per mg of protein at 30°C, pH 8.8) (Liberek et al., 1991). The turnover number for ATP hydrolysis by DnaK is in the range 0.02-1/min, depending on the preparation of DnaK used (Jordan and McMacken, 1995; Liberek et al., 1991). The *E.coli* DnaJ stimulates the intrinsically low ATPase rate of DnaK by a factor of 500-15000 (Laufen et al., 1999; Russell et al., 1999). However, with the *Thermus thermophilus* DnaK system, no stimulation of the DnaK by DnaJ was observed (Klostermeier et al., 1999). The *E.coli* DnaJ (Molecular weight of 41 kDa) binds substrates with a similar consequence as DnaK and was proposed to be a chaperone on its own right.

1.2.3.3. Structure and Function of GrpE

GrpE acts as nucleotide exchange factor for DnaK. It enhances the rate of nucleotide exchange of DnaK up to 5,000-fold (Packschies et al., 1997). GrpE homologs exist in various bacteria, eukaryotic mitochondria and chloroplast. However, no nucleotide exchange factor for Hsp70 has been definitively identified in the eukaryotic cytosol and endoplasmic reticulum (Buchberger et al., 1997), although such a function has been proposed for the Bcl2-associated athanogene 1 (Bag-1) protein (Brehmer et al., 2001;Sondermann et al., 2001).

To assist DnaK function GrpE and DnaK should physically interact with each other. Harrison with co-workers (1997) determined the crystal structure of the GrpE_{Eco}-DnaK_{Eco} ATPase domain complex at 2.8 Å resolution and found that a dimer of GrpE interacts in an asymmetric fashion with the DnaK_{Eco} ATPase domain. The structure of the GrpE_{Eco} dimer (Mr = 22 kDa) may be divided into three regions: paired N-terminal α -helices (residues 40-88), four-helix bundles (residues 89-13), and the C-terminal β -domains (139-197) (Fig. 1.7).

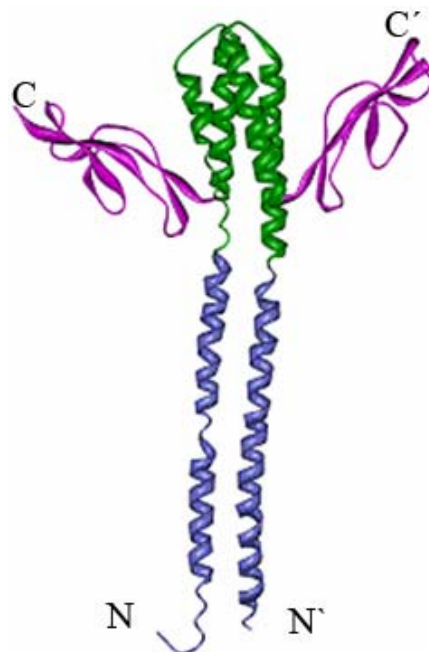


Figure 1.7: Crystal structure of GrpE from *E.coli* (Harrison et al., 1997) (PDB-ID: 1DKG). The general GrpE domains are shown in different color: N-terminal α -helices, *blue*; four-helix bundles, *green*; C-terminal β -domains, *violet*.

Residues 1-33 are thought to exist in a disordered, flexible state. The two long helices in the dimer do not form a canonical coiled-coil but instead lie nearly in the same plane.

Association of DnaK_{Eco} with GrpE_{Eco} is stable in the absence of added nucleotides and is disrupted by Mg²⁺/ATP (Buchberger et al., 1994b). There are some evidences that GrpE mediates nucleotide exchange by inducing an opening of the nucleotide binding cleft of DnaK. Packschies *et al.* (1997) kinetically showed that the initial weak binding of GrpE to DnaK-ADP complex is followed by an isomerization of the ternary complex which leads to weakening of nucleotide binding and finally to its rapid dissociation. They also demonstrated that the displacement mechanism of ADP by GrpE is associative. This means that the binding sites of GrpE and ADP are either distinct or only partially overlapping. Thus, these observations are in line with what has been reported about the crystal structure of a complex of the DnaK_{Eco} ATPase domain with GrpE_{Eco} (Harrison et al., 1997). Harrison and co-workers (1997) demonstrated that the nucleotide-binding pocket is disrupted in the GrpE-DnaK complex by the mechanical opening of the DnaK structure. The maximum stimulation of nucleotide exchange (k_{off}) by the *T.thermophilus* GrpE is 80,000-fold in comparison to a 5,000-fold stimulation by *E.coli* GrpE (Groemping et al., 2001; Packschies et al., 1997).

Several studies have shown that GrpE is probably more than just a nucleotide exchange factor; it is also involved in substrate release. Using a radioactively labelled permanently unfolded form of lactalbumin (RCMLA, reduced carboxymethylated lactalbumin) Harrison and co-workers (1997) showed that the N-terminal residues of GrpE_{Eco} (amino acids 1-33) are required for dissociation of the substrate from ADP-DnaK_{Eco}-RCMLA complex. Mally and Witt (2001) have kinetically shown that GrpE_{Eco} binding to an ADP-DnaK-peptide (or DnaK-peptide) complex increases peptide k_{off} and k_{on} values by ~200-fold and ~60-fold, respectively, providing evidence that GrpE_{Eco} induces a conformational change in the C-terminal polypeptide binding domain of DnaK_{Eco}. In addition it has been demonstrated directly that the GrpE_{Eco} mutant containing the only tail region is able to release bound substrate from DnaK_{Eco} (Mehl et al., 2001).

1.3. Scope of this Thesis

The participation of molecular chaperones in solubilization of unfolded proteins probably accounts for the role of chaperones in the acquisition of thermotolerance. The studies presented here were an attempt to ascertain the role of the DnaK system from the thermophilic eubacterium *T.thermophilus* in repair of thermally and chemically denatured proteins *in vitro*. In order to study the mechanism of the DnaK system (DnaK, DnaJ, GrpE) together with ClpB in assisting protein folding it was necessary to find suitable model substrates for this chaperone machinery.

A key question of the functional cycle of the DnaK_{Th} system is the mechanism by which the co-chaperone GrpE controlled ATPase cycle is coupled to the productive association of DnaK with substrates. The goal of this work was to experimentally explore the influence of nucleotides and substrates on the interaction of the molecular chaperone DnaK and its co-chaperone GrpE. In regard with the DnaK-GrpE interactions we studied whether a covalent link between the ATPase domain (amino acids 1-381) and the peptide binding domain (amino acids 382-615) of DnaK is necessary for interaction with GrpE.

To further explore these DnaK-GrpE interactions on the level of individual GrpE domains, the interactions between DnaK and the GrpE α -helical domain were monitored in the absence and presence of ADP, ATP and a substrate protein.

In the last part of this work we tried to map specific locations where the end of the long NH₂-terminal α -helix of GrpE interacts with the DnaK's substrate binding domain. In this type of experiment two different GrpE cysteine mutants were engineered, GrpE(N5C) and GrpE(V17C). Covalent coupling of environmentally sensitive fluorophores to these cysteine mutants allowed for spectroscopic monitoring of conformational changes.

2. Materials and Methods

2.1. Enzymes and Chemicals

Enzymes and chemicals used in this work are listed in Table 2.1.

Table 2.1: Enzymes and chemicals

Product	Producer
Acrylamid – solution (30 %), (NH ₄) ₂ SO ₄	AppliChem (Darmstadt)
Ethanol, Acetic acid, HCl, Isopropanol, Potassium acetate, Sodium acetate, K ₂ HPO ₄ , KH ₂ PO ₄ , KCl, MgCl ₂ , NaCl, NaOH, Urea	J.T. Baker (Deventer, Holland)
TCA	Fluka (Neu -Ulm)
DTT, EDTA, Glycerol, HEPES, IPTG, Kanamycin	Gerbu (Gaiberg)
GdnHCl	Sigma-Aldrich (Steinheim, Germany)
Na ₂ HPO ₄ , NaH ₂ PO ₄	Merck, Darmstadt
DNA standard (kb- Marker)	New England Biolabs (Frankfurt)
NADH, Protease inhibitor (tablets), LDH (pig muscle), NADH	Roche Diagnostics (Mannheim)
Tris, Agarose, Ethidium bromide	Roth (Karlsruhe)
APS, Bromphenol blue, Coomassie Blue-R250/G250, SDS, TEMED	Serva (Heidelberg)
ADP, ATP, BSA, PMSF, TFA, Pyruvate, LDH (<i>Bacillus stearothermophilus</i>), β-Mercaptoethanol	Sigma-Aldrich (Taufkirchen)
<i>Pfu</i> DNA-polymerase	Stratagene (Amsterdam, Holland)
Agar, Yeast extract, Select peptone 140	GibcoBRL (Karlsruhe)

2.2. Microbiological Methods

2.2.1. Site-Directed Mutagenesis

The QuikChange site-directed mutagenesis kit was used to make point mutations in proteins under investigation, GrpE(N5C), GrpE(V17C). The QuikChange site-directed mutagenesis method was performed using *Pfu* DNA polymerase, which replicates both plasmid strands with high fidelity and without displacing the mutant oligonucleotide primers, and a thermal cycler. PCR was performed with aliquots of 50 μ l of the reaction mixture including pet27b vector as a DNA template as listed in Table 2.2. Primers used for mutagenesis are listed in Table 2.3. PCR cycling parameters for the QuikChange site-directed mutagenesis method are shown in Table 2.4.

Following temperature cycling, 1 μ l *Dpn* I restriction enzyme (10 U/ μ l) was directly added to the amplification reaction, gently and thoroughly mixed and incubated at 37° C for 1 hour to digest the parental (nonmutated) supercoiled dsDNA.

The nicked vector DNA incorporating the desired mutations was then transformed into *E.coli* (XL1-Blue) competent cells. 50 μ l 10 % glycerol stock solution of XL1-Blue competent cells were gently thawed on ice, mixed with 5 μ l of the nicked vector and transformed into Micro-Electroporation Chamber. The conditions for electroporation were as follows: the resistance on the Voltage Booster was 800 ohms, the Pulse Control was 25 μ F, the total voltage was 1.5 kV with time constant 10 ms. The transformation reaction was incubated in 1 ml 2YT medium at 37 °C for 1 hour followed by plating out on agar plates containing kanamycin (50 μ g/ml) that is prescribed by the plasmid vector transformed. 1 colony was incubated at 37 °C for more than 16 hours in 3 ml 2YT medium with kanamycin (50 μ g/ml).

Then the plasmid DNA was purified using Plasmid Mini Kit (Qiagen, Hilden), and after PCR-sequencing the integrity of the plasmid obtained was confirmed by DNA sequencing. Conditions for PCR-sequencing reaction are shown in Table 2.5 and Table 2.6.

Table 2.2: Reaction mixture for a single-copy chromosomal locus PCR amplification

Component	Amount per reaction
Distilled water	40.6 μ l
10 \times cloned <i>Pfu</i> DNA polymerase reaction buffer	5.0 μ l
dNTPs (25 mM each dNTP)	0.4 μ l
DNA template (100 ng/ μ l)	1.0 μ l
Primer #1 (100 ng/ μ l)	1.0 μ l
Primer #2 (100 ng/ μ l)	1.0 μ l
<i>Pfu Turbo</i> DNA polymerase (2.5 U/ μ l)	1.0 μ l
Total reaction volume	50.0 μ l

Table 2.3: Primer sequencing for mutagenesis

Mutant	Primer	Sequencing
GrpE(N5C)	GrpEN5C-for	5'-GGA GCG GTG CCA CGA GAA CAC CCT GGA G-3'
	GrpEN5C-rev	5'-CTC CAG GGT GTT CTC GTG GCA CCG CTC C-3'
GrpE(V17C)	GrpEV17C-for	5'-GAC CTG GAG GCC TGT GGC CAG GAG GCC-3'
	GrpEV17C-rev	5'-GGC CTC CTG GCC ACA GGC CTC CAG GTC-3'

Table 2.4: PCR cycling parameters for *Pfu Turbo* DNA polymerase with single-block temperature cyclers

Cycles	Temperature	Time
1	95°C	30 seconds
16	95°C	30 seconds
	55°C	1 minute
	68°C	2 minutes/kb of plasmid length
-	4°C	Forever

Table 2.5: Reaction mixture for DNA-sequencing

Component	Amount per reaction
DNA (1 µg/ml)	1.0 µl
Primer (T7 promoter or T7 terminator primer)	0.3 µl
Terminator kit	4.0 µl
Water	4.7 µl
Total volume	10 µl

Table 2.6: PCR cycling parameters for DNA sequencing

Cycles	Temperature	Time
1	96 °C	30 seconds
25	96 °C	30 seconds
	50 °C	15 seconds
	60 °C	4 minutes
-	4 °C	Forever

2.2.2. Agarose Gel Electrophoresis of DNA

To pour a gel, agarose powder was mixed with TAE buffer to concentration 1% (w/v), then heated in a microwave oven until completely melted. Ethidium bromide (final concentration 0.5 µg/ml) was added to the gel at this point to facilitate visualization of DNA after electrophoresis. After cooling the solution to about 60 °C it was poured into a casting tray containing a sample comb and allowed to solidify at room temperature. Samples containing DNA mixed with 1:5 Sample buffer were then pipetted into the sample wells, and a current 10V/cm was applied. To visualize DNA, the gel was placed on an ultraviolet transilluminator at 302 nm.

- TAE buffer: 90 mM Tris, pH 8.3, 90 mM Acetic acid, 2 mM EDTA
- Sample buffer: 0.25 % Bromphenolblue, 0.25% Xylencyanol, 40% Sucrose in 50 mM EDTA, pH 8.0

2.2.3. Growth of *E.coli* Cells

Thermophile chaperones were expressed in *E.coli* BL21 (DE3) cells (Studier and Moffatt, 1986). The bacteria were grown to mid-logarithmic phase ($OD_{600} = 0.5-0.8$) in 2YT medium supplemented with 50 $\mu\text{g/ml}$ kanamycin. The medium was sterilized by autoclaving at 121 $^{\circ}\text{C}$ for 30 minutes. Antibiotic was added as sterile-filtered solution. Expression of the proteins was induced by addition of IPTG to a final concentration of 1 mM. The cells were harvested by centrifugation four hours after induction (Sorvall Rotor H6000A, 5000 rpm, 4 $^{\circ}\text{C}$, 15 minutes). The cell pellet was dissolved in 50 mM Tris/HCl pH 7.5 followed by centrifugation, freezing in liquid nitrogen and storage at -80 $^{\circ}\text{C}$.

- 2YT medium (1L): 16 g Peptone, 10 g Yeast extract, 5 g NaCl, pH 7.2

2.3. Fluorescent Labelling of Single Cysteine Mutants

To perform fluorescent measurements GrpE protein was labelled with extrinsic, environmentally sensitive fluorophores. Wild type GrpE from *T.thermophilus* contains no cysteine residues. Therefore two different GrpE cysteine mutants were engineered, GrpE(N5C) and GrpE(V17C). Alexa Fluor® 488 C₅ maleimide and *N,N'*-dimethyl-*N*-(iodoacetyl)-*N'*-(7-nitrobenz-2-oxa-1,3-diazol-4-yl)ethylenediamine (IANBD amide) (Molecular Probes, Eugene, USA) were covalently coupled to the single cysteine residues in GrpE(N5C) and GrpE(V17C). Chemical structures of the fluorophores are shown in Fig. 2.1.

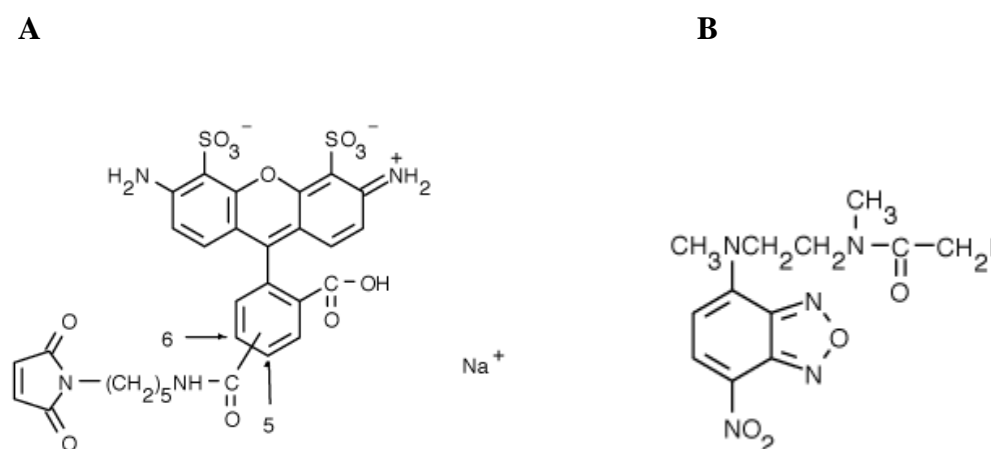


Figure 2.1: Chemical structure of Alexa Fluor® 488 (A) and IANBD amide (B).

Fluorescent labelling was done using a standard procedure for the thiol-reactive probes (Haugland, 1996). In a typical labelling reaction 10 mM Alexa488 maleimide in H₂O or IANBD amide in DMF were added dropwise to 1 ml of a 100 μM sample of single GrpE cysteine mutant in a DTT-free buffer to give approximately 20 moles of reagent for each mole of protein. The reagent was added to the protein solution as it is stirring. The sample was incubated overnight at 4° C in the dark and then 10 mM DTT was added to consume excess thiol-reactive reagent. Then the conjugant was separated on gel filtration column, such as Sephadex G-25 (NAP 5, Amersham Biosciences, Uppsala) and dialysed 2 x 5 h against buffer A. Concentration of the conjugated protein was determined using the Bradford colorimetric assay. The degree of labelling was calculated using the following formula:

$$\frac{A_x}{\epsilon} \times \frac{\text{MW of protein}}{\text{mg protein/mL}} = \frac{\text{moles of dye}}{\text{moles of protein}} \quad (2.1)$$

A_x - the absorbance value of the dye at the absorption maximum wavelength

ϵ - molar extinction coefficient of the dye at the absorption maximum wavelength (Alexa maleimide $\epsilon_{488} = 72\,000\text{ M}^{-1}\text{ cm}^{-1}$, IANBD amide $\epsilon_{493} = 25\,000\text{ M}^{-1}\text{ cm}^{-1}$).

- Buffer A: 20 mM Tris/HCl pH 7.5, 25 mM KCl, 1 mM MgCl₂, 2 mM DTE

2.4. Protein Methods

2.4.1. Protein Purification

2.4.1.1. Proteins without His-Tag

DnaK, GrpE, GrpE (N5C), GrpE (V17C), GrpE(Δ C), and DnaJ were purified as described (Groemping and Reinstein, 2001;Klostermeier et al., 1998;Klostermeier et al., 1999). The DnaK truncated mutants DnaK(1-381) and DnaK(382-615) were engineered by Dr. Seidel and purified by P.Herde. GrpE(Δ C) was engineered by Dr. Groemping (Groemping and Reinstein, 2001).

Overproducing *E.coli* cells with proteins under investigation were dissolved in lysis buffer with protease inhibitor, homogenized using a homogenizer (Novodirect, Kehl, Germany) and disrupted in a microfluidizer (Microfluidics, Newton, Massachusetts, USA) at a pressure of 600 kPa and a temperature of 4 °C. In case of GrpE proteins, after centrifugation for 30 minutes at 4 °C (Beckman Ti-45 rotor, 35000 rpm) 0.28 g of ammonium sulphate per ml of supernatant (45% saturation) was added and incubated at 4 °C for 30 minutes. To precipitate DnaK proteins, 0.136 g/ml of ammonium sulphate per ml of supernatant (25% saturation) was added and incubated at 4 °C for 30 minutes followed by centrifugation (40 minutes at 35000 rpm, 4 °C in the BeckmanTi-45-Rotor) and an additional precipitation by adding 0.321 g/ml of ammonium sulphate per ml of supernatant (75% saturation). After 30 minutes, the precipitate of the crude extract was centrifuged for 40 minutes at 4 °C (Beckman Ti-45 rotor, 35000 rpm). The protein pellet was resuspended in approximately 150 ml of buffer A and then dialyzed twice against 2 L of buffer A for 4 hours and over night. The dialysed sample was treated for 30 minutes at 75 °C followed by 30 minutes at 4 °C centrifugation (Beckman Ti-45 rotor, 35000 rpm). Then the supernatant was applied to an equilibrated EMD-DEAE column (300 ml, Merck, Darmstadt, Germany) with a flow rate of 3 ml/min. DnaK was eluted between 175 and 330 mM KCl. GrpE was eluted between 200 and 300 mM KCl. After analysis by SDS-PAGE, the fractions containing proteins under investigation were pooled and concentrated in Amicon chambers (Amicon, Beverly, USA). The sample was directly loaded onto a gel filtration column (Superdex 200, Pharmacia, 320 ml) to remove excess potassium from solution. The gel filtration column was washed with the gel filtration buffer at run 2 ml/min. The gel filtration fractions were pooled and dialysed against 2 L storage buffer for 4 hours and over night. Then proteins were concentrated in Amicon chamber (until approximately 20 mg/ml) and frozen at -80°C.

- Lysis buffer (used for DnaK proteins): 50 mM Tris/HCl pH 7.5, 25 mM KCl, 5 mM MgCl₂, 2 mM DTE, 2 mM EDTA, 1 mM PMSF, 10% (v/v) Glycerol, protease inhibitor cocktail
- Lysis buffer (used for GrpE proteins): 50 mM Tris/HCl pH 7.5, 100 mM KCl, 5 mM EDTA, 1 mM PMSF, 10% (v/v) Glycerol, protease inhibitor cocktail
- Buffer A (used for DnaK protein): 50 mM Tris/HCl pH 7.5, 25 mM KCl, 5 mM MgCl₂, 2 mM DTE, 2 mM EDTA)

- Buffer A (used for GrpE proteins): 50 mM Tris/HCl pH 7.5, 25 mM KCl, 2 mM EDTA, 10% (v/v) Glycerol
- Buffer B (used for DnaK protein): 50 mM Tris/HCl pH 7.5, 1 M KCl, 5 mM MgCl₂, 2 mM DTE, 2 mM EDTA
- Buffer B (used for GrpE proteins): 50 mM Tris/HCl pH 7.5, 1 M KCl, 2 mM EDTA, 10% (v/v) Glycerol
- Gel filtration buffer (used for DnaK protein): 50 mM Tris/HCl pH 7.5, 100 mM Na₂SO₄, 5 mM EDTA
- Gel filtration buffer (used for GrpE proteins): 50 mM Tris/HCl pH 7.5, 200 mM KCl, 2 mM EDTA, 10% (v/v) Glycerol
- Storage buffer (used DnaK proteins): 50 mM Tris/HCl pH 7.5, 200 mM KCl, 5 mM MgCl₂, 2 mM EDTA
- Storage buffer (used GrpE protein): 20 mM Tris/HCl pH 7.5, 25 mM KCl

2.4.1.2. Purification of 6xHis-Tagged Protein

The overproducing *E.coli* cells with DnaK_{Chis} were dissolved in lysis buffer with protease inhibitor, then homogenized using homogenizer (Novodirect, Kehl, Germany) and disrupted in microfluidizer (Microfluidics, Newton, Massachusetts, USA) at a pressure of 600 kPa and a temperature of 4 °C. To precipitate DnaK_{Chis} proteins 0.136 g/ml of ammonium sulphate per ml of supernatant (25% saturation) was added and incubated at 4 °C for 30 minutes followed by centrifugation (40 minutes at 35000 rpm, 4 °C in the BeckmanTi-45-Rotor) and an additional precipitation by adding 0.321 g/ml of ammonium sulphate per ml of supernatant (75% saturation). After 30 minutes, the precipitate of the crude extract was centrifuged for 40 minutes at 4 °C (Beckman Ti-45 rotor, 35000 rpm). The protein pellet was resuspended in approximately 150 ml of wash buffer and then dialyzed twice against 2 L of wash buffer for 4 and 14 hours. Then the protein solution was loaded onto the equilibrated Ni-NTA column (40

ml, Qiagen, Hilden) with a flow rate of 2 ml/min. The Ni-NTA column was equilibrated with 2 column volumes of wash buffer. DnaK_{Chis} was eluted between 323-500 mM Imidazole. After analysis by SDS-PAGE, the peak fractions were pooled and concentrated in Amicon chamber (Amicon, Beverly, USA) and frozen at - 80°C.

- Lysis buffer (50 mM Tris/HCl pH 7.5, 25 mM KCl, 5 mM MgCl₂, 2 mM DTE, 2 mM EDTA, 1 mM PMSF, 10% (v/v) Glycerol, protease inhibitor cocktail)
- Wash buffer: 50 mM Tris/HCl pH 7.5, 50 mM Imidazole; 100 mM NaCl
- Elution buffer: 50 mM Tris/HCl pH 7.5, 1 M Imidazole; 100 mM NaCl

2.4.2. SDS-Polyacrylamide Gel Electrophoresis (SDS-PAGE)

Protein separation by SDS-PAGE (Laemmli, 1970) was used to determine the relative abundance of major proteins in a sample, their approximate molecular weights, purity and in what fractions they can be found.

Separating gel consisted of 15% acrylamide, 0.4% bisacrylamide, 375 mM Tris/HCl, pH 8.8 and 0.1% SDS. Stacking gel was prepared by mixing 4.5% acrylamide, 0.1% bisacrylamide, 125 mM Tris/HCl, pH 6.8 and 0.06% SDS. Polymerization of acrylamide and bisacrylamide monomers was induced by APS and TEMED (50 µl 10% APS, and 5 µl TEMED per 10 ml).

Approximately 5 µg of sample protein was combined with Sample loading buffer in ratio 1:3 and boiled at 95 °C for 10 minutes to fully denature the protein. The electrophoresis was carried out in Biorad Mini 2D-Gel chamber (Biorad, München, Germany) with SDS-running buffer at constant amperage 40 mA per gel.

Protein standard (Marker) consisted of a number of proteins with known molecular weight such as Phosphorylase b (94.0 kDa), Bovine serum albumin (67.0 kDa), Ovalbumin (43.0 kDa), Carboanhydrase (30.0 kDa), Trypsin inhibitor (20.1 kDa) and α-Lactalbumin (14.4 kDa) (LMW Proteinmarker, Amersham, Freiburg, Germany).

After electrophoresis the gel was stained with staining solution. For rapid destaining, the gel was washed in multiple changes of destaining solution.

- Sample loading buffer (4x): 130 mM Tris/HCl, pH 6.8, 200 mM DTE, 4% (w/v) SDS, 0.01% (w/v) Bromphenol blue, 20% (v/v) Glycerol
- SDS-running buffer: 25 mM Tris, 192 mM Glycin, 0.01% (w/v) SDS
- Staining solution: 25% (v/v) Isopropanol, 10% (v/v) Acetic acid, 0.1% (w/v) Coomassie Blue-R250, 0.01% Coomassie Blue-G250
- Destaining solution: 20% (v/v) Acetic acid, 10% (v/v) Ethanol

2.4.3. Determination of Nucleotides in Protein Solution

In order to get information about nucleotide content of DnaK 16 μ l of the protein was incubated with 4 μ l 50% (w/v) TCA solution for 10 minutes at 0 °C followed by centrifugation at 14000 rpm, for 10 minutes at 4 °C. After that the supernatant was neutralized with 20 μ l of 2 M KOAc and applied to the ODC Hypersil Reversed Phase C-18 column (5 μ m, 120 x 4.6 mm, Bischoff, Leonberg) equilibrated with 50 mM KPi, pH 6.8. To get a calibration curve the same procedure was applied for the nucleotide solution consisting of 10 μ M ATP, 10 μ M ADP and 10 μ M AMP. Nucleotide peaks detected on a calibration curve correspond to nucleotide at a concentration of 10 μ M. Therefore the corresponding peaks on the sample chromatogram can be used to calculate the nucleotide content in a protein solution.

2.4.4. Protein Affinity Chromatography

2.4.4.1. Ni-NTA Affinity Chromatography

84 μM GrpE(ΔC) was incubated together with 25 μM of a C-terminally His-tagged DnaK (DnaK_{Chis}) for 1 hour at 30 °C in wash buffer. After incubation the proteins were loaded onto 2.0 ml Ni-NTA column (QIAGEN, CA) equilibrated with wash buffer. After washing of the column with the wash buffer until baseline recovery, bound DnaK_{Chis} protein was eluted with elution buffer containing 250 mM Imidazole. Protein peak fractions were pooled and analysed by 15% SDS-PAGE.

- Wash buffer: 50 mM NaH₂PO₄, 100 mM NaCl, 5 mM MgCl₂, 10 mM β -mercaptoethanol, 10% glycerol
- Elution buffer: 50 mM NaH₂PO₄, 100 mM NaCl, 5 mM MgCl₂, 10 mM β -mercaptoethanol, 10% glycerol, 250 mM Imidazole

2.4.4.2. Co-elution Experiment with DnaK and ATP-Agarose

C8-attached ATP-agarose (80 μl , Sigma-Aldrich, Taufkirchen) was incubated together with 30 μl 100 μM DnaK for 2 hours at 30 °C in agarose buffer. The resin was washed in batch procedure to remove unbound protein. Then, 30 μl of purified co-chaperones (GrpE, GrpE(ΔC)) at a concentration of 400 μM were added and incubated together with resin for 2 hours at 30 °C. The resin was washed with ten volumes of agarose buffer and bound proteins were finally eluted by incubating agarose buffer containing 5 mM ATP for 1.5 hour at 30 °C together with the resin. Non-specific binding was determined using resin without DnaK bound. Aliquots representing 10% of eluates were analysed by SDS-PAGE.

- Agarose buffer: 20 mM Tris/HCl pH 7.5, 25 mM KCl, 1 mM MgCl₂

2.5. Spectroscopic Methods

Absorption spectroscopy measurements of protein concentration were performed using DU 650 photometer (Beckman, Palo Alto, USA).

2.5.1. Determination of Protein Concentration

Protein concentrations were determined spectrophotometrically by the method of Ehresmann (Ehresmann et al., 1973) by measuring absorption at 228.5 nm and 234.5 nm in a Quartz cuvette. The protein concentration in mg/ml was calculated according to equation:

$$c = (A_{228.5} - A_{234.5})/3.14 \quad (2.2)$$

$A_{228.5}$: absorption at 228.5 nm

$A_{234.5}$: absorption at 234.5 nm

c: protein concentration in mg/ml

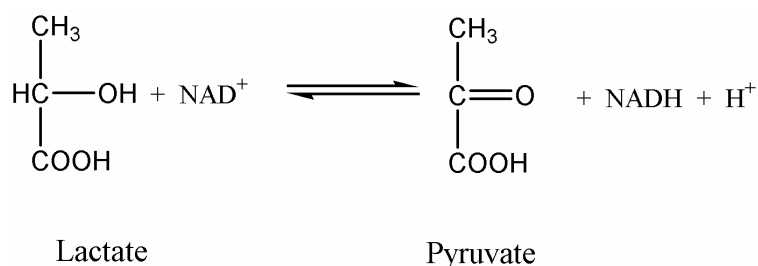
Since fluorescent dyes used for protein labelling are able to absorb UV light between 220 and 240 nm the concentration of the labelled proteins was determined by the method of Bradford (Bradford, 1976). The method is based on the proportional binding of the dye Coomassie Brilliant Blue G-250 to proteins. Within the linear range of the assay (~5-25 $\mu\text{g/ml}$), the more protein present, the more Coomassie binds. Coomassie absorbs at 595 nm. The protein concentration of a test labelled sample was determined by comparison to that of non-labelled protein which exhibited a linear absorbance profile in this assay.

2.5.2. Chaperone-Assisted Reactivation of Lactate dehydrogenase

The chaperone activity of the DnaK system (DnaK, DnaJ, GrpE) in the absence and presence of the chaperone ClpB was monitored via reactivation of chemically and temperature

denatured Lactate dehydrogenase from *S.scrofa* (pig) muscle (LDH_{Ssc}) and heat inactivated Lactate dehydrogenase from *B.stearothermophilus* (LDH_{Bst}).

The enzyme Lactate dehydrogenase (EC 1.1.1.27) catalysis the reaction:



The steady-state assay of LDH activity is based on the nicotineamide adenine dinucleotide coenzyme of LDH, NADH, spectroscopic properties. NADH absorbs radiation at 340 nm in reduced form, whilst the oxidized NAD⁺ form does not absorb at this wavelength. The LDH activity was monitored with absorption spectroscopy using the iEMS Reader (Labsystems, Helsinki, Finland) for titerplates (8x12).

LDH_{Ssc} at a concentration of 30 μM was denatured with 6 M urea or 2 M GdnHCl in denaturation buffer at 30 °C for 30 minutes. Heat denaturation of LDH_{Ssc} (0.5 μM) was performed for 40 minutes at 60 °C in denaturation buffer. Renaturation in the presence of the DnaK system alone (3.2 μM DnaK, 0.8 μM DnaJ, 0.4 μM GrpE(wt)/GrpE(N5C)/GrpE(V17C)) or together with the chaperone ClpB (0.5 μM) was initiated by 120-fold dilution with NADH buffer in the presence of 1 mg/ml BSA and 1 mM ATP at 30 °C. A sample of the refolding solution was transferred into the activity assay (NADH buffer, 1 mg/ml BSA, 3 mM pyruvate, 0.4 mM NADH) at the indicated times. LDH activity was followed by recording the changes in absorbance at 340 nm of a 500-μl mixture at 30 °C. The activity of the refolded LDH was calculated as a percentage of positive control.

- Denaturation buffer: 50 mM Tris/HCl, pH 7.5, 50 mM KCl, 5 mM MgCl₂, 10 mM DTE, 0.05 mg/ml BSA
- NADH buffer: 50 mM Tris/HCl, pH 7.5, 50 mM KCl, 5 mM MgCl₂, 4 mM EDTA, 4 mM DTE, 0.4 mM NADH

2.5.3. Circular Dichroism (CD)

CD spectra were recorded with a Jasco-J710 spectropolarimeter (JASCO, Tokyo, Japan) from 200 to 250 nm in a cuvette with 0.1 cm thickness at a scan-rate of 20 nm/minute, 0.2 nm resolution, 1 nm bandwidth, a time-constant of one second and a sensitivity of 20 mdeg. The temperature was held constant at 25 °C using a water-bath. Protein concentrations were 1 and 2 mg/ml. CD spectra were buffer corrected.

- CD buffer: 20 mM NaH₂PO₂ (pH 7.04), 20 mM KCl, 5 mM MgCl₂

The detected ellipticity in mDegree was transformed into mean residue ellipticity (Degree cm²dmol⁻¹) according to formula:

$$[\Theta]_{\text{MRE}} = \Theta \cdot 100 / (c \cdot d \cdot N) \quad (2.3)$$

$[\Theta]_{\text{MRE}}$: mean residue ellipticity in Degree cm²dmol⁻¹

$[\Theta]$: ellipticity measured in Degree

c: protein concentration in M

d: thickness in cm

N: number of amino acids of the protein under investigation

2.5.4. Fluorescence Spectroscopy

2.5.4.1. Equilibrium Fluorescence Measurements

2.5.4.1.1. Tryptophan Fluorescence

Fluorescence was measured with a Fluoromax-3 Spectrofluorometer (JY Horiba, USA) using a 1-cm-square quartz cuvette. 2 μ M DnaK(1-381) was incubated in standard fluorescence buffer in the absence or presence of GdnHCl for 1 hour at 25 °C followed by emission spectra detection. The emission and excitation slit widths were set at 9 and 10 nm respectively. The excitation wavelength was 287 nm. The temperature of the measurement was kept at 25 \pm 0.5 °C.

- Standard fluorescence buffer (SFB): 50 mM Tris/HCl, pH 7.5, 100 mM KCl, 5 mM MgCl₂, 2 mM EDTA, 2 mM DTE

2.5.4.1.2. IANBD Fluorescence

Measurements were performed with a Fluoromax-3 Spectrofluorometer (JY Horiba, USA). Excitation was at 498 nm and emission was recorded from 520 to 680 nm with a 7-nm slit width. Spectra were determined after incubation of 1 μ M GrpE(N5C)IANBD and 1 μ M GrpE(V17C)IANBD with 20 μ M DnaK, 20 μ M DnaK-ADP, 20 μ M DnaK-ATP, and 20 μ M DnaK-P3 in SFB for 1 hour at 25 °C. P3 is a 10-mer peptide derived from p53 tumor suppressor protein with the sequence FYQLAKTCPV. To get a DnaK-P3 complex, 40 μ M DnaK was incubated with 1600 μ M peptide P3 for 1 hour at 25 °C. DnaK in ATP bound state and in ADP bound form was generated by incubation of 100 μ M DnaK with 2 mM Mg²⁺/ATP (2 mM Mg²⁺/ADP) To determine emission peak maxima, data were fitted by nonlinear regression analysis to a Gaussian peak function using Microsoft Excel.

2.5.4.2. Fluorescence Correlation Spectroscopy (FCS)

FCS was performed on the basis of a confocal laser scanning microscope (MRC-1024, Biorad) extended correlation measurements. Rhodamine-Green, GrpE(V17C)IANBD, and GrpE(V17C)Alexa488 were excited 488-nm line of an argon laser. The intensity fluctuations were detected by a single photon counting avalanche photodiode (SPAD, EGBG) and processed with a digital correlator (ALV, Langen, Germany). The power of the laser beam entering the microscope was set to 0.1 mW for the Ar⁺ laser for solution of Rhodamine-Green; 1 mW for GrpE(V17C) labeled with IANBD; 0.1 mW for GrpE(V17C) labeled with Alexa488. Autocorrelation curve of free GrpE(V17C)Alexa488 at a concentration of 40 nM and autocorrelation curve of the same protein in the presence of 4 μM DnaK, 4 μM DnaK in a complex with ADP, 4 μM DnaK in a complex with ATP, and mixture of 4 μM DnaK(1-381) and 4 μM DnaK(382-615) were recorded in standard fluorescence buffer in sample volume of 50 μl. All experimental autocorrelation functions (ACF), except ACF of IANBD labelled GrpE(V17C) and Rhodamine Green, were fitted by a single species model (Eq. 2.4), ignoring the triplet state. Translational diffusion time (τ_d) derived from this formula was calculated using Origin 5.0.

$$G(\tau) - 1 = \frac{1 - T + T^* \exp(-\tau / \tau_T)}{N * (1 + \tau / \tau_d) * (1 + (r/z)^2 * \tau / \tau_d)^{0.5}} \quad (2.4)$$

T: average of fraction of molecules in the excited triplet state

τ_T : triplet relaxation time

N: average number of fluorescent molecules in the Gaussian detection volume

r: radial distances

z: axial distances

τ_d : characteristic time for translational diffusion of the single species

To analyse contribution of the standard fluorescence buffer used in FCS measurements into fluorescent signal, we performed FCS measurements of the buffer. As shown in Fig. 2.2, standard fluorescence buffer contains no fluorescent molecules. The count rate shown in Fig.

2.2A possibly results from unspecific light scattering and does not describe a single species correlation function as shown in Fig. 2.2B. Hence fluorescent signals detected in FCS measurements come only from the labeled GrpE molecules.

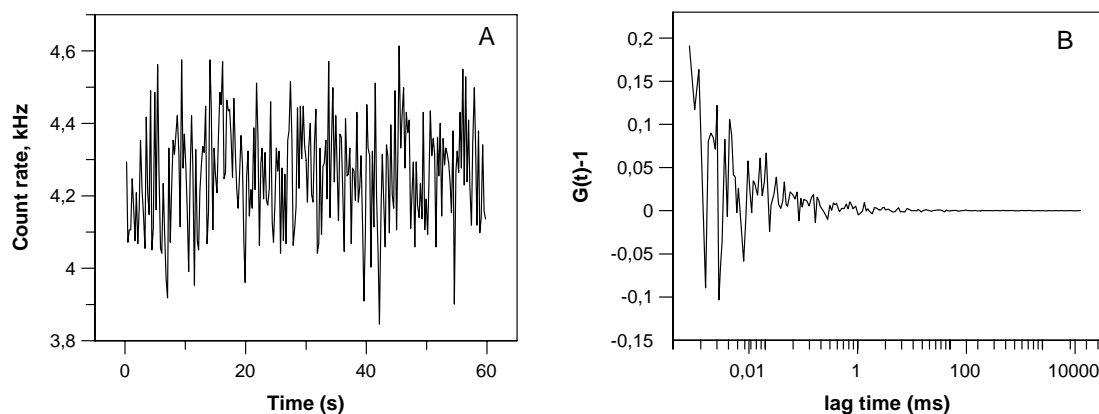


Figure 2.2: Count rate (A) and autocorrelation function (B) of the standard fluorescence buffer.

Laser power was 1 mW.

2.6. Differential Scanning Calorimetry (DSC)

The scans were performed with a scan rate of 60 deg. C/hour in a VP-DSC-Microcalorimeter (MicroCal, Northampton, MA). The samples were dialysed for 18 hours at room temperature against the same DSC buffer that was used to establish the baseline with a final protein concentration of 40 μ M for DnaK and 80 μ M for GrpE(Δ C). The samples and reference solutions were degassed for at least 5 min at room temperature and carefully loaded into the cells to avoid bubble formation. Cells were carefully cleaned before each experiment. The volume of the calorimetric cell was 0.5 ml. A background scan recorded with buffer in both cells was subtracted from each scan. The reversibility of thermal transitions was checked by examining the reproducibility of the calorimetric trace in the second heating of the sample immediately after first cooling from the first scan.

- DSC buffer: 20 mM Hepes/NaOH (pH 7.5), 100 mM KCl, 5 mM MgCl₂

3. Results

3.1. Establishing New Substrates for the DnaK-ClpB Chaperone System from *T.thermophilus*

3.1.1. Lactate dehydrogenase from *S.scrofa* Muscle (LDH_{Ssc})

In order to study the mechanism of the DnaK system (DnaK, DnaJ, GrpE) and ClpB from *Thermus thermophilus* to assist protein folding *in vitro* it was necessary to find a substrate for this chaperone machinery. As a model substrate we considered Lactate dehydrogenase (EC 1.1.1.27, LDH) since it fulfils a number of relevant criteria: it populates intermediates during its folding process (Jaenicke and Seckler, 1997); its enzymatic activity readily determined by a sensitive spectroscopic assay, can be utilized to monitor its folding status. LDH catalyses interconversion of lactate and pyruvate using nicotineamide adenine dinucleotide, NADH, as co-enzyme. The steady-state assay of LDH activity is based on the NADH spectroscopic properties. NADH absorbs radiation at 340 nm in reduced form, whilst the oxidized NAD⁺ form does not absorb at this wavelength. Lactate dehydrogenase from *S. scrofa* (pig) muscle (LDH_{Ssc}) is a homotetramer with a subunit molecular weight of 31 kDa. The complex of LDH_{Ssc} with NADH was solved at 2.2 Å resolution (Dunn et al., 1991). To find conditions at which LDH_{Ssc} is saturated with the substrate (pyruvate), a microtiterplate based assay had been performed. Enzymatic activity of LDH_{Ssc} was measured over a range of pyruvate concentrations from 0.2 mM to 5 mM. Kinetic constants of LDH_{Ssc} were determined at 25°C. Normal Michaelis-Menten enzyme kinetic shown in Fig. 3.1.1 demonstrates that 5 nM LDH was saturated by 3 mM pyruvate. The rate dependence on pyruvate followed Michaelis-Menten kinetics, with apparent K_m value of 0.26 mM; apparent V_{max} was about 0.0039 $\Delta A_{340}/s$ corresponding to k_{cat} of about 125/s. The maximum velocity and K_m values reported

in the literature and presented in this work are different because we studied kinetics of the backward reaction (pyruvate reduction) in comparison to the forward reaction (lactate oxidation) used by others (Chen and Engel, 1975).

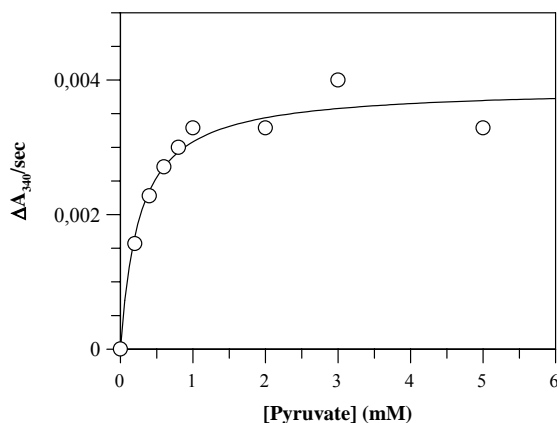


Figure 3.1.1: Michaelis-Menten kinetics of Lactate dehydrogenase from *S.scrofa* muscle (LDH_{Ssc}). The measurement of the LDH_{Ssc} (5 nM) activity was carried out in 150 μ l of NADH buffer: (50 mM Tris/HCl pH 7.5, 50 mM KCl, 5 mM EDTA, 2 mM DTE, 0.2 mM NADH), with 1 mg/ml BSA and pyruvate at different concentrations (from 0.2 mM to 5 mM). The initial value was recorded without LDH_{Ssc}. From the calculated value of V_{\max} (0.0039 $\Delta A_{340}/\text{s}$), the corresponding catalytic rate constant was determined ($k_{\text{cat}} = 125/\text{s}$).

3.1.1.1. Chemical (urea, GdnHCl) and Temperature Denaturation of LDH_{Ssc}

Before study the DnaK-ClpB assisted reactivation of a substrate protein, we monitored denaturation of LDH_{Ssc} by two of the best known chemical agents, such as urea and GdnHCl and inactivation induced by high temperature. As shown in Fig. 3.1.2, 30 minutes incubation of 500 nM LDH_{Ssc} at increasing concentrations of urea leads to a progressive decrease in the reaction rate; nearly complete inactivation of LDH_{Ssc} was observed at 3 M urea.

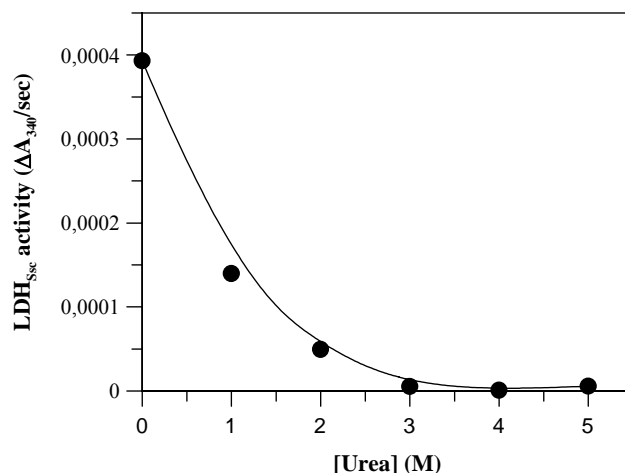


Figure 3.1.2: Effect of urea on the activity of LDH_{Ssc}. LDH_{Ssc} (500 nM) was denatured at 25 °C for 30 minutes in denaturation buffer with urea at different concentrations (from 1 to 5 M). The first point was recorded from a “denaturation” mixture free of urea. After denaturation LDH_{Ssc} was diluted one hundred fold into the NADH buffer. LDH_{Ssc} activity was thus measured with 5 nM LDH_{Ssc}, 5 mM pyruvate, 0.2 mM NADH.

The effect of GdnHCl on LDH_{Ssc} activity was qualitatively similar to those obtained with urea denaturation: the extent of LDH_{Ssc} deactivation diminished as the concentration of GdnHCl was raised (Fig. 3.1.3). It was found that GdnHCl at a concentration of 1 M caused significant loss of the LDH_{Ssc} activity due to denaturation of the enzyme. In comparison to GdnHCl, urea at a concentration of 3 M was necessary to induce inactivation of 500 nM LDH_{Ssc}. GdnHCl was found to be a stronger denaturant than urea.

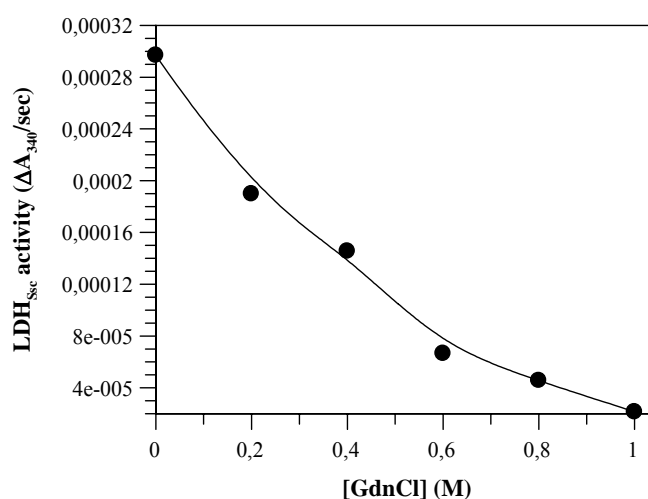


Figure 3.1.3: GdnHCl denaturation of LDH_{Ssc}. LDH_{Ssc} (500 nM) was denatured at 25 °C for 30 minutes in denaturation buffer with GdnHCl at different concentrations (from 0.2 to 1 M). The first value was recorded with solution free of GdnHCl. After denaturation LDH_{Ssc} was diluted one hundred fold into the NADH buffer. LDH_{Ssc} activity was thus measured with 5 nM LDH_{Ssc}, 5 mM pyruvate, 0.2 mM NADH.

To determine the conditions for maximal inactivation the effect of 2 M GdmCl on the activity of LDH_{Ssc} at various concentrations was monitored. Experiments consisted of two steps: in the first step LDH_{Ssc} (at different concentrations) was incubated at 25 °C for 30 minutes (inactivation) in denaturation buffer in the presence of 2 M GdnHCl which was followed by the second incubation at 25 °C for 210 minutes (reactivation) in NADH buffer and in the presence of 1 mM ATP and 1 mg/ml BSA. To control the influence of GdnHCl on LDH_{Ssc} denaturation the enzyme was incubated at different concentrations at 25 °C for 30 minutes in the absence of denaturant. The result was remarkable: incubation of LDH_{Ssc} at concentrations ranging from 1 to 35 μM in the presence of 2 M GdnHCl produced a progressive decrease in its activity (Fig. 3.1.4, filled circles). In the absence of denaturant the LDH_{Ssc} enzymatic activity did not change significantly and corresponded to about 98% of native control (Fig. 3.1.4, open circles). Based on the data obtained we could assume that increase in concentration of LDH_{Ssc} at a constant concentration of denaturant, GdnHCl, causes fast aggregation of the denatured LDH_{Ssc} molecules that accounts for a progressive decrease of the enzymatic activity.

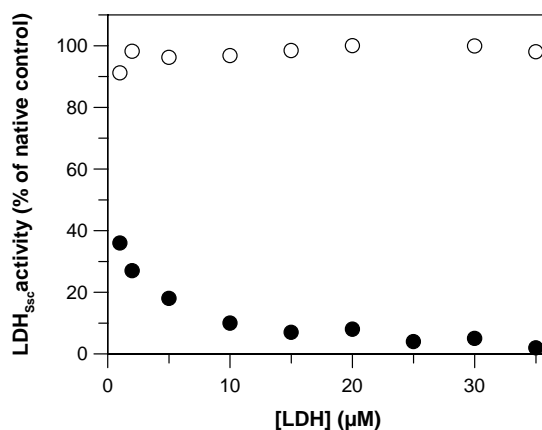


Figure 3.1.4: Concentration dependence of the LDH_{Ssc} denaturation with 2 M GdnCl. LDH_{Ssc} (at different concentrations ranging from 1 to 35 μM; concentration refers to monomer) was denatured at 25 °C for 30 minutes in denaturation buffer in the absence (open circles) or presence of 2 M GdnHCl (filled circles). After dilution to a final concentration of 20 nM LDH_{Ssc} was incubated at 25 °C for 210 minutes in NADH buffer with 1 mg/ml BSA, 1 mM ATP. LDH_{Ssc} activity was measured with 5 nM LDH, 3 mM pyruvate and 0.8 mM NADH.

To assign thermostability of LDH_{Ssc} the enzymatic activity of this protein was determined after 30 minutes incubation in the range from 35 to 80 °C. In addition, to detect whether the co-factor NADH has any influence on the heat denaturation of LDH_{Ssc} the enzyme was denatured in the absence and presence of NADH.

It was observed that 30 minutes incubation of LDH_{Ssc} (50 nM) in the range from 35 to 80 °C resulted in remarkable decrease of the enzymatic activity (Fig. 3.1.5). It was detected that LDH_{Ssc} lost its activity much faster in the absence of the co-factor (NADH) than in its presence. The maximal denaturation of LDH_{Ssc} in the absence of NADH was detected at 60°C, whereas in the presence of NADH significant decrease in the LDH_{Ssc} activity was observed at 70 °C, which is 10 degrees higher than in the presence of the co-factor. The obtained results provide the evidence that the co-factor NADH stabilises LDH_{Ssc}.

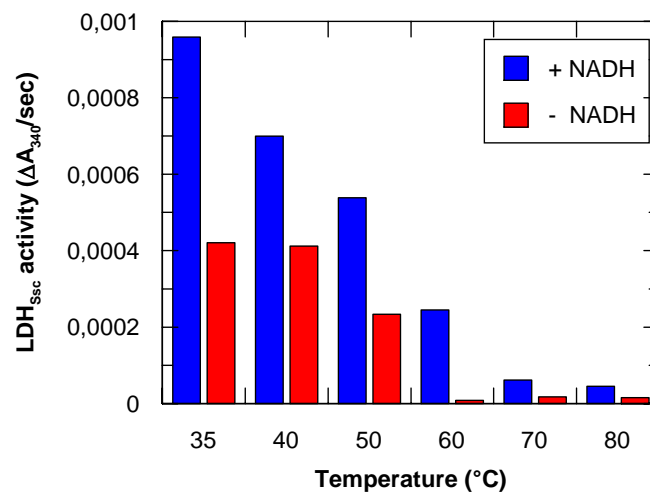


Figure 3.1.5: Thermal denaturation of LDH_{Ssc}. LDH_{Ssc} (50 nM) was incubated for 30 minutes at different temperatures (from 35 to 80 °C) either in the absence (shown in red) or presence of 0.8 mM NADH (shown in blue). LDH_{Ssc} activity was determined in microtiter plates over a five minute period. LDH_{Ssc} activity was measured with 5 nM LDH, 3 mM pyruvate and 0.8 mM NADH.

3.1.1.2. Refolding of urea-, GdnHCl- and Thermally Denatured LDH_{Ssc} Mediated by the DnaK_{Tth}-ClpB_{Tth} Chaperone System

In order to test the ability of the DnaK system (DnaK, DnaJ, GrpE) in the absence and presence of the chaperone ClpB from *T.thermophilus* to reactivate denatured proteins, we measured the enzymatic recovery of chemically (urea and GdnHCl) and thermally inactivated Lactate dehydrogenase (LDH_{Ssc}).

The experiment consisted of two steps: incubation of LDH_{Ssc} with urea or GdnHCl was immediately followed by the dilution and second incubation in the absence or presence of chaperones. LDH_{Ssc} (30 μM) was denatured in denaturation buffer with 6 M urea or 2 M GdnHCl for 30 minutes at 30 °C. Renaturation of LDH_{Ssc} was initiated by 120-fold dilution of the denatured enzyme in NADH buffer. It was also checked out in the presence of the DnaK

system alone (3.2 μM DnaK, 0.8 μM DnaJ, 0.4 μM GrpE) and in the presence of the DnaK system together with the chaperone ClpB (0.5 μM). During refolding, samples were withdrawn at certain time intervals, diluted 250-fold into assay buffer and the absorption of the LDH_{Ssc} cofactor NADH in this reaction-mix was measured in microtiter plates over a five hour period. Results of this experiment are shown in Fig. 3.1.6. Spontaneous recovery of the enzymatic activity was up to 9% of that of native LDH_{Ssc}. The yield of recovered LDH_{Ssc} activity assisted by chaperones was increased with incubation time. It was detected that maximal reactivation of LDH_{Ssc} assisted by the DnaK system alone is 34%, whereas an additional presence of the ClpB chaperone gives rise to recovery of LDH_{Ssc} up to 50%. As shown in Figure 3.1.6, the end value of the chaperone mediated reactivation of LDH_{Ssc} may not be reached after 300 minutes of incubation. However, according to the data obtained, we could conclude that urea denatured LDH_{Ssc} could be a suitable model substrate for the DnaK_{Tth} system alone and for the DnaK_{Tth}-ClpB_{Tth} machinery as well.

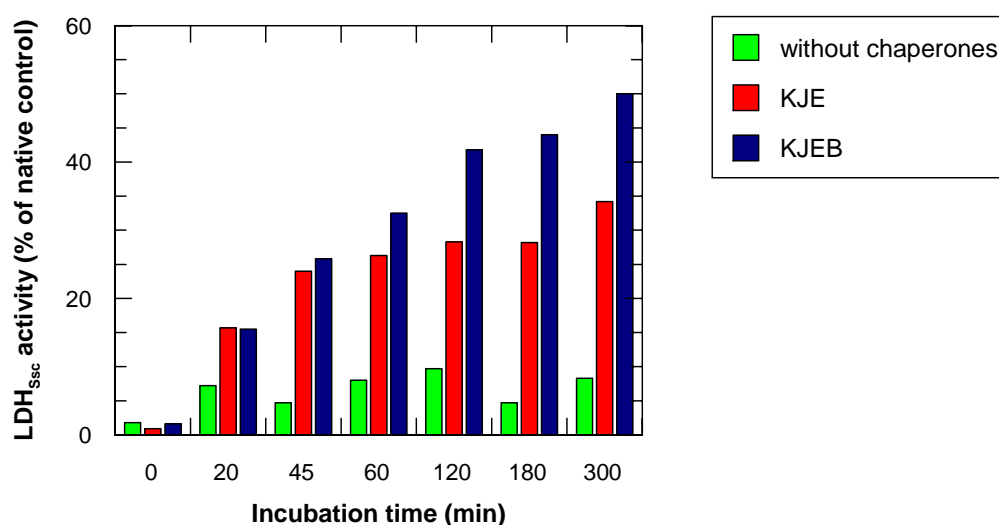


Figure 3.1.6: Refolding of urea denatured LDH_{Ssc} mediated by the DnaK_{Tth}-ClpB_{Tth} chaperone system. LDH_{Ssc} (30 μM) was incubated at 30 °C for 30 minutes in NADH buffer with 6 M urea. After 120-fold dilution the refolding of urea-denatured LDH_{Ssc} was monitored in a reaction containing buffer alone (shown in green), the DnaK system (3.2 μM DnaK, 0.8 μM DnaJ, 0.4 μM GrpE) (shown in red), and the DnaK system together with 0.5 μM ClpB (shown in blue). The yield of refolding was normalized to the activity of native LDH_{Ssc}.

Continuous observation of LDH_{Ssc} activity over 300 minutes indicated that spontaneous recovery of the enzymatic activity of GdnHCl-denatured LDH_{Ssc} was up to 3% of that of native LDH_{Ssc}. (Fig. 3.1.7, shown in green). The DnaK system alone (Fig. 3.1.7, shown in

red) gave rise to a recovery of active enzyme up to 12% after 300 minutes of incubation. Renaturation was significantly noticed after 30 minutes incubation of denatured LDH_{Ssc} with ClpB and the DnaK system. It was also found to be maximum (38%) after 5 hours of incubation (Fig. 3.1.7, shown in blue). It was observed a “lag phase” of about 30 minutes, during which the LDH_{Ssc} activity regain was very low even in the presence of ClpB and DnaK/DnaJ/GrpE. This suggests that LDH_{Ssc} may undergo repetitive cycles of binding to different chaperones before being released to solution in an active state.

As shown in Figure 3.1.7, the end value of the chaperone assisted reactivation of GdnHCl-denatured LDH_{Ssc} may be not achieved after 300 minutes incubation and therefore incubation period should be extended. However, even in 5 hours incubation we observed chaperone mediated reactivation of LDH_{Ssc} and besides the highest yield of the enzymatic activity was detected in the presence of the DnaK-ClpB chaperone machinery.

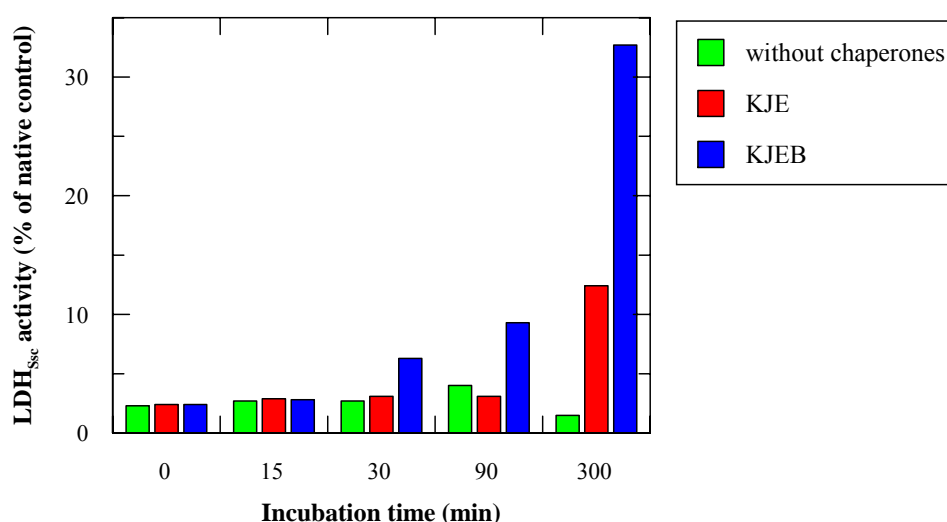


Figure 3.1.7: Refolding of GdnHCl denatured LDH_{Ssc} mediated by the DnaK_{Tth}-ClpB_{Tth} chaperone system.

LDH_{Ssc} (30 μM) was denatured at 30 °C for 30 minutes with 2 M GdnHCl. After dilution to a concentration of 30 nM LDH_{Ssc} was incubated at 30 °C either in buffer alone (shown in red) or in the presence of the DnaK system alone (3.2 μM DnaK, 0.8 μM DnaJ, 0.4 μM GrpE) (shown in red), or in the presence of the DnaK system together with 0.5 μM ClpB (shown in blue).

To study the ability of molecular chaperones to assist reactivation of heat-inactivated enzyme, LDH_{Ssc} at a concentration of 500 nM was incubated at 60 °C in the presence of 0.8 mM NADH for 40 minutes. The inactivation period was immediately followed by the second incubation of fivefold diluted LDH_{Ssc} into NADH buffer with 1 mg/ml BSA, 1 mM ATP at 30°C either in the absence or presence of chaperones (3.2 μM DnaK, 0.8 μM DnaJ, 0.4 μM

GrpE, 0.5 μ M ClpB) (recovery period). During incubation samples were withdrawn at certain time intervals, diluted fivefold into assay solution (NADH buffer, 1 mg/ml BSA, 5 mM pyruvate, 0.4 mM NADH) and the absorption of NADH in 150 μ l of this mixture was measured in microtiter plates over a five minute period. LDH_{Ssc} activity was expressed as a percent of activity of this enzyme prior to heat inactivation.

In this experiment we recorded reactivation of heat-denatured LDH_{Ssc} mediated by the DnaK system together with the chaperone ClpB. Elevated temperature is known to denature the protein by disrupting its hydrophobic core. The result of denaturation is the formation of unstable species with exposed hydrophobic surfaces which may tend to assume an alternatively stable conformation in the form of aggregates. The molecular chaperone ClpB was shown to modify the nature of large turbid aggregates toward subsequent solubilization and assist protein refolding together with the DnaK system (Goloubinoff et al., 1999; Schlee et al., 2004). Therefore the chaperone assisted reactivation of thermally denatured LDH_{Ssc} was investigated in the presence of both DnaK system and the chaperone ClpB.

It was detected that in the absence of chaperones, approximately 34% of heat-inactivated LDH_{Ssc} were active (Fig. 3.1.8, open circles). In addition, during reactivation period the spontaneous reactivation of LDH_{Ssc} was not increased more than 34%. It is possible to assume that 34% of the LDH_{Ssc} molecules were refolded immediately after denaturation or they were not unfolded. In the presence of chaperones the amount of reactivated LDH_{Ssc} was increased to 60% (Fig. 3.1.8, filled circles). Taking into account that in the absence of chaperones 34% of heat-inactivated LDH_{Ssc} were active we could conclude that chaperones reactivated only additional 20% of heat denatured LDH_{Ssc}.

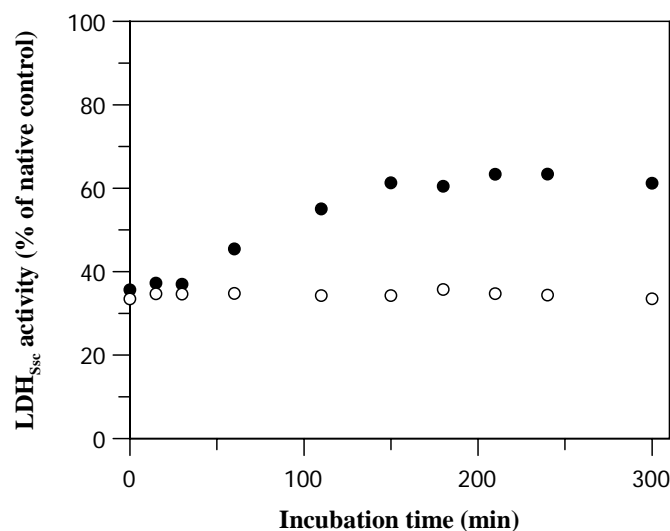


Figure 3.1.8: Reactivation of LDH_{Ssc} by chaperones after heat denaturation in the presence of NADH. LDH_{Ssc} (0.5 μ M) was denatured for 40 minutes at 60 °C in buffer (50 mM Tris/HCl pH 7.5, 50 mM KCl, 5 mM MgCl₂, 10 DTE, 0.05 mg/ml BSA) in the presence of 0.8 mM NADH. Then LDH_{Ssc} was diluted fivefold into NADH buffer without chaperones (open circles) or with 3.2 μ M DnaK, 0.8 μ M DnaJ, 0.4 μ M GrpE and 0.5 μ M ClpB (filled circles) and incubated at 30 °C. LDH_{Ssc} activity was determined at the indicated times during the recovery period.

To obtain a differently inactivated LDH_{Ssc} as a suitable substrate for the DnaK-ClpB system we applied a number of additional conditions: the denaturation temperature was increased up to 70 °C; the LDH_{Ssc} concentration was 10 fold higher than in previous experiment; denaturation was performed in the absence of the co-enzyme NADH. In addition, to test the inactivation of the enzyme during exposure to different period at elevated temperature, LDH_{Ssc} (5 μ M) was inactivated at 70 °C for 2, 5, 10, 15, 20 and 30 minutes. After denaturation the enzyme was diluted to fivefold into NADH buffer without chaperones or in the presence of chaperones and incubated at 30 °C for 270 minutes. LDH_{Ssc} activity was determined at the indicated times of denaturation. It was observed that even a short period (2 minutes) of LDH_{Ssc} exposure to 70 °C resulted in the irreversible loss of more than 98% of LDH_{Ssc} activity (Fig. 3.1.9, open circles). However, the maximal recovery of the enzymatic activity was only 5% of native control in the presence of the components of the DnaK-ClpB system (Fig. 3.1.9, filled circles). It could be possible that mesophilic LDH_{Ssc} exposed at elevated temperature immediately loses enzymatic activity due to changes in its three-dimensional structure and then it starts to form aggregates via hydrophobic interactions in such a way that disaggregation not being possible by chaperones. It is also very likely that reactivation of the eukaryotic LDH_{Ssc} is very slow and may span long time periods.

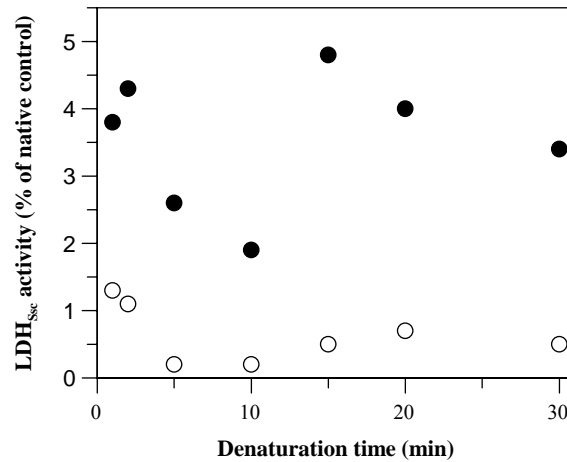


Figure 3.1.9: Reactivation of LDH_{Ssc} by chaperones after different time interval of heat denaturation. LDH_{Ssc} (5 μ M) was denatured at 70 °C for 2, 5, 10, 15, 20 and 30 minutes in buffer (50 mM Tris/HCl pH 7.5, 50 mM KCl, 5 mM MgCl₂, 10 mM DTE, 0.05 mg/ml BSA). Then LDH_{Ssc} was diluted to tenfold and incubated at 30 °C for 270 min without chaperones (open circles) or with 3.2 μ M DnaK, 0.8 μ M DnaJ, 0.4 μ M GrpE and 0.5 μ M ClpB (filled circles).

3.1.2. Lactate dehydrogenase from *B.stearothermophilus* (LDH_{Bst})

The previous experiment showed that LDH from *S.scrofa* muscle (LDH_{Ssc}) was completely denatured after incubation at 70 °C for only 2 minutes and significant reactivation of the enzymatic activity was not detected in the presence of the DnaK system together with the chaperone ClpB. As an alternative to LDH from mesophilic organism we chose the thermophilic LDH from *B.stearothermophilus* (LDH_{Bst}). The oligomeric state of the *B.stearothermophilus* LDH_{Bst} is the same as LDH from *S.scrofa* muscle; it is a tetramer composed of four identical subunits. The molecular weight of the enzyme (in its tetrameric form) was found to be 135 kDa, each of the subunits approximately 36 kDa (Schär and Zuber, 1979).

To study whether heat denatured LDH_{Bst} could be a substrate for the DnaK-ClpB chaperone machinery we investigated first the kinetic properties of the enzyme. The kinetic properties were evaluated with 0.1 μ M LDH_{Bst} in reaction buffer in the presence of 1 mg/ml BSA at different pyruvate concentrations at 25 °C. 150 μ l of this reaction mixture were placed in wells of microtiter plates and the absorption at 340 nm was measured. Michaelis-Menten kinetics of LDH_{Bst} is shown in Fig. 3.1.10. The value of V_{\max} is 0.0024 A_{340}/s corresponding to k_{cat} of about 13/s and the K_m is 3.3 mM. The kinetic data obtained differ from those reported by other authors. Jackson and colleagues (1992) estimated the k_{cat} for the pyruvate reduction of 317/s and the K_m value of 5.2 mM at 25 °C and pH 6.0 in reaction buffer. The k_{cat} and K_m estimated directly from the saturation curves by Schär and Zuber (1979) were $2 \cdot 10^5/s$ and 6.6 mM, respectively at 37 °C in reaction buffer (0.1 M triethanolamine hydrochloride/NaOH, pH 6.0). The detected diversities on the kinetic properties of LDH_{Bst} could be explained by different conditions used: the composition and pH of the assay buffer, temperature.

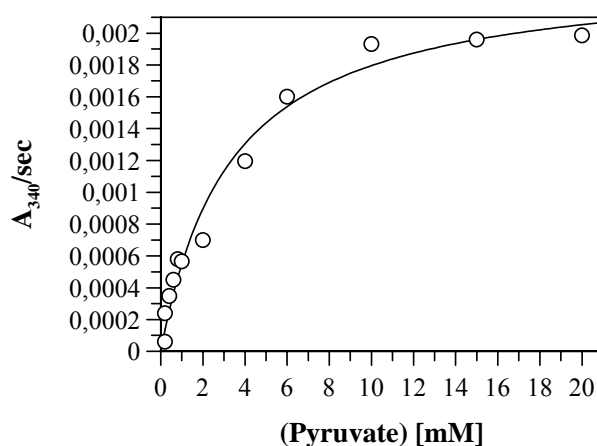


Figure 3.1.10: Michaelis-Menten kinetics of Lactate dehydrogenase from *B.stearothermophilus* (LDH_{Bst}). The measurement of the LDH_{Bst} (100 nM) activity was carried out in 150 μ l of reaction buffer (50 mM MOPS-NAOH pH 7.5, 5 mM MgCl₂, 150 mM KCl, 1 mM DTT, 0.2 mM NADH) with 1 mg/ml BSA and pyruvate at different concentrations (from 0.2 to 20 mM). From the calculated value of V_{\max} (0.0024 $\Delta A_{340}/s$), the corresponding catalytic rate constant was determined ($k_{\text{cat}} = 13/s$).

3.1.2.1. Refolding of Thermally Denatured LDH_{Bst} Mediated by the DnaK_{Tth}-ClpB_{Tth} Chaperone System

To get insight into ability of the DnaK-ClpB chaperone system to assist reactivation of thermally inactivated LDH_{Bst} the enzyme was first incubated at 80 °C for 30 minutes in buffer (inactivation period) and subsequently incubated at 40 °C either in the absence or in the presence of the DnaK-ClpB chaperone system (recovery period). As depicted in Fig. 3.1.11 (open circles), in the absence of chaperones LDH_{Bst} was completely unable to recover from thermal inactivation. Observation of the LDH_{Bst} activity over 300 minutes indicated that when denatured LDH_{Bst} was incubated in the presence of ClpB and the DnaK system, reactivation of the enzymatic activity started immediately and reached 40% of native control (Fig. 3.1.11, filled circles). These results clearly show that heat-inactivated *B.stearothermophilus* Lactate dehydrogenase could be a suitable model substrate for the DnaK-ClpB chaperone system.

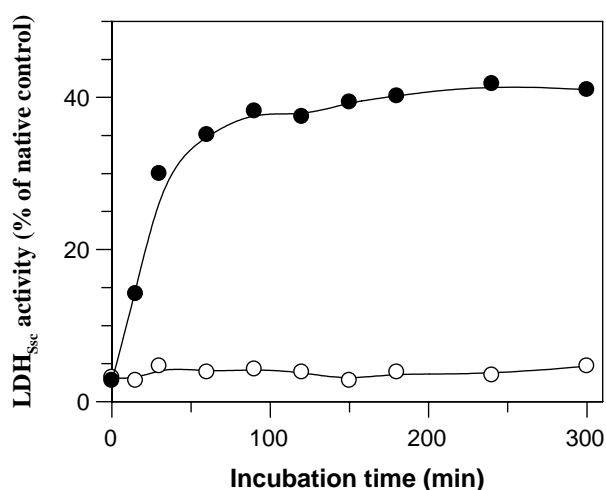


Figure 3.1.11: Refolding of heat-denatured LDH_{Bst} mediated by the DnaK_{Tth}-ClpB_{Tth} chaperone system. LDH_{Bst} (1 μM) was incubated at 80 °C for 30 minutes, leading to its inactivation and then incubated at 40 °C in reaction buffer in the absence (open circles) or presence of 3.2 μM DnaK, 0.8 μM DnaJ, 0.4 μM GrpE, 0.5 μM ClpB (filled circles). The LDH_{Bst} activity was determined at the indicated time intervals after incubation at 40 °C. The enzymatic activity of LDH_{Bst} after heat denaturation was measured with 100 nM LDH_{Bst}, 15 mM pyruvate and 0.2 mM NADH. The yield of refolding was normalized to the activity of native LDH_{Bst}.

3.2. Investigation of the Interactions between DnaK and GrpE

3.2.1. Protein Affinity Chromatography

On the basis of the crystal structure of GrpE from *E.coli* it has been proposed that structurally different regions of GrpE are responsible for two important functions of this protein in the DnaK chaperone cycle: stimulation of nucleotide exchange and release of bound substrate from DnaK. The β -sheet domain is supposed to constitute the major factor of nucleotide exchange stimulation (Brehmer et al., 2001; Harrison et al., 1997). Consistently, GrpE_{Tth} lacking the C-terminal β -sheet domain does not accelerate nucleotide exchange from DnaK_{Tth} (Groemping and Reinstein, 2001). It has been assumed that the long α -helical tail region of GrpE is responsible for interaction with the peptide binding domain of DnaK and hence stimulates release of a bound substrate from DnaK (Mally and Witt, 2001; Mehl et al., 2001).

The 3D structure of the GrpE_{Eco} was used to model a structure of GrpE_{Tth} based on a sequence similarity of 61% and an identity of 27%. Schematic representation of the domain position in GrpE_{Tth} and a ribbon image of the modelled structure of GrpE_{Tth} are shown in Fig. 3.2.1. The α -helical domain is colored in blue, the β -sheet domain is shown in red. Using a C-terminally truncated version of GrpE lacking the β -sheet domain (GrpE(Δ C)) (Fig. 3.2.1A) it is possible to investigate interactions between DnaK and GrpE without influence of the β -sheet domain.

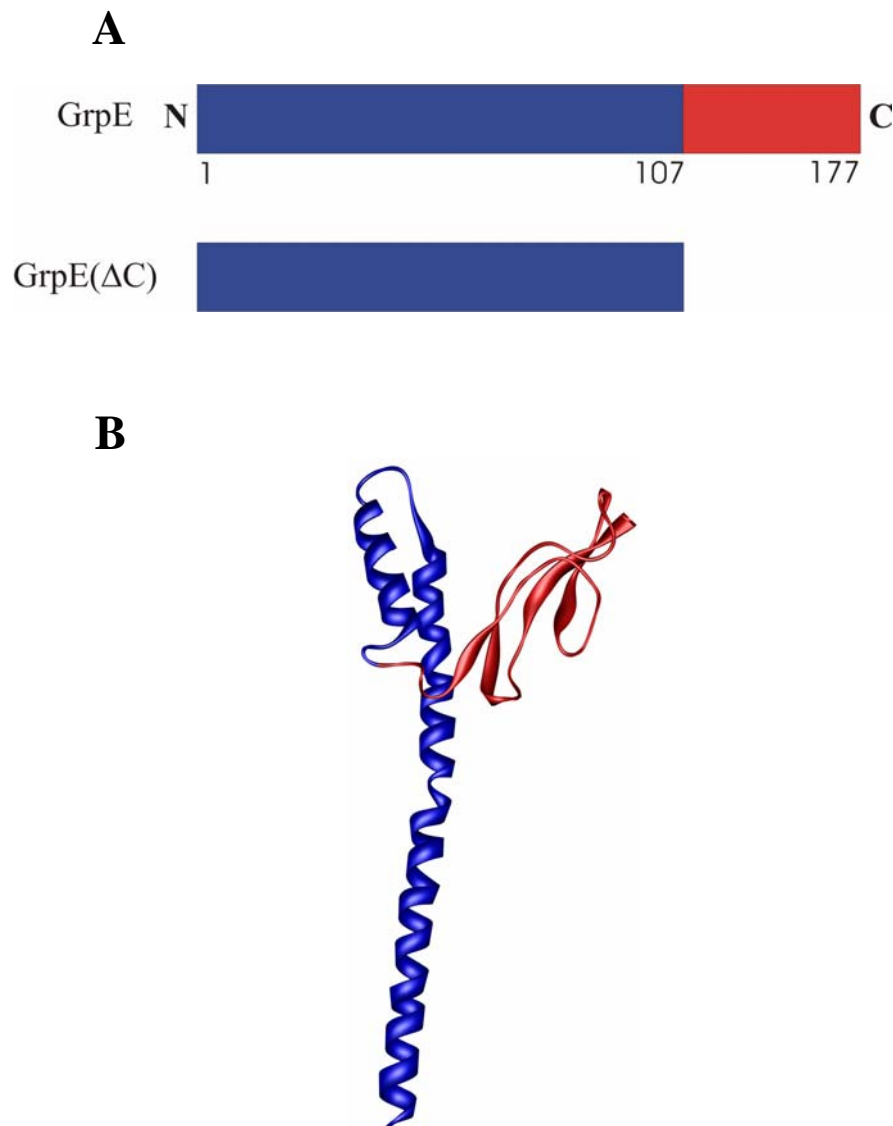


Figure 3.2.1: Structural features of GrpE from *Thermus thermophilus*. (A) Schematic representation of the domain portion of GrpE_{Tth} (upper picture) and structure of the GrpE(ΔC) mutant. Numbers refer to amino acid positions in the GrpE_{Tth} protein. (B) Ribbon representation of the modeled structure of GrpE_{Tth}. The α-helical domain is shown in blue, the β-sheet domain is shown in red. One monomer of GrpE_{Tth} was modeled by alignment to the dimeric structure of GrpE_{Eco} using SWISS-MODEL – Internet based tools for automated comparative protein modeling (Groemping and Reinstein, 2001;Peitsch, 1996).

The aim of this work was to study the interaction between GrpE (only with its α-helical domain (GrpE(ΔC)) and DnaK in the absence and presence of nucleotides, such as Mg²⁺/ADP and Mg²⁺/ATP. We employed a column containing nickel-nitrilotriacetic acid (Ni-NTA) as ligand since DnaK was engineered to contain six adjacent histidine residues at the C terminus so as to carry out qualitative analysis of interaction between DnaK_{Chis} and GrpE(ΔC) via Ni-NTA affinity chromatography. The DnaK_{Chis} protein has a selective affinity for an

immobilized chelate absorbent such as Ni^{2+} . The interaction between the His residues and the Ni^{2+} ions is reversible and the bound protein can be eluted under mild conditions with increasing amount of imidazole. The imidazole ring is part of the structure of histidine. Therefore imidazole itself can also bind to the nickel ions and disrupt the binding of histidine residues in a tagged protein. In the experiment performed, GrpE(Δ C) was not histidine tagged. Consequently, it can only be co-eluted in a complex with DnaK_{Chis}.

3.2.1.1. Interaction between GrpE(Δ C) and DnaK_{Chis} in the Absence of Nucleotides

In order to study the interaction between DnaK and GrpE(Δ C), 25 μM DnaK was incubated for 1 hour at 30 °C with 84 μM GrpE(Δ C) in wash buffer. After incubation, the mixture was loaded onto the Ni-NTA column and washed with wash buffer. Then the bound proteins were eluted with the elution buffer containing 250 mM Imidazole. The GrpE(Δ C) protein was co-eluted with DnaK_{Chis} but not with DnaK wild type (Fig. 3.2.2A, B). To confirm the interaction between DnaK_{Chis} and GrpE(Δ C), GrpE(Δ C) was loaded alone onto this column. Notably, the GrpE(Δ C) mutant was detected only in the wash fractions but not in the eluate (Fig. 3.2.2C). Hence, the C-terminally truncated GrpE does not bind non-specifically to Ni-NTA resin.

Taken together the results of the above experiments suggest that GrpE(Δ C) can directly interact with DnaK_{Chis}.

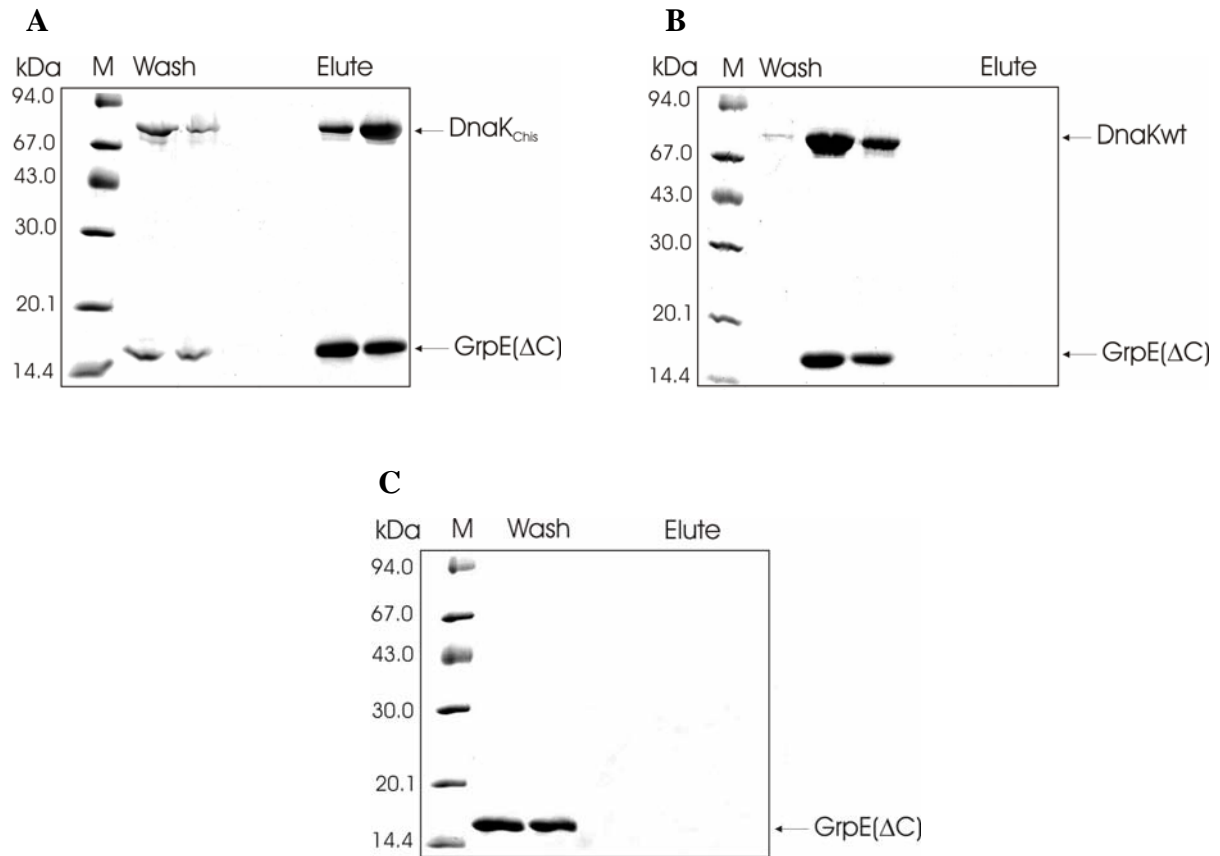


Figure 3.2.2: Interaction between DnaK_{Chis} and GrpE(ΔC) on Ni-NTA column.

(A) DnaK_{Chis} (25 μM) was incubated with GrpE(ΔC) (84 μM) at 30 °C for 1 hour in wash buffer (50 mM NaH₂PO₄, 100 mM NaCl, 5 mM MgCl₂, 10 mM β-mercaptoethanol, 10% glycerol). After that the proteins were loaded onto the Ni-NTA column, washed with wash buffer until base line recovery and eluted with the elution buffer (50 mM NaH₂PO₄, 100 mM NaCl, 5 mM MgCl₂, 10 mM β-mercaptoethanol, 10% glycerol, 250 mM Imidazole). Protein peak fractions were pooled and analysed by 15% SDS-PAGE. M-Molecular weight standard (see Materials and methods).

(B) Control 1: test for non-specific binding of GrpE(ΔC) to the Ni-NTA column in the presence of DnaK wild type (DnaK wt). DnaK wt (25 μM) was incubated with GrpE(ΔC) (84 μM) at 30 °C for 1 hour in wash buffer. After that the proteins were loaded onto the Ni-NTA column, washed with wash buffer until base line recovery and eluted with the elution buffer.

(C) Control 2: test for non-specific binding of GrpE(ΔC) to the Ni-NTA column. GrpE(ΔC) (84 μM) was loaded onto the Ni-NTA column, washed with wash buffer until base line recovery and eluted with the elution buffer.

3.2.1.2. Interaction of DnaK_{Chis} with Protein Substrate (LDH_{Ssc})

The following experiments were carried out to check whether the C-terminal peptide binding region of DnaK_{Chis} containing six adjacent histidine residues interacts with a protein substrate. Urea denatured Lactate dehydrogenase from *S.scrofa* muscle (LDH_{Ssc}) was used as a substrate protein. In addition, we also tested whether GrpE(Δ C) competes with LDH_{Ssc} for the peptide binding domain of DnaK_{Chis}. According to Qiagen kit, urea does not disturb interaction of the His tagged protein with Ni-NTA column. The enzyme LDH_{Ssc} at a concentration of 193 μ M was denatured by incubating with 3 M urea for 30 minutes at 30 °C. This denatured protein at a concentration of 100 μ M was then incubated with 5 μ M DnaK_{Chis} and 10 μ M GrpE(Δ C) for 1 hour at 30 °C followed by loading of the sample onto the Ni-NTA column, which was then washed with wash buffer until base line recovery and eluted with the elution buffer. As shown in Fig. 3.2.3A, LDH_{Ssc} co-eluted with DnaK_{Chis}, indicating the existence of a binary complex composed of DnaK_{Chis} and LDH_{Ssc}. The result of this experiment also showed that GrpE(Δ C) could be almost completely replaced by LDH_{Ssc}.

In order to test whether urea-denatured LDH_{Ssc} interferes in GrpE wild type interaction with DnaK_{Chis}, we performed the same experiment as described above but instead of the GrpE(Δ C) mutant we used GrpE wild type. It was observed that GrpE wild type interacts with DnaK_{Chis} in the presence of urea unfolded LDH_{Ssc} possibly via the β -sheet domain (Fig. 3.2.3B). The interaction of GrpE wild type with DnaK_{Chis} in the presence of the substrate (LDH_{Ssc}) was also confirmed by loading GrpE wild type alone onto the Ni-NTA column. As shown in Fig. 3.2.3C, this protein was observed only in the wash fractions, indicating that it does not unspecifically bind to Ni-NTA resin.

To analyse whether urea denatured LDH_{Ssc} exhibits non-specific binding to Ni-NTA resin, the denatured LDH_{Ssc} (100 μ M) was loaded onto the column, extensively washed with wash buffer and eluted with the elution buffer. No LDH_{Ssc} protein was present in the elution fractions, demonstrating that it does not bind non-specifically to the Ni-NTA resin (Fig. 3.2.3D). Therefore, LDH_{Ssc} detected in elution fractions together with DnaK_{Chis} is very likely due to specific complex formation. The results of this experiment clearly show that peptide binding domain of DnaK reversibly connected to the Ni-NTA column via six histidine residues is able to bind substrate. Taking into account that DnaK_{Chis} interacts with substrate

protein which is in excess but not with GrpE(Δ C) we can propose that GrpE(Δ C) and urea denatured LDH_{Ssc} bind to the same or at least overlapping sites on DnaK.

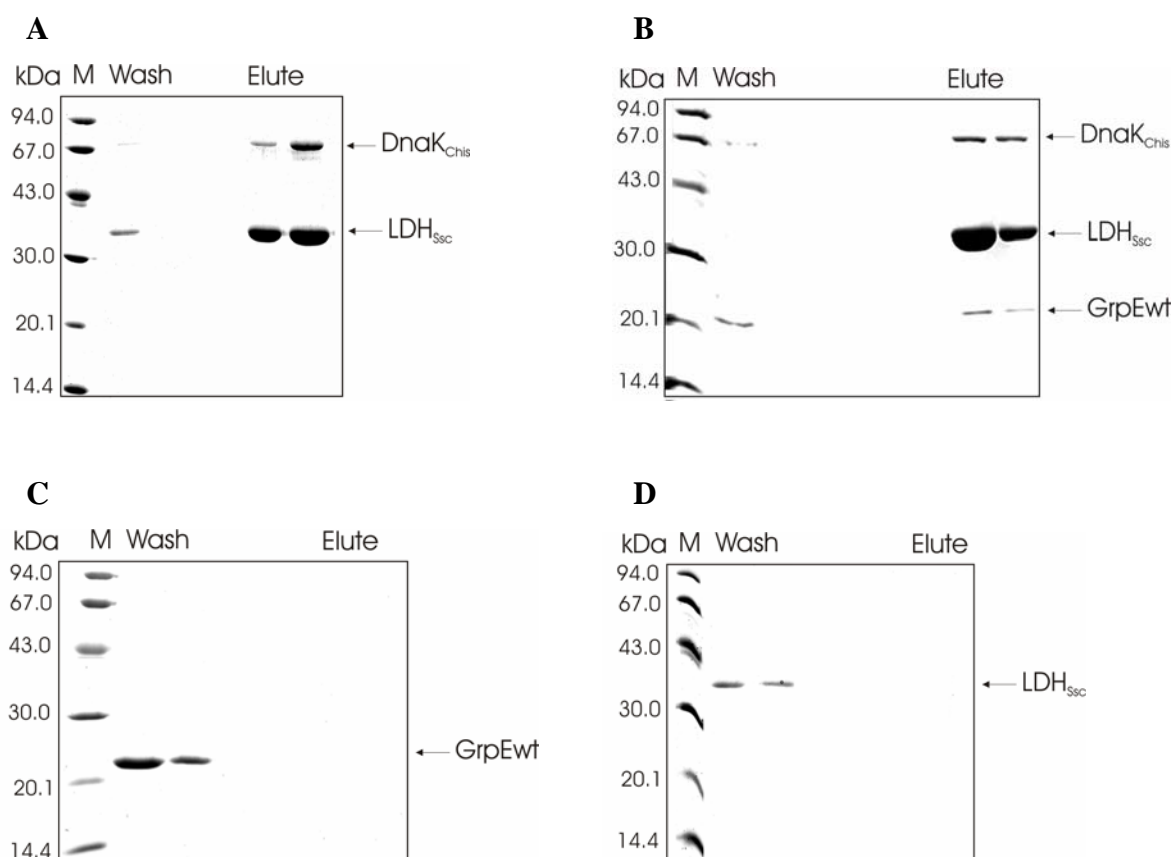


Figure 3.2.3: Binding of GrpE(Δ C) to DnaK_{Chis} in the presence of excess of Lactate dehydrogenase from *S.scrofa* muscle (LDH_{Ssc}).

(A) DnaK_{Chis} (5 μ M) was incubated with GrpE(Δ C) (10 μ M) and with urea denatured LDH_{Ssc} (100 μ M) at 30 $^{\circ}$ C for 1 hour in wash buffer (50 mM NaH₂PO₄, 100 mM NaCl, 5 mM MgCl₂, 10 mM β -mercaptoethanol, 10% glycerol). After that the proteins were loaded onto the Ni-NTA column, washed with wash buffer until base line recovery and eluted with the elution buffer (50 mM NaH₂PO₄, 100 mM NaCl, 5 mM MgCl₂, 10 mM β -mercaptoethanol, 10% glycerol, 250 mM Imidazole). Protein peak fractions were pooled and analysed by 15% SDS-PAGE. M-molecular weight standard (see Materials and Methods).

(B) Control 1: test for interaction between GrpE wild type and DnaK_{Chis} in the presence of excess of urea denatured LDH_{Ssc}. The experiment was performed as described in (A) but instead of GrpE(Δ C) we used GrpE wild type.

(C) Control 2: test for non-specific binding of GrpE wild type (GrpE wt) to the Ni-NTA column. GrpE wt (84 μ M) was loaded onto the Ni-NTA column, washed with wash buffer until base line recovery and eluted with the elution buffer.

(D) Control 3: test for non-specific binding of urea denatured LDH_{Ssc} to the Ni-NTA column. LDH_{Ssc} (100 μ M) was loaded onto the Ni-NTA column, washed with wash buffer until base line recovery and eluted with the

elution buffer.

3.2.1.3. Effect of Mg^{2+} /ADP and Mg^{2+} /ATP on the GrpE(Δ C)-DnaK_{Chis} Interactions

Using Ni-NTA columns we investigated whether Mg^{2+} /ADP affects the ability of GrpE(Δ C) to interact with DnaK_{Chis}. To this experiment similar conditions were applied as prior but in addition, both wash buffer and elution buffer contained 1 mM Mg^{2+} /ADP. It was observed that GrpE(Δ C) co-eluted with DnaK_{Chis}, demonstrating that a GrpE(Δ C)-DnaK_{Chis} complex is very likely to be formed (Fig. 3.2.4A). Neither in the presence of DnaK wild type nor in the absence of His-tagged DnaK, the GrpE(Δ C) protein was detected in the elution fractions (Fig. 3.2.4B, C).

In order to test the ability of the β -sheet domain of GrpE to interact with DnaK in the presence of Mg^{2+} /ADP, we blocked binding of the α -helical domain of GrpE wild type to DnaK_{Chis} by adding an excess of urea denatured LDH_{Ssc}. In this experiment, we detected GrpE wild type in the elution fractions together with DnaK_{Chis} and LDH_{Ssc}, indicating that interaction between DnaK and GrpE in the presence of ADP occurs not only via the α -helical domain of GrpE but also the β -sheet domain is involved in the interaction (Fig. 3.2.4D).

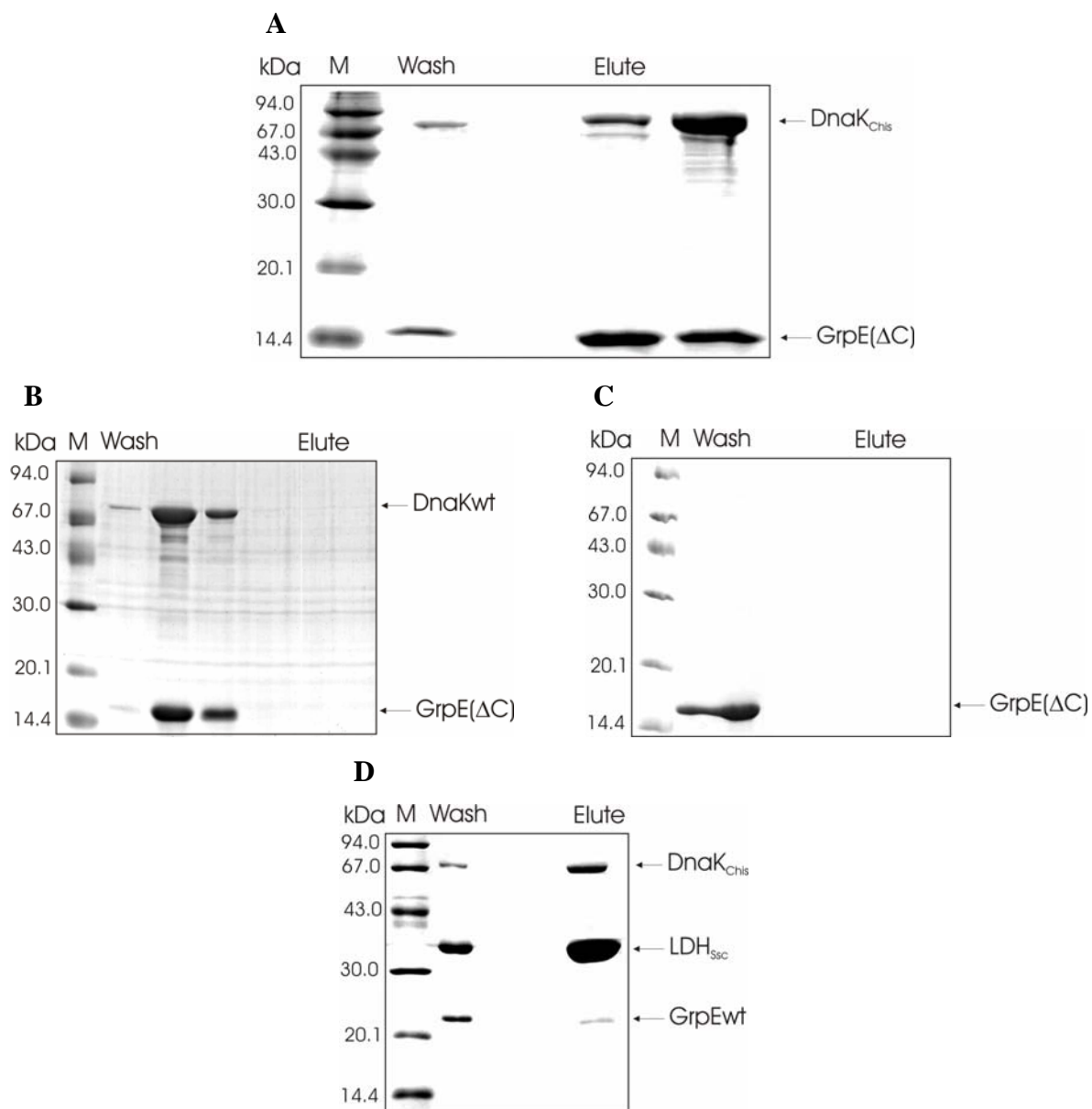


Figure 3.2.4: Interaction between DnaK_{Chis} and GrpE(ΔC) in the presence of Mg²⁺/ADP on Ni-NTA column.

(A) DnaK_{Chis} (25 μM) was incubated with GrpE(ΔC) (84 μM) at 30 °C for 1 hour in wash buffer (50 mM NaH₂PO₄, 100 mM NaCl, 5 mM MgCl₂, 10 mM β-mercaptoethanol, 10% glycerol, 1 mM Mg²⁺/ADP). After that the proteins were loaded onto the Ni-NTA column, washed with wash buffer until base line recovery and eluted with the elution buffer (50 mM NaH₂PO₄, 100 mM NaCl, 5 mM MgCl₂, 10 mM β-mercaptoethanol, 10% glycerol, 250 mM Imidazole, 1 mM Mg²⁺/ADP). Protein peak fractions were pooled and analysed by 15% SDS-PAGE. M-molecular weight standard (see Materials and Methods). (B) Control 1: test for non-specific binding of GrpE(ΔC) to the Ni-NTA column in the presence of DnaK wild type (DnaK_{wt}). DnaK wt (25 μM) was incubated with GrpE(ΔC) (84 μM) at 30 °C for 1 hour in wash buffer. After that the proteins were loaded onto the Ni-NTA column, washed with wash buffer until base line recovery and eluted with the elution buffer. (C) Control 2: test for non-specific binding of GrpE(ΔC) to the Ni-NTA column in the presence of Mg²⁺/ADP. GrpE(ΔC) (84 μM) was loaded onto the Ni-NTA column, washed with wash buffer until base line recovery and eluted with the elution buffer. (D) Control 3: test for interaction between GrpE wild type and DnaK_{Chis} in the presence of Mg²⁺/ADP and excess of urea denatured LDH_{Ssc}. The experiment was performed as described in Figure 3.2.3A but instead of GrpE(ΔC) we used GrpE wild type.

To determine whether GrpE(Δ C) forms a complex with DnaK_{Chis} in the presence of Mg²⁺/ATP, we incubated 25 μ M DnaK_{Chis} together with 84 μ M GrpE(Δ C) in wash buffer for 1 hour at 30 °C. Both wash buffer and elution buffer contained 1 mM Mg²⁺/ATP. GrpE(Δ C) was detected only in the wash fractions, but not in the imidazole elution samples, demonstrating that the DnaK_{Chis}-GrpE(Δ C) complex is very likely not formed (Fig. 3.2.5). This experiment together with the previous studies of the GrpE(Δ C)-DnaK_{Chis} interactions in the absence of any nucleotides and in the presence of Mg²⁺/ADP shows that GrpE helix binding is coupled to ADP/ATP state of DnaK.

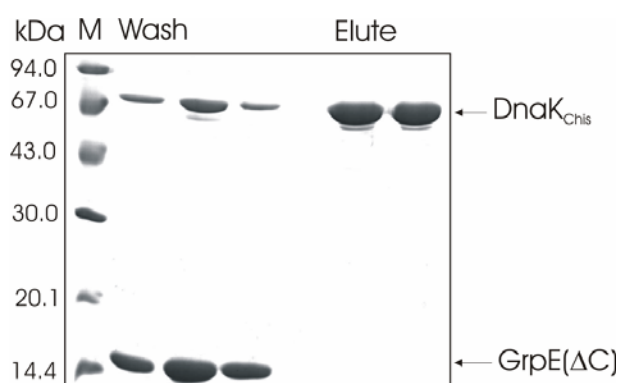


Figure 3.2.5: Effect of Mg²⁺/ATP on the interaction between DnaK_{Chis} and GrpE(Δ C) on Ni-NTA column.

DnaK_{Chis} (25 μ M) was incubated with GrpE(Δ C) (84 μ M) at 30 °C for 1 hour in wash buffer (50 mM NaH₂PO₄, 100 mM NaCl, 5 mM MgCl₂, 10 mM β -mercaptoethanol, 10% glycerol, 1 mM Mg²⁺/ATP). After that the proteins were loaded onto the Ni-NTA column, washed with wash buffer until base line recovery and eluted with the elution buffer (50 mM NaH₂PO₄, 100 mM NaCl, 5 mM MgCl₂, 10 mM β -mercaptoethanol, 10% glycerol, 250 mM Imidazole, 1 mM Mg²⁺/ATP). Protein peak fractions were pooled and analysed by 15% SDS-PAGE. M-molecular weight standard (see Materials and Methods).

The above experimental results indicating that GrpE(Δ C) does not interact with DnaK in the presence of ATP were confirmed by performing co-elution experiments and using the ability of DnaK wild type to bind to C8-coupled ATP-agarose. The first lane shown in Fig. 3.2.6, indicates single DnaK bound to the ATP-agarose. We did not observe non-specific interaction of GrpE wild type with ATP-agarose (Fig. 3.2.6, lane 2). However, when DnaK was coupled to the ATP-agarose and incubated with GrpE wild type, GrpE wild type co-eluted with DnaK due to complex formation (Fig. 3.2.6, lane 4). Notably, co-elution did not occur when DnaK was incubated with GrpE(Δ C) (Fig. 3.2.6, lane 3). This agrees with results from experiments with Ni-NTA columns and indicates that in the presence of Mg²⁺/ATP the complex between

GrpE(Δ C) and DnaK_{Chis} does not form. It is possible to propose that ATP bound to the ATPase domain of DnaK influences the interaction of GrpE and DnaK in such a way that the α -helical domain of GrpE does not bind to DnaK. However, the observed complex between GrpE wild type and DnaK wild type in co-elution experiment with C8-coupled ATP-agarose suggests that the GrpE protein does not lose contact with DnaK completely in the presence of ATP but still interacts via the β -sheet domain.

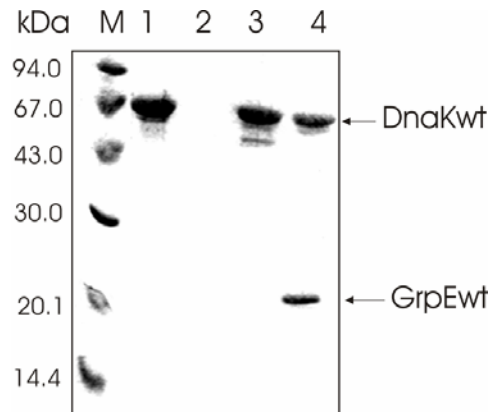


Figure 3.2.6: Co-elution of GrpE wild type with DnaK immobilized on ATP-agarose. DnaK (100 μ M) was immobilized on C8-coupled ATP-agarose and incubated in agarose buffer alone (lane 1), with 400 μ M GrpE(Δ C) (lane 3), with 400 μ M GrpE wild type (lane 4) as described in Materials and Methods. The lane 2 corresponds to control for non-specific binding of GrpE wild type with the ATP-agarose. After intensive washing chaperones were eluted with 5 mM Mg^{2+} /ATP and aliquots representing 10% of eluates were resolved by 15% SDS-PAGE. M-molecular weight standard (see Materials and Methods).

3.2.2. Differential Scanning Calorimetry

Previous experiments using Ni-NTA columns showed that GrpE(Δ C) binds to the C-terminally His-tagged DnaK in the absence and presence of Mg^{2+} /ADP at room temperature. The objective of the present study was to identify interactions between these proteins through studies of the behavior of their thermally induced denaturation. Differential scanning calorimetry is a direct method to measure the thermal unfolding of proteins interacting with each other. This approach reveals the structural changes that occur in the proteins as a result of their interaction. Protein-protein interactions studied by differential scanning calorimetry were observed on a number of protein complexes, such as barstar-barnase and myosin subfragment 1-F-actin (Makarov et al., 1994; Martinez et al., 1995; Nikolaeva et al., 1996).

3.2.2.1. Thermal Stability of DnaK and GrpE(Δ C)

Complex formation is often associated with an increase in thermal stability of the complex compared to its constituents. Therefore it was essential to know the temperature dependence of the unfolding enthalpies of the individual reacting species.

Fig. 3.2.7 shows the DSC scan of DnaK. This thermogram was recorded in DSC buffer (20 mM HEPES/NaOH (pH 7.5), 100 mM KCl, 5 mM $MgCl_2$), a protein concentration of 40 μ M and a scan rate of 60 deg. C/hour. Under these conditions the denaturation curve of DnaK exhibits a sharp intense endothermic peak with a T_m of 94.6 °C. The thermogram shows a negative slope with the exothermic peak at 120 °C. These features are known to result from aggregation of denatured protein and/or from secondary exothermic chemical reactions caused by high temperatures such as cystine destruction, thiol-catalysed disulfide interchange, oxidation of cysteine residues, deamidation of asparagine and glutamine residues, and hydrolysis of peptide bonds at aspartic acid residues (Volkin et al., 1997; Volkin and Klibanov, 1987; Volkin and Klibanov, 1992). Aggregation usually causes distortion of the

DSC curve, with noisy traces at higher temperatures due to convection of clumpy aggregates in the DSC cell. Such aggregation is difficult to control or predict. It is a kinetic phenomenon, likely to be dependent on protein concentrations, DSC scan rates, etc. The distortion of the DSC peak leads to lower values for the apparent T_m and lower values for ΔH_{cal} . For this reason the thermogram detected after the first scan of DnaK could not be used for calculation of absolute values for the calorimetric enthalpy (ΔH_{cal}).

To test reversibility of thermal denaturation of DnaK, the sample in the calorimetric cell was cooled down to the initial temperature after first heating to 130 °C and rescanned to 130 °C (Fig. 3.2.7, dotted line). It was detected that the position of the T_m of the thermal denaturation (94.3 °C) was recovered during the second scan. This peak corresponds to the thermal denaturation of the native DnaK protein. However, the reversibility of DnaK after heating to 130 °C was extremely low. The obtained calorimetric data indicate that after thermally induced denaturation of DnaK, only a negligible amount of protein was able to renature.

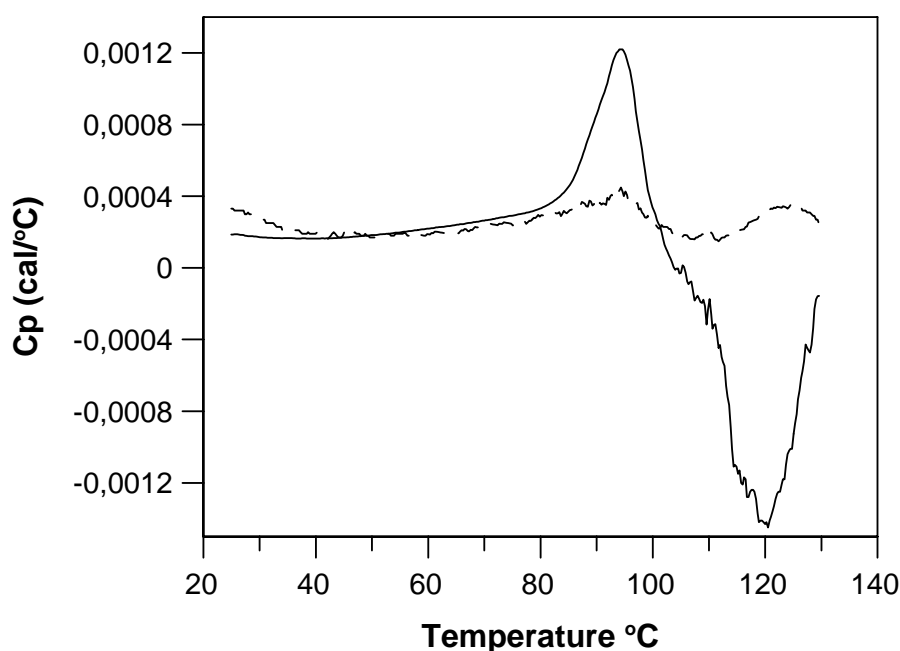


Figure 3.2.7: DSC scans of DnaK. The DnaK (40 μ M) thermogram was obtained in DSC buffer (20 mM Hepes/NaOH pH 7.5, 100 mM KCl, 5 mM $MgCl_2$) (*straight line*). After cooling to 20 °C the same sample was reheated to 130 °C (*dotted line*).

The thermal unfolding of GrpE(Δ C), the second component of the DnaK-GrpE(Δ C) complex, was studied using the same calorimetric approach. The thermogram in Fig. 3.2.8 illustrates the thermal denaturation of GrpE(Δ C) that exhibits a denaturation curve with a T_m at 93.5 °C. The calorimetric reversibility of the thermally induced transition was checked by reheating the protein solution in the calorimetric cell after cooling from the first run. The position of maximum of the peak after second heating was detected at 90.5 °C. The observed shift in T_m towards lower temperatures reflects a reduced thermostability of GrpE(Δ C) after heating to 130 °C.

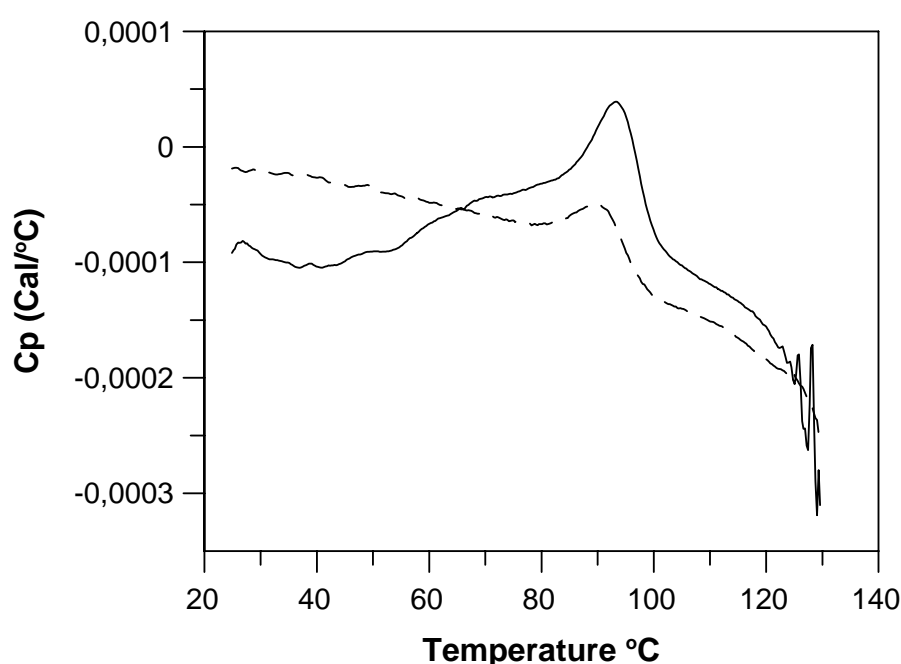


Figure 3.2.8: DSC scans of GrpE(Δ C). The GrpE(Δ C) (80 μ M) thermogram was obtained in DSC buffer (20 mM Hepes/NaOH pH 7.5, 100 mM KCl, 5 mM MgCl₂) (*straight line*). After cooling to 20 °C the same sample was reheated to 130 °C (*dotted line*).

3.2.2.2. Study of the Interactions between DnaK and GrpE(Δ C)

Taking into account the calorimetric data obtained from the study of the individual DnaK and GrpE(Δ C) we started to investigate complex formation between these two proteins. Fig. 3.2.9A (red line) shows the thermal stability of the DnaK and GrpE(Δ C) mixture in DSC buffer. The calorimetric curve demonstrates one peak with a maximum at 94.6 °C. The steep negative slope which was reproducibly observed from 20 to 80 degree centigrades where the mixture was heated can be explained as a result of dissociation of the DnaK-GrpE(Δ C)

complex. The thermogram shows a sharp exothermic peak with maximum at 104 °C. This means that heating was accompanied by energy release, which is likely due to aggregation and precipitation of unfolded proteins. On the basis of the thermograms of the individual DnaK and GrpE(Δ C) and a sample containing both proteins, it is evident that the thermal transition of the mixture corresponds to the thermal denaturation of DnaK alone (Fig.3.2.9A, red line and black line). To find out whether DnaK interacts with GrpE(Δ C) by forming a stable complex, the thermogram calculated as a sum of DnaK and GrpE(Δ C) denaturation curves was compared with the experimentally obtained thermogram. If proteins do not interact with each other, both curves should be identical. It is obvious from Fig. 3.2.9B that the calculated curve (dark yellow line) is similar to the experimentally detected one (red line). This leads to the conclusion that the DSC method is not suitable to detect complex formation of DnaK with GrpE(Δ C). One possible explanation could be the complex might be stable at low temperatures only but not at high temperatures which could disrupt the potentially weak interactions, leaving the proteins to denature as individual components.

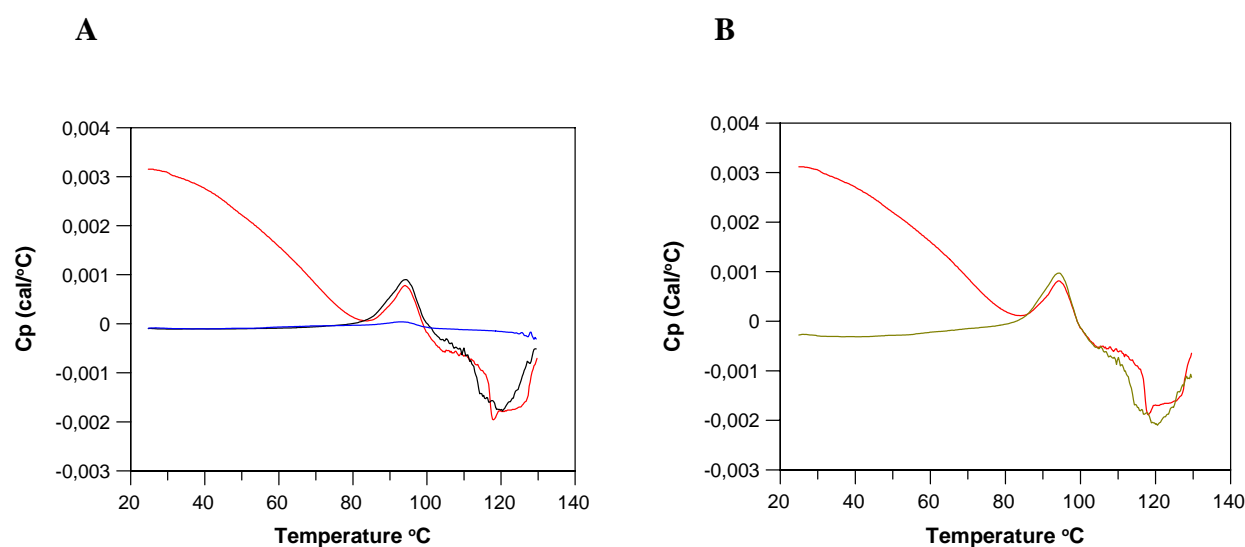


Figure 3.2.9: Study of the interactions between DnaK and GrpE(Δ C) by DSC. (A) Thermogram of DnaK, GrpE(Δ C) and a sample containing both DnaK and GrpE(Δ C). Thermal denaturation of DnaK (40 μ M) (*black line*), GrpE(Δ C) (80 μ M) (*blue line*) and the sample containing both DnaK (40 μ M) and GrpE(Δ C) (80 μ M) (*red line*) was performed under the same buffer conditions (20 mM Hepes/NaOH pH 7.5, 100 mM KCl, 5 mM MgCl₂). The unfolding of proteins was performed at a scan rate 60 deg. C/hour from 20 to 130 °C. (B) Comparison of the theoretical and practical heat capacity curves of the DnaK-GrpE(Δ C) mixture. The red line represents the thermogram of the DnaK-GrpE(Δ C) mixture experimentally obtained as described in (A). The dark yellow line corresponds to a thermal curve calculated as a sum of thermograms of the individual DnaK and GrpE(Δ C) proteins.

3.2.2.3. Influence of Mg^{2+}/ADP on the Thermal Stability of DnaK, GrpE(ΔC) and DnaK-GrpE(ΔC) complex

Previous experiments using Ni-NTA columns showed that in the presence of Mg^{2+}/ADP (but not Mg^{2+}/ATP) GrpE(ΔC) binds to a C-terminally His-tagged DnaK at room temperature. To identify the interaction between DnaK and GrpE(ΔC) in the presence of Mg^{2+}/ADP through studies of their melting behaviour, differential scanning calorimetry measurements had been performed. To determine a possible complex formation in the presence of Mg^{2+}/ADP , the process of thermal induced denaturation of the individual DnaK and GrpE(ΔC) proteins was examined first.

To determine the thermal stability 40 μM DnaK was incubated in DSC buffer with 1 mM Mg^{2+}/ADP in the calorimetric cell at 20 °C for 30 minutes followed by heating from 20 to 130 °C. Fig. 3.2.10 (straight line) shows the DSC scan of DnaK in the presence of Mg^{2+}/ADP . The calorimetric curve contains one endothermic peak with a maximum at 101 °C. Above 104°C a negative slope of the postdenaturation baseline arises, which is likely to be due to aggregation and precipitation of unfolded DnaK. The reversibility of thermal transition after heating to 130 °C was checked by examining the reproducibility of the thermal transition in the second heating of the same sample immediately after fast cooling from the first run. We observed that DnaK in the presence of Mg^{2+}/ADP underwent a partially reversible denaturation after heating to 130 °C (Fig. 3.2.10, dotted line). A 7 °C shift in the transition maximum towards lower temperatures produced by second run can be detected. This finding shows that the fraction of DnaK which is able to renature after cooling from 130 to 20 °C exhibits less thermostability.

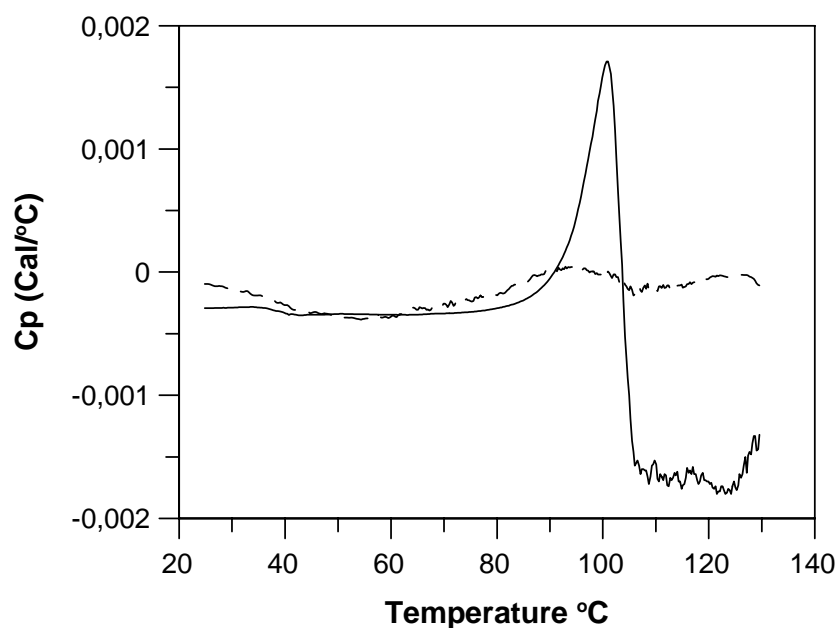


Figure 3.2.10: DSC scans of DnaK in the presence of Mg^{2+}/ADP . The thermogram of 40 μM DnaK was obtained in DSC buffer (20 mM Hepes/NaOH pH 7.5, 100 mM KCl, 5 mM $MgCl_2$, 1 mM Mg^{2+}/ADP) (*straight line*). After cooling to 20 $^{\circ}C$ the same sample was reheated to 130 $^{\circ}C$ (*dotted line*).

To analyse the thermal denaturation of GrpE(ΔC) in the presence of Mg^{2+}/ADP , this protein was heated in DSC buffer containing Mg^{2+}/ADP . The thermogram in Figure 3.2.11 (straight line) illustrates the denaturation of 80 μM GrpE(ΔC) in the presence of 1 mM Mg^{2+}/ADP that exhibits a single thermal transition with maximum at 94.3 $^{\circ}C$. Rescanning the sample after heating to 130 $^{\circ}C$ showed that heat denaturation of GrpE(ΔC) was partially reversible (Fig. 3.2.11, dotted line). Two repetitive scans of the same protein sample also show a difference in the position of the peak maximum (93.5 $^{\circ}C$ for the first scan and 90.6 $^{\circ}C$ for the second scan). This observation indicates that GrpE(ΔC) was less thermostable after heating to 130 $^{\circ}C$.

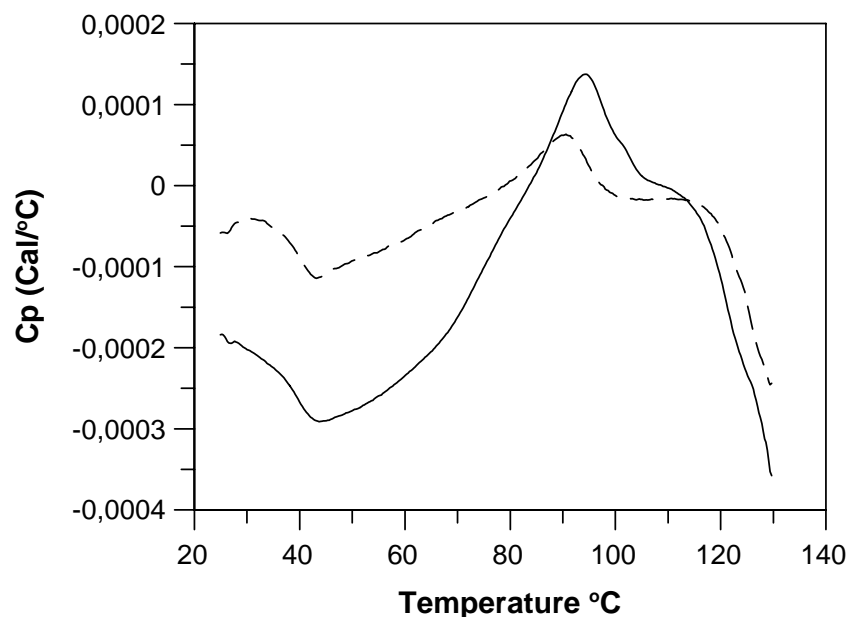


Figure 3.2.11: Thermal transition of GrpE(Δ C) in the presence of Mg^{2+} /ADP. The thermogram of 80 μ M GrpE(Δ C) was obtained in DSC buffer (20 mM HEPES/NaOH pH 7.5, 100 mM KCl, 5 mM $MgCl_2$, 1 mM Mg^{2+} /ADP) (*straight line*). DSC scan of second heating is shown by *dotted line*.

To evaluate an influence of Mg^{2+} /ADP on the thermal denaturation of DnaK and GrpE(Δ C), thermograms of these proteins obtained in the absence and in the presence of the nucleotide were compared.

As shown in Fig. 3.2.12A, the difference in the position of T_m after heat denaturation of GrpE(Δ C) in the presence and absence of Mg^{2+} /ADP is negligible and corresponds to about 0.8 $^{\circ}C$ that could be within the error limits. These data are in good agreement with previously published experiments showing that GrpE does not interact with nucleotides (Reid and Fink, 1996). The nucleotide exchange factor GrpE facilitates the exchange of DnaK-bound ADP for ATP and binds directly to DnaK (Harrison et al., 1997). It was observed that Mg^{2+} /ADP significantly increases the thermal stability of DnaK by shifting the maximum of its thermal transition by about 6.4 $^{\circ}C$ to higher temperatures, from 94.6 $^{\circ}C$ to 101.0 $^{\circ}C$ (Fig. 3.2.12B). The observed stabilization with Mg^{2+} /ADP reflects the nucleotide binding capacity of DnaK.

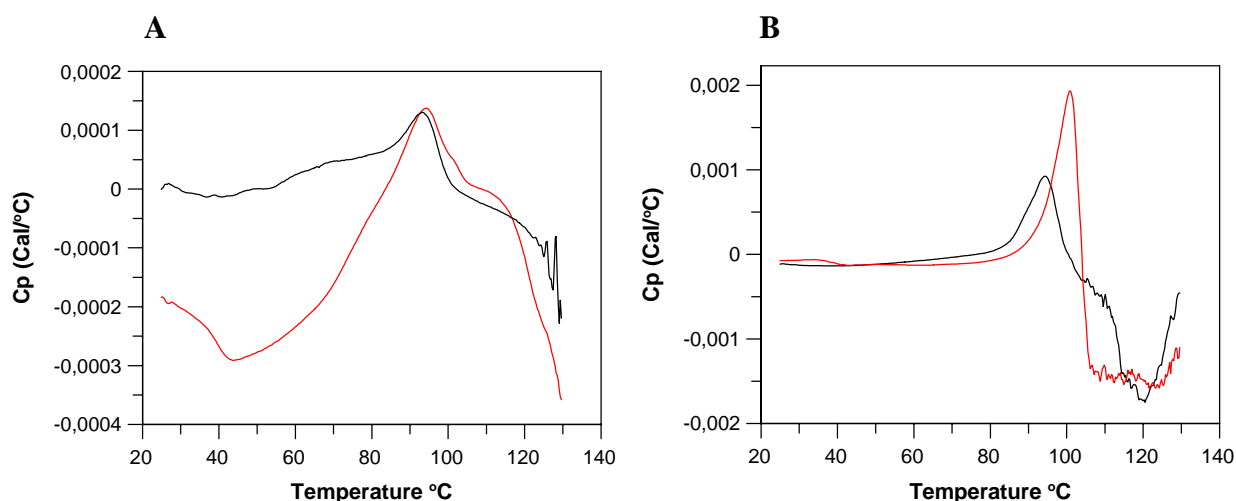


Figure 3.2.12: Thermal stability of GrpE(Δ C) and DnaK in the absence and presence of Mg^{2+} /ADP. Thermograms of 80 μ M GrpE(Δ C) (**A**) and 40 μ M DnaK (**B**) were obtained in DSC buffer (20 mM Hepes/NaOH pH 7.5, 100 mM KCl, 5 mM $MgCl_2$) in the absence (*black line*) and presence of 1 mM Mg^{2+} /ADP (*red line*).

To study whether the complex of DnaK and GrpE(Δ C) is formed in the presence of Mg^{2+} /ADP, both proteins were heated at the same conditions in DSC buffer containing 1 mM Mg^{2+} /ADP. The observed T_m of the sample containing DnaK (40 μ M) and GrpE(Δ C) (80 μ M) at 100.6 $^{\circ}$ C was comparable with the maximum thermal transition of DnaK (40 μ M) denatured alone (101.0 $^{\circ}$ C), suggesting that interaction between these proteins was not detected (Fig. 3.2.13A). In addition, to check whether protein-protein interactions exist, we summarized scans of individual proteins and compared practical and theoretical heat denaturation curves. The data presented in Fig. 3.2.13B show that the DSC profile of the sample containing both DnaK and GrpE(Δ C) has almost the same shape as the calculated curve for the individual proteins.

Taken together, the experimentally obtained data and calculated summed curve of the individual proteins give rise to assume that in the presence of Mg^{2+} /ADP interactions between DnaK and GrpE(Δ C) could not be detected by the changes in denaturation profiles.

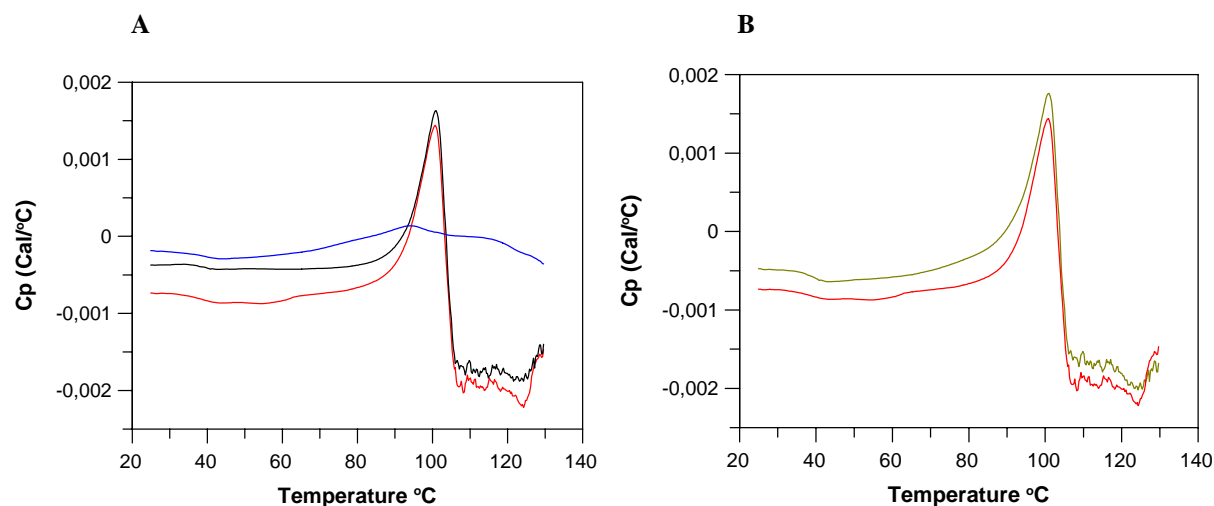


Figure 3.2.13: Study of the interactions between DnaK and GrpE(Δ C) in the presence of Mg^{2+} /ADP by DSC. (A) Thermogram of DnaK, GrpE(Δ C) and a sample containing both DnaK and GrpE(Δ C). DnaK (40 μ M) (black line), GrpE (80 μ M) (blue line) and the sample containing both DnaK (40 μ M) and GrpE (80 μ M) (red line) were scanned under the same buffer conditions (20 mM Hepes/NaOH pH 7.5, 100 mM KCl, 5 mM $MgCl_2$, 1 mM Mg^{2+} /ADP). The unfolding of proteins was performed at a scan rate 60 deg. C/hour from 20 to 130 °C. **(B)** Comparison of the theoretical and practical heat capacity curves of the DnaK-GrpE(Δ C) mixture. The red line represents the thermogram of the DnaK-GrpE(Δ C) mixture experimentally obtained as described in (A). The dark yellow line corresponds to a thermal curve calculated as a sum of thermograms of the individual DnaK and GrpE(Δ C) proteins.

3.2.2.4. Temperature Dependence of the DnaK-GrpE(Δ C) Interactions

In order to verify whether the DnaK-GrpE(Δ C) interactions are temperature sensitive, an additional experiment with Ni-NTA columns had been performed. The C-terminally His-tagged DnaK (DnaK_{Chis}) used in this experiment is able to reversibly interact with the Ni^{2+} ions. The bound DnaK_{Chis} can be eluted under mild conditions with increasing amount of imidazole. The GrpE(Δ C) protein was not histidine tagged. Consequently, it can only be co-eluted in a complex with DnaK_{Chis}.

To detect the influence of temperature on binding of GrpE(Δ C) with DnaK_{Chis}, these proteins were incubated in wash buffer at 30, 55 and 70 °C for 1 hour. Then the proteins were loaded onto the Ni-NTA column. After intensive washing of the column until baseline recovery the

bound proteins were eluted with the elution buffer containing 250 mM imidazole. DnaK_{Chis} and GrpE(Δ C), found in elution fractions after incubation at 30 and 55 °C, suggest that these proteins interact at 30 °C and 55 °C (Fig. 3.2.14A, B). Fig. 3.2.14C demonstrates that after incubation of the DnaK_{Chis}-GrpE(Δ C) mixture at 70 °C the GrpE(Δ C) mutant was detected only in wash fractions. This finding shows that a temperature of 70 °C very likely causes dissociation of the DnaK_{Chis}-GrpE(Δ C) complex or prevents its formation, respectively. Therefore the DnaK-GrpE(Δ C) interactions are indeed temperature sensitive and the DSC method is not suitable to detect complex formation between these proteins.

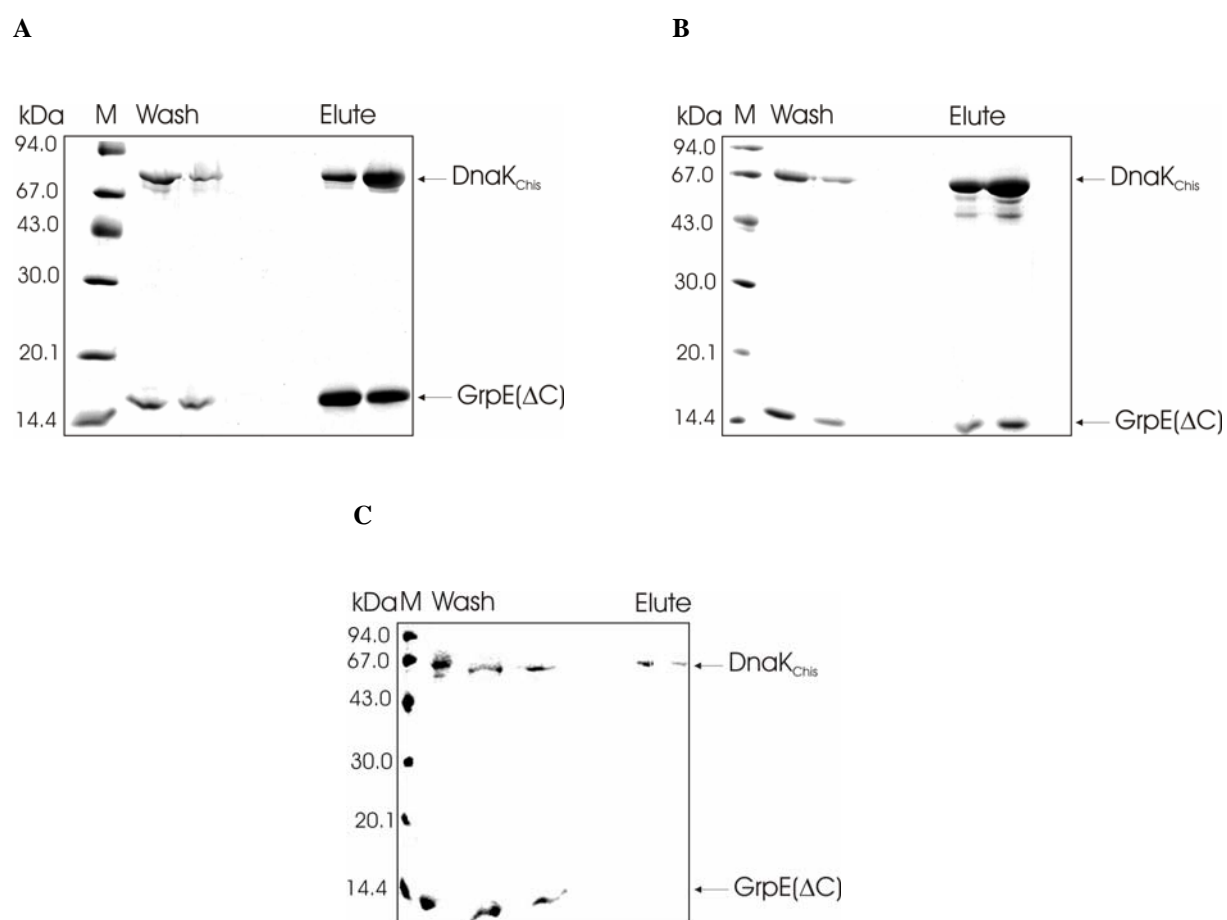


Figure 3.2.14: Interaction of GrpE(Δ C) with DnaK_{Chis} at different temperatures. DnaK_{Chis} (25 μ M) was incubated with GrpE(Δ C) (84 μ M) at (A) 30, (B) 55 and (C) 70 °C for 1 hour in wash buffer (50 mM NaH₂PO₄, 100 mM NaCl, 5 mM MgCl₂, 10 mM β -mercaptoethanol, 10% glycerol). After that the proteins were loaded onto the Ni-NTA column, washed with wash buffer until base line recovery and then eluted with the elution buffer (50 mM NaH₂PO₄, 100 mM NaCl, 5 mM MgCl₂, 10 mM β -mercaptoethanol, 10% glycerol, 250 mM Imidazole). Protein peak fractions were pooled and analysed by 15% SDS-PAGE. M-molecular weight standard (see Materials and Methods).

To verify whether GrpE(Δ C) binds unspecifically to the Ni-NTA resin after incubation at 30 and 55 °C, the protein was incubated at these temperatures for 1 hour and then loaded onto the Ni-NTA column. The GrpE(Δ C) protein detected only in wash fractions shows that it does not bind unspecifically to the Ni-NTA column after incubation at 30 and 55 °C (Fig. 3.2.15A, B). Therefore the detected co-elution of GrpE(Δ C) with DnaK_{Chis} in previous experiments could be explained by complex formation between them.

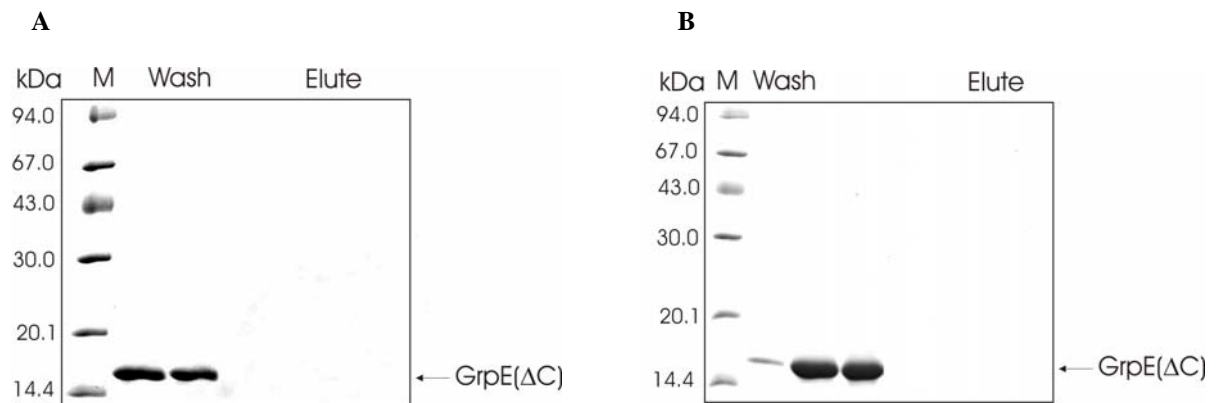


Figure 3.2.15: Test for non-specific binding of GrpE(Δ C) to the Ni-NTA column. GrpE(Δ C) (84 μ M) was incubated in wash buffer (50 mM NaH₂PO₄, 100 mM NaCl, 5 mM MgCl₂, 10 mM β -mercaptoethanol, 10% glycerol) for 1 hour at 30 °C (A) and 55 °C (B). Then proteins were loaded onto the Ni-NTA column, washed with wash buffer until base line recovery and then eluted with the elution buffer (50 mM NaH₂PO₄, 100 mM NaCl, 5 mM MgCl₂, 10 mM β -mercaptoethanol, 10% glycerol, 250 mM imidazole). Protein peak fractions were pooled and analyzed by 15% SDS-PAGE. M-molecular weight standard (see Materials and Methods).

3.2.3. Fluorescence Spectroscopy

3.2.3.1. Site specific DnaK-GrpE Interactions

In spite of the well documented fact that the C-terminal part of GrpE including the β -sheet domain binds to the ATPase domain of DnaK and stimulates nucleotide release the specific location where the GrpE's N-terminal tail part interacts with DnaK's substrate binding domain is still unknown. Based on the crystal structure of GrpE_{Eco} in a complex with the ATPase domain of DnaK_{Eco} it has been proposed that GrpE_{Eco} might interact with the peptide binding domain of DnaK_{Eco} (Harrison et al., 1997). The hypothesis that the flexible GrpE_{Eco} N-terminal region including residues 1-33 is involved in interaction with the peptide binding domain of DnaK was supported by surface resonance measurements (Chesnokova et al., 2003). In addition, using radioactively labeled carboxymethylated α -lactalbumin, a permanently unfolded model substrate of DnaK, it was observed that the flexible tail region of GrpE_{Eco} including residues 1 to 33 is necessary for dissociation of a complex between DnaK_{Eco} and substrate (Harrison et al., 1997).

In this work we performed equilibrium fluorescence measurements to yield qualitative information about the site specific interactions between DnaK and the N-terminal part of GrpE. Fluorescence changes are critically dependent on the location of the fluorophore which has to be positioned in a region where the microenvironment changes with formation of the complex. The fluorophore should therefore be placed either in the protein-protein interface itself, or in a region that undergoes a local conformational change upon complex formation. Wild type GrpE_{Th} contains no cysteine residues. Site-directed mutagenesis was used to engineer two GrpE mutants with incorporated a cysteine residue at position 5 (N5→C) and 17 (V17→C). Cysteine residues were then available for modification with an IANBD amide probe molecule. Sites of labeling were chosen according to number of predictions that the N-terminal part of GrpE including residues 1-33 is involved in substrate release from DnaK (Harrison et al., 1997; Mally and Witt, 2001; Mehl et al., 2001). IANBD amide has the advantage of having a small molecular weight (419.18 Da) and strong fluorescence signal. The fluorescence of this dye is highly sensitive to changes in the solvation level of the fluorophore. The strong environmental dependence of the emission spectra and quantum

yields of IANBD makes this probe useful for investigation protein interactions. When a protein conjugate with this dye undergoes a change in conformation, a change in fluorescence intensity and a blue or red shift in emission is often observed (Shore et al., 1995).

To evaluate whether the biological activity of the GrpE cysteine mutants corresponds to biological activity of GrpE wild type, the reactivation of urea denatured Lactate dehydrogenase from *S.scrofa* muscle (LDH_{Ssc}) assisted by the DnaK system was investigated. The DnaK system includes DnaK, DnaJ and GrpE proteins. The results presented in Fig. 3.2.16 show that the yield of refolding of the denatured LDH_{Ssc} in the presence of DnaK, DnaJ and GrpE wild type is comparable to that obtained with DnaK, DnaJ and the GrpE cysteine mutants, GrpE(N5C) and GrpE(V17C). These findings indicate that substitution of both asparagine and valine residues to cysteine does not influence significantly on biological activity of GrpE.

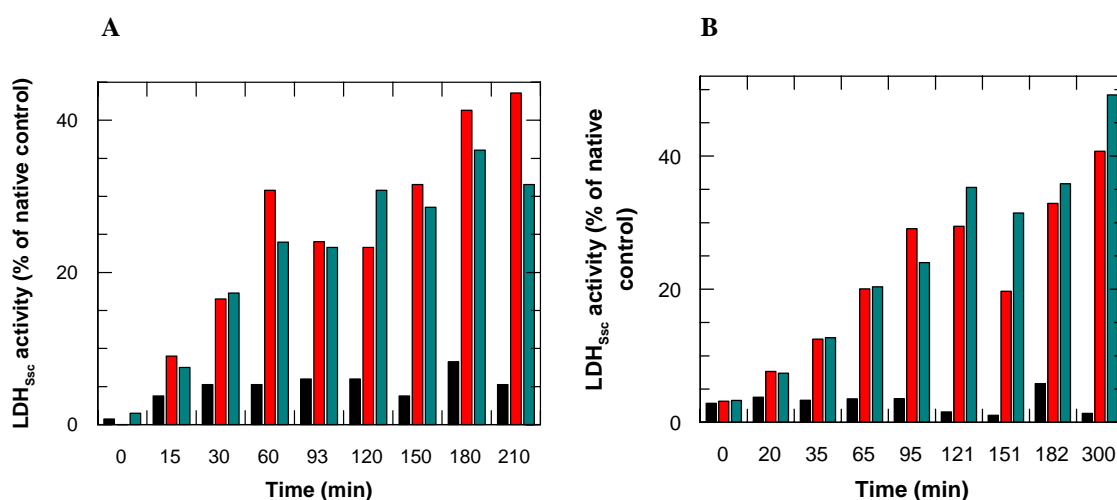


Figure 3.2.16: Biological activity of GrpE(N5C) and GrpE(V17C). LDH_{Ssc} at a concentration of 30 μ M was denatured in 6 M urea, 50 mM Tris/HCl, pH 7.5, 50 mM KCl, 5 mM MgCl₂, 10 mM DTE, 0.05 mg/ml BSA, at 30 °C for 30 min. Renaturation in the absence (*black column*) or presence of DnaK system including 3.2 μ M DnaK, 0.8 μ M DnaJ, 0.4 μ M GrpE(wt) (*red column*)/GrpE(N5C) (*cyan column*, **A**)/GrpE(V17C) (*cyan column*, **B**) was initiated by 120-fold dilution with NADH buffer at 30 °C. A sample of the refolding solution was transferred into the activity assay at the indicated times. The activity of the refolded LDH_{Ssc} was calculated as a percentage of native control.

In order to test whether the N-terminal part of GrpE at position 5 and 17 is able to interact with the peptide binding domain of DnaK fluorescence emission spectra of the IANBD fluorophore covalently coupled to the single cysteine mutations was recorded before and after incubation with DnaK. Since the IANBD emission spectra of GrpE(N5C)IANBD and

GrpE(V17C)IANBD were analyzed before and after incubation for 1 hour at 25 °C, we first tested influence of the incubation on the fluorescence intensity and position of the IANBD maximum. Fig. 3.2.17A and Fig. 3.2.18A show fluorescence emission spectra of GrpE(N5C)IANBD and GrpE(V17C)IANBD before and after incubation for 1 hour at 25 °C. The IANBD labeled GrpE(N5C) had an emission peak at 550.5 nm, which was not shifted after incubation. The fluorescence intensity was also unchanged. The position of the IANBD emission peak of the GrpE(V17C)IANBD mutant was shifted by 0.5 nm towards longer wavelength after incubation, however such a shift could be within the error limits. Change in a fluorescence intensity of GrpE(V17C)IANBD was not observed. According to measurements performed we could conclude that incubation for 1 hour at 25 °C itself does not influence on the emission spectra of GrpE(N5C)IANBD and GrpE(V17C)IANBD.

Fig. 3.2.17B shows the fluorescence emission spectra of 1 μM GrpE(N5C)IANBD before and after incubation with 20 μM DnaK. The position of emission peak was shifted from 548.5 to 547.0 nm, while fluorescence intensity was not changed. As shown in Table 3.2.2, small changes in position of emission maximum occurred when 1 μM GrpE(V17C)IANBD was incubated with 20 μM DnaK. In detail, a 2.5 nm emission blue shift was observed without change fluorescence intensity. Taking into account a negligible shift in position of the IANBD emission maximum without detectable change fluorescence intensity after incubation of GrpE(N5C)IANBD and GrpE(V17C)IANBD with DnaK we can not make a final conclusion about binding of GrpE at position 5 and 17 into the substrate binding pocket of DnaK. It is also very likely that labeled regions of GrpE do not undergo a local conformational change upon complex formation.

In order to evaluate whether different nucleotides and peptide bound to DnaK have any influence on interaction with the labeled N-terminal part of GrpE, the extrinsic fluorescence emission was registered and compared under identical conditions before and after incubation with DnaK in different states (ADP-, ATP- and peptide bound state). The peptide (P3) used in this experiment is a 10-mer peptide derived from p53 tumor suppressor protein with the sequence FYQLAKTCPV. Fig. 3.2.17C, D, E and Fig. 3.2.18C, D, E show fluorescence emission spectra of GrpE(N5C)IANBD and GrpE(V17C)IANBD before and after incubation with DnaK in ADP-, ATP- and peptide bound states. It was observed that incubation of GrpE(N5C)IANBD with DnaK in the ADP-bound form resulted in 0.5 nm blue shift accompanied by 7% decrease of fluorescence intensity. The addition of DnaK-ATP to

GrpE(N5C)IANBD affected both the fluorescence intensity and the position of the fluorescence maximum in GrpE(N5C)IANBD. The fluorescence was decreased by 7% with emission shift by 2.5 nm towards shorter wavelength. The recorded decrease in GrpE(N5C)IANBD fluorescence intensity and a blue shift after incubation with DnaK with an occupied peptide binding domain (peptide P3) were 17% and 0.5 nm, respectively. Based on a small shift (0.5-2.5 nm) in position of emission maximum of GrpE(N5C)IANBD accompanied by fluorescence intensity decrease (7-17%) after incubation with DnaK in different states (ADP-, ATP- and peptide bound state) we can not make a final conclusion about interaction of GrpE at position of 5 with DnaK when its nucleotide binding and peptide binding domains are occupied by nucleotide and peptide, respectively.

As compiled in Table 3.2.2, the addition of DnaK in different states (ADP-, ATP- and peptide bound state) to another GrpE mutant, GrpE(V17C)IANBD, resulted in a decrease of the fluorescence signal of 9-17%. The emission wavelength was concurrently shifted by 2-3 nm. These observations suggest that GrpE at position 17 is very likely undergoes local conformational changes as a result of binding of DnaK in different states.

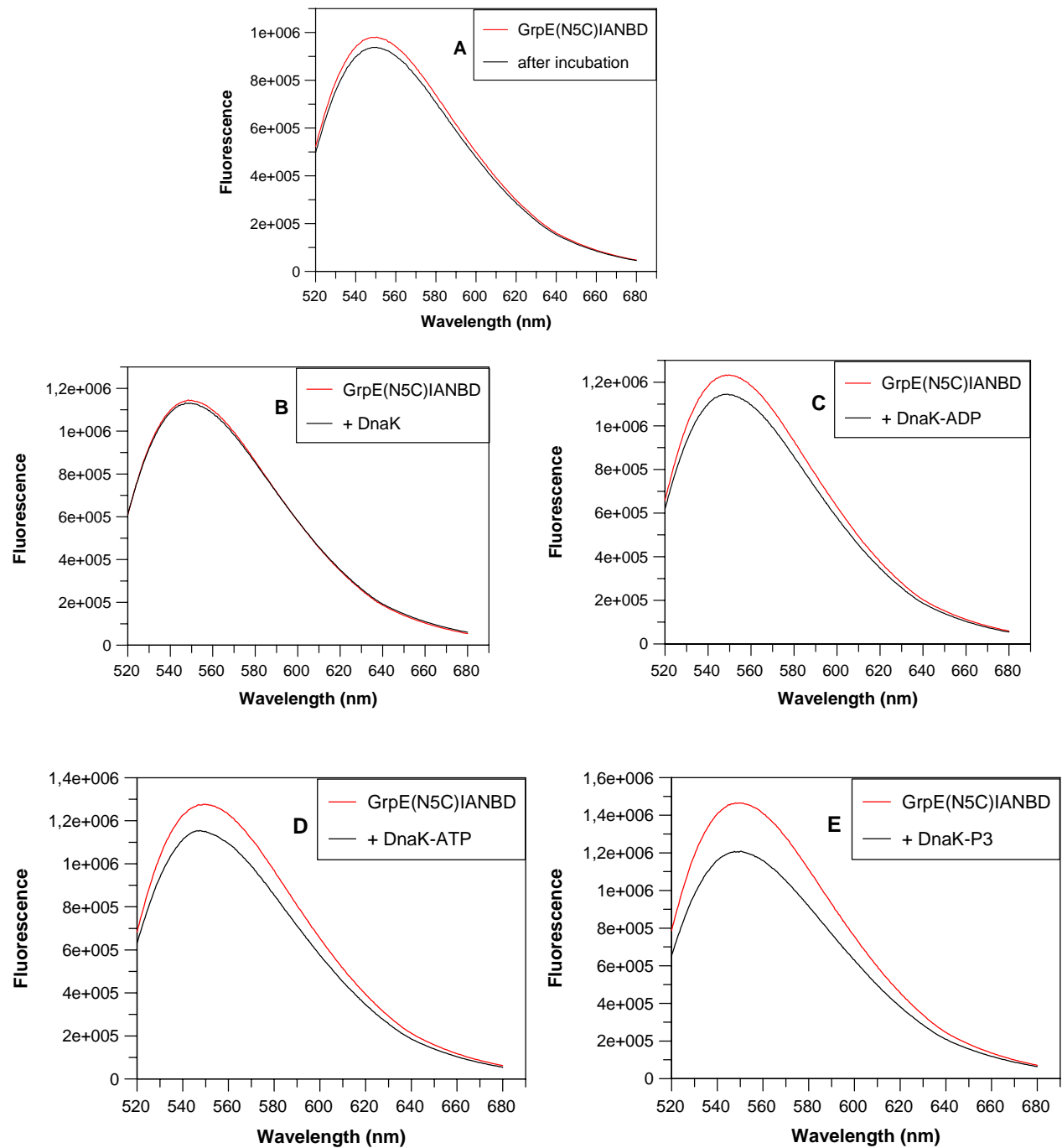


Figure 3.2.17: IANBD fluorescence spectra of GrpE(N5C)IANBD. Emission spectra of IANBD fluorescence of GrpE(N5C)IANBD at a concentration of $1 \mu\text{M}$ before (*red line*) and after 1-hour incubation (*black line*) at 25°C in the standard fluorescence buffer alone (A), in the presence of $20 \mu\text{M}$ DnaK (B), $20 \mu\text{M}$ DnaK in a complex with ADP (C), $20 \mu\text{M}$ DnaK in a complex with ATP (D), $20 \mu\text{M}$ DnaK in a complex with peptide P3 (E) were recorded between 520 and 680 nm at a fixed wavelength of 498 nm.

Table 3.2.1: Fluorescence emission peak wavelength and fluorescence intensity change of GrpE(N5C)IANBD before and after incubation in the standard fluorescence buffer alone and in the presence of DnaK in different states (nucleotide free, ADP-, ATP- and peptide bound state). To determine peak maximum fluorescence emission spectra shown in Fig. 3.2.17 were fitted by nonlinear regression analysis to a Gaussian peak function using Microsoft Excel.

Sample	Emission peak maximum of GrpE(N5C)IANBD alone, nm	Emission peak maximum of GrpE(N5C)IANBD after incubation, nm	IANBD emission peak shift, nm	Fluorescence intensity change, %
(A) GrpE(N5C)IANBD	550.5	550.5	-	-
(B) + DnaK	548.5	547.0	1.5	-
(C) + DnaK-ADP	548.5	549.0	0.5	7
(D) + DnaK-ATP	550.0	547.5	2.5	7
(E) + DnaK-P3	549.5	550.0	0.5	17

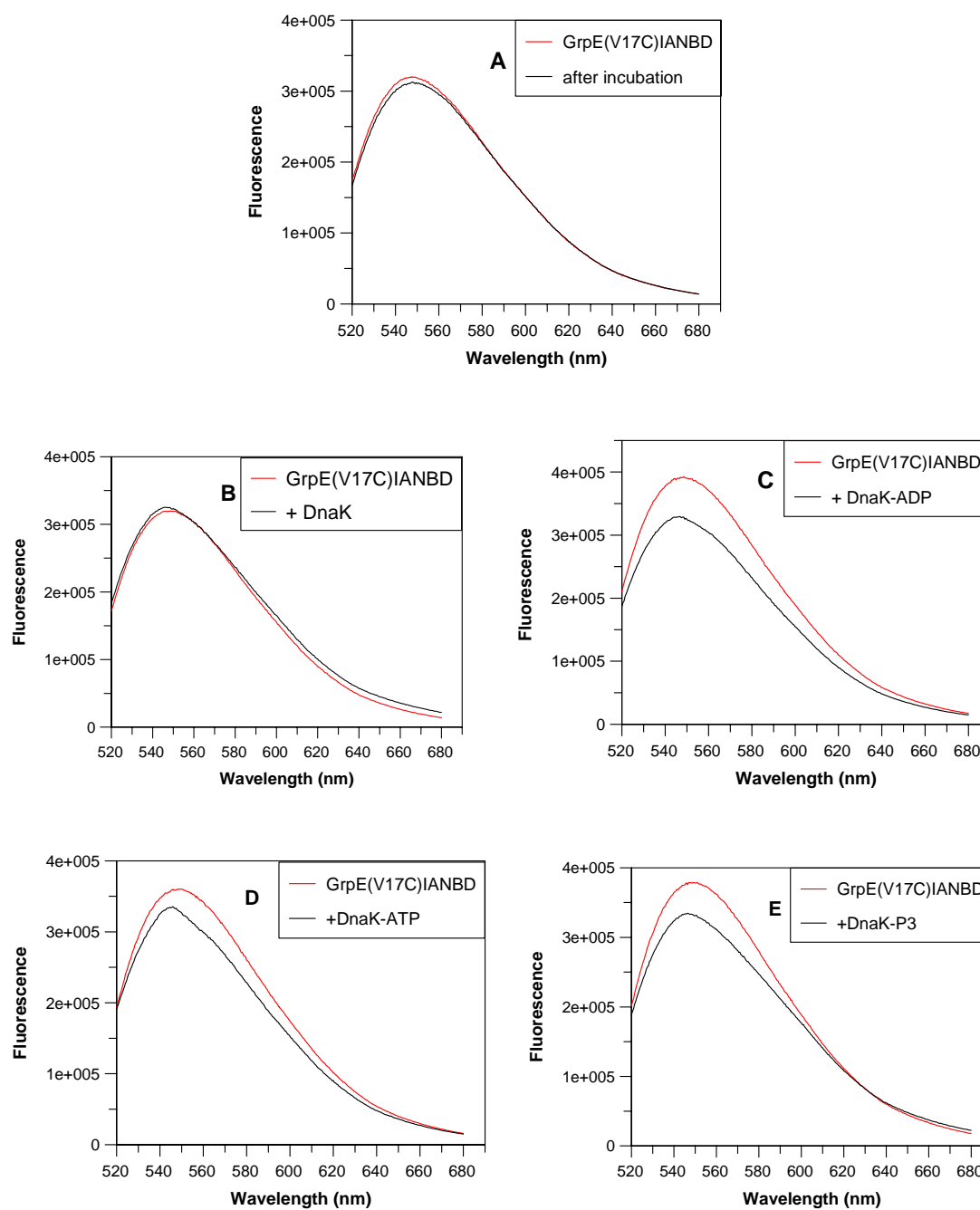


Figure 3.2.18: IANBD fluorescence spectra of GrpE(V17C)IANBD. Emission spectra of IANBD fluorescence of GrpE(V17C)IANBD at a concentration of 1 μ M before (*red line*) and after 1-hour incubation (*black line*) at 25 $^{\circ}$ C in the standard fluorescence buffer alone (A), in the presence of 20 μ M DnaK (B), 20 μ M DnaK in a complex with ADP (C), 20 μ M DnaK in a complex with ATP (D), 20 μ M DnaK in a complex with peptide P3 (E) were recorded between 520 and 680 nm at a fixed wavelength of 498 nm.

Table 3.2.2: Fluorescence emission peak wavelength and fluorescence intensity change of GrpE(V17C)IANBD before and after incubation in the standard fluorescence buffer alone and in the presence of DnaK in different states (nucleotide free, ADP-, ATP- and peptide bound state). To determine peak maximum fluorescence emission spectra shown in Fig. 3.2.18 were fitted by nonlinear regression analysis to a Gaussian peak function using Microsoft Excel.

Sample	Emission peak maximum of GrpE(V17C)IANBD alone, nm	Emission peak maximum of GrpE(V17C)IANBD after incubation, nm	IANBD emission peak shift, nm	Fluorescence intensity change, %
(A) GrpE(V17C)IANBD	547.5	548.0	0.5	-
(B) + DnaK	548.5	546	2.5	-
(C) + DnaK-ADP	548.5	546.5	2.0	17
(D) + DnaK-ATP	549.0	546.0	3.0	10
(E) + DnaK-P3	548.5	546.5	2.0	9

3.2.4. Fluorescence Correlation Spectroscopy (FCS)

Fluorescence correlation spectroscopy (FCS) measurements were performed to yield qualitative information about interactions between whole GrpE and DnaK in different states (nucleotide free, ADP-, ATP- and peptide bound state). This technique is applied to measure protein-protein interactions by monitoring translational diffusion (τ_d) time of a fluorescently labelled protein. In contrast to other fluorescence techniques, the parameter of primary interest is not the emission intensity itself, but rather spontaneous intensity fluctuations of single dye-labelled molecules measured in a microscopic detection volume of about 10^{-15} L (1 femtoliter) defined by a tightly focused laser beam. The time required for the passage of fluorescent molecules through the tiny volume element is determined by the diffusion coefficient which is related to the size and shape of a molecule (Pramanik and Rigler, 2001). Therefore, in contrast to equilibrium fluorescence measurements where fluorescence changes are dependent on the location of the fluorophore, FCS measurements have the advantage that any interaction between proteins is monitored directly without dependence on the position of the label.

3.2.4.1. Use of the Alexa488 and IANBD (amide) Fluorophores Coupled to GrpE(V17C) for the FCS Measurements

GrpE(V17C) mutant was labeled with two different fluorophores, such as Alexa488 and IANBD amide, to detect which of them is suitable for the FCS measurements.

Fig. 3.2.19 shows fluorescence count rate and corresponding autocorrelation functions of GrpE(V17C)IANBD and GrpE(V17C)Alexa488. For GrpE(V17C)Alexa488 no triplet state population at the applied excitation power (0.1 mW) was detected and therefore the experimental ACF was fitted by single species model (Eq. 2.4 shown in Material and Methods), ignoring triplet state.

We observed that the count rate per fluorescent molecule (cpm) was strongly dependent on fluorophore and the laser power used. The cpm reached for GrpE(V17C)Alexa488 was 6 kHz/molecule (laser power 0.1 mW, the concentration of GrpE(V17C)Alexa488 was 40 nM). Such low laser power applied at low GrpE(V17C)Alexa488 concentration gave strong fluorescent signal and high count rate per molecule. This shows that Alexa488 labeled GrpE(V17C) is suitable for the FCS measurements. In the case with IANBD-labeled GrpE(V17C), we obtained 0.5 kHz/molecule (laser power 1 mW, the concentration of GrpE(V17C)IANBD was 500 nM). Such high laser intensity at 12.5 fold molar excess of IANBD labeled GrpE(V17C) than Alexa488 labeled GrpE(V17C) could cause bleaching, aggregation or even disruption of the protein. In addition, the fluorescence signal of GrpE(V17C)IANBD was very noisy and too low to be detectable by FCS. Because IANBD-labeled GrpE(V17C) is generally not well suited for the FCS measurements we used Alexa488-labeled GrpE cysteine mutant.

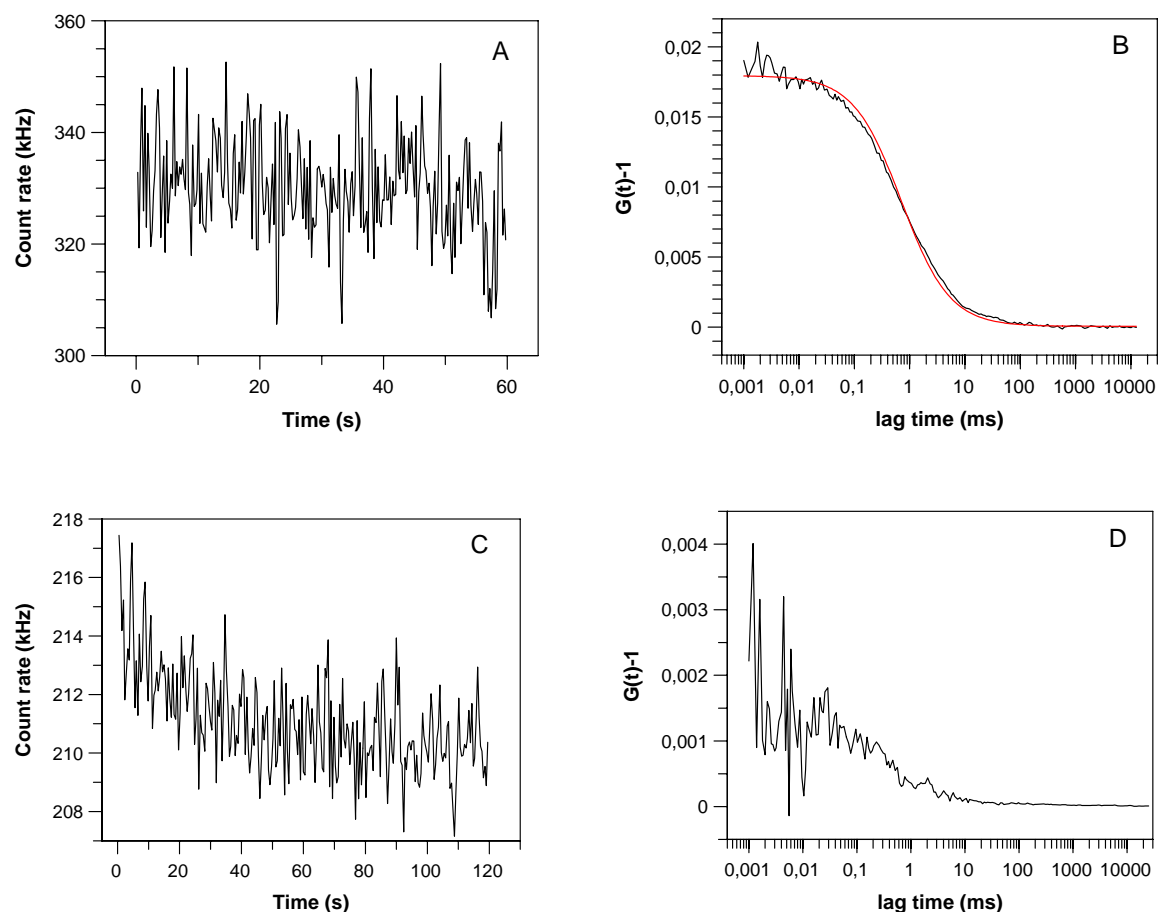


Figure 3.2.19: Count rate and autocorrelation function of GrpE(V17C)Alexa488 and GrpE(V17C)IANBD.

(A) Count rate of GrpE(V17C)Alexa488 (laser power ca.0.1 mW, 488 nm; the concentration of GrpE(V17C)Alexa488 was 40 nM).

(B) Autocorrelation function of GrpE(V17C)Alexa488. The red line represents fit according to a one component model (eq. 2.4 see Materials and Methods), ignoring triplet state.

(C) Count rate of GrpE(V17C)IANBD (laser power ca.1 mW, 488 nm; the concentration of GrpE(V17C)IANBD was 500 nM).

(D) Autocorrelation function of GrpE(V17C)IANBD.

3.2.4.2. Conformational Stability of the Nucleotide Binding and Peptide Binding Domains of DnaK

Because the tertiary structures of the two DnaK_{Eco} domains have been determined separately and the full length of DnaK has not been solved, it is not known how the ATPase and peptide binding domains are arranged relatively to each other, and it remains elusive how the conformational changes are communicated. According to the crystallographic data GrpE from

E.coli binds to the single ATPase domain of DnaK (Harrison et al., 1997). Using fluorescently labelled peptide it was kinetically shown that GrpE_{Eco} induces conformational change in the peptide binding domain of the DnaK_{Eco} molecule (Mally and Witt, 2001). However, whether GrpE is able to bind to the single peptide binding domain lacking a covalent link with the ATPase domain is still unknown. To evaluate the importance of structural coupling between the nucleotide binding domain (NBD, amino acids from 1 to 382) and the peptide binding domain (PBD, amino acids from 383 to 615) of DnaK_{Th} for interaction with GrpE_{Th}, we studied binding of the Alexa488 labelled GrpE(V17C) to a mixture of both domains.

The crystal structure of DnaK from *T.thermophilus* is not solved. As members of the highly conserved Hsp70 family, DnaK_{Eco} and DnaK_{Th} display a high level of sequence homology (73%) with an identity of 55%. The 3D structures of the DnaK_{Eco} nucleotide binding and peptide binding domains were used to model a structure of these domains from *T.thermophilus*. Ribbon representation of the modelled DnaK_{Th} nucleotide binding and peptide binding domains is shown in Fig. 3.2.20. These domains were expressed in *E.coli* cells, purified and used for the above mentioned experiments.

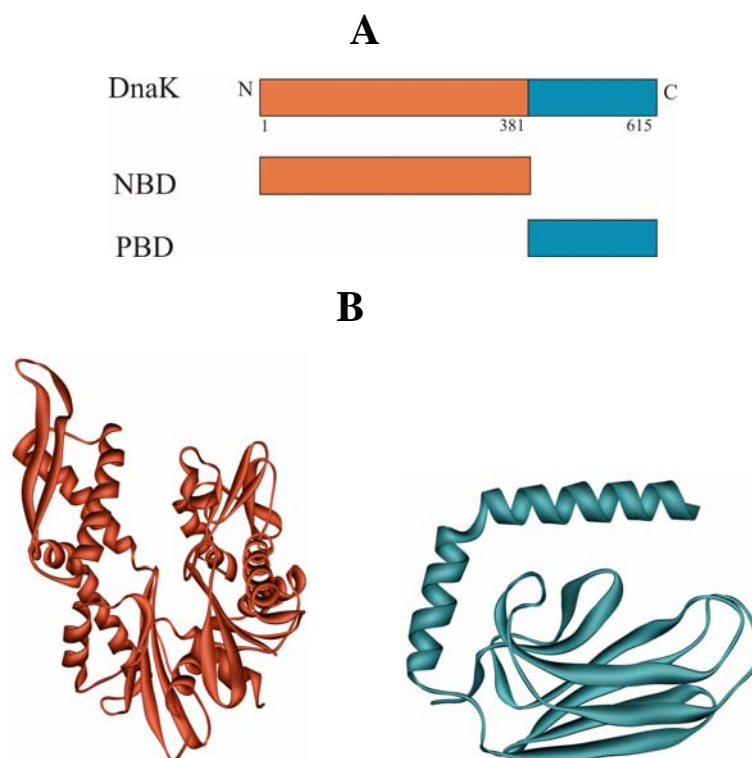


Figure 3.2.20: Structural features of DnaK from *Thermus thermophilus*.

(A) Schematic representation of the domain position in DnaK_{Th} and structure of the nucleotide binding (NBD) domain and peptide binding domain (PBD). Numbers refer to amino acid positions in the DnaK_{Th} protein.

(B) Ribbon representation of the modeled structure of the nucleotide binding domain (shown in red) and peptide binding domain (shown in cyan) of DnaK_{Th}. NBD and PBD were modeled by alignment to the NBD and PBD structure from *E.coli* (Harrison et al., 1997;Zhu et al., 1996) using SWISS-MODEL – Internet based tools for automated comparative protein modeling (Peitsch, 1996).

Before study the importance of the covalent link between the ATPase domain and peptide binding domain of DnaK for interaction with GrpE it was necessary to investigate the conformational stability of the individual domains. To detect if folding of the single nucleotide binding and peptide binding domains coincides with whole DnaK, circular dichroism spectra (CD) were recorded in the far-UV wavelength region (Fig. 3.2.21). The CD spectrum of DnaK ATPase and peptide binding domains closely resembles that of full-length DnaK. It shows the two negative peaks at 208 and 222 nm, which are characteristic for α -helical proteins. Thus the separation of ATPase and peptide binding domains from each other did not influence the folding of the each domain significantly.

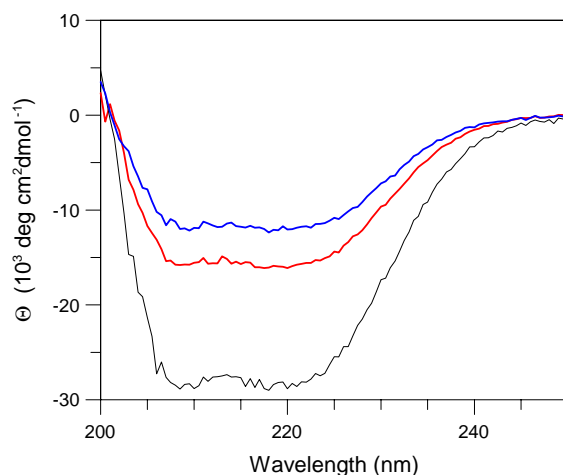


Figure 3.2.21: Secondary structure of DnaK_{Tth} wild type, the nucleotide binding and peptide binding domains of DnaK_{Tth}. Far-UV CD spectra of DnaK_{Tth} wild type (2 mg/ml; *red line*), ATPase (1 mg/ml; *black line*) and Peptide binding domains (2 mg/ml; *blue line*) are expressed as mean molar residue ellipticity (Θ). The spectra were measured at a sensitivity of 20 mdeg, a time constant of 1 s, 1 nm bandwidth, 0.2 nm resolution in 20 mM sodium phosphate, pH 7.04, 5 mM MgCl₂, 20 mM KCl. The temperature was held constant at 25 °C using a water-bath.

In addition to CD measurements, to verify the conformation stability of the nucleotide binding domain of DnaK (NBD) equilibrium fluorescence measurements were performed. NBD contains one tryptophan at position 231. As shown in Fig. 3.2.22 (red line), its emission maximum is centered around 308 nm, indicating that the spectrum is mainly due to tryptophan residue. Addition of 1 M, 3 M and 4 M GdnHCl to the sample produced a significant (about 49%) decrease in fluorescence intensity (Fig. 3.2.22). This suggests that the tryptophan in NBD is buried in the interior of the molecule. After incubation of NBD with 3 M and 4 M GdnHCl a significant red shift in emission spectra from 308 to 355 nm was detected. This effect reflects the change of microenvironment of the NBD's tryptophan residue to a more polar one and indicates a change in conformation of the protein. The detected 47 nm red shift accompanied by a 49% decrease of fluorescence shows that the single ATPase domain of DnaK is folded properly.

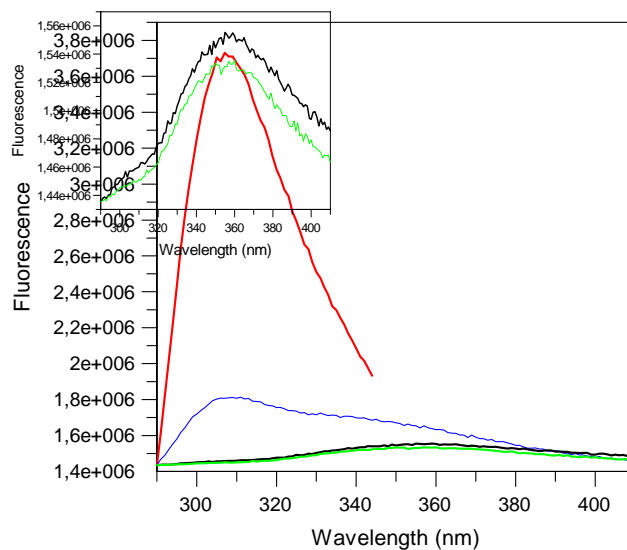


Figure 3.2.22: Conformational stability of the nucleotide binding domain of DnaK_{Tth} (NBD). The conformational changes in NBD induced by GdnHCl were analysed using fluorescence spectroscopy. 2 μ M NBD was incubated in standard fluorescence buffer in the absence (*shown in red*) or presence of 1 M GdnHCl (*shown in blue*), 3 M GdnHCl (*shown in black*), and 4 M GdnHCl (*shown in green*) for 1 hour at 25 °C followed by tryptophan emission spectra monitoring. The emission and excitation widths were set at 9 and 10 nm respectively. The excitation wavelength was 287 nm. The temperature was kept at 25 °C.

3.2.3. Interactions between GrpE(V17C)Alexa488 and DnaK

In this work we investigated whether the covalent linkage between the nucleotide binding (NBD) and peptide binding domains (PBD) of DnaK is important for interaction of GrpE with DnaK. When a mixture of 4 μ M NBD and 4 μ M PBD was added to 0.04 μ M GrpE(V17C)Alexa488 the diffusion time of the labelled GrpE(V17C) was increased from 0.583 ms to 0.888 ms that may be judged as to be association between these proteins (Tab. 3.2.3). According to the FCS measurements performed we can propose that the single nucleotide binding (NBD) and peptide binding domains (PBD) of DnaK lacking a covalent link are able to interact in the presence of GrpE.

To detect whether GrpE(V17C)Alexa488 interacts with DnaK in different states autocorrelation curve of the 0.04 μ M GrpE(V17C)Alexa488 was recorded in the absence and presence of 4 μ M DnaK, 4 μ M DnaK-ADP, 4 μ M DnaK-ATP and 4 μ M DnaK-P3 (Fig.

3.2.23). The peptide (P3) used in this experiment is a 10-mer peptide derived from p53 tumor suppressor protein with the sequence FYQLAKTCPV.

Because FCS is intrinsically sensitive to the mass changes occurring upon binding of one protein to another, the increase in estimated diffusion time from 0.583 ms (free GrpE(V17C)Alexa488) to 0.959 ms (in the presence of DnaK), 0.955 ms (in the presence of DnaK-ADP), 0.842 ms (in the presence of DnaK-ATP) and 0.867 ms (in the presence of DnaK-P3) demonstrates that GrpE(V17C)Alexa488 bound to DnaK in different states became less mobile due to a complex formation between these proteins (Tab. 3.2.3). According to the results obtained we can propose that the interaction between DnaK and GrpE from *T.thermophilus* is not coupled to the nucleotide state of DnaK as well as DnaK with the occupied peptide binding domain is able to interact with GrpE.

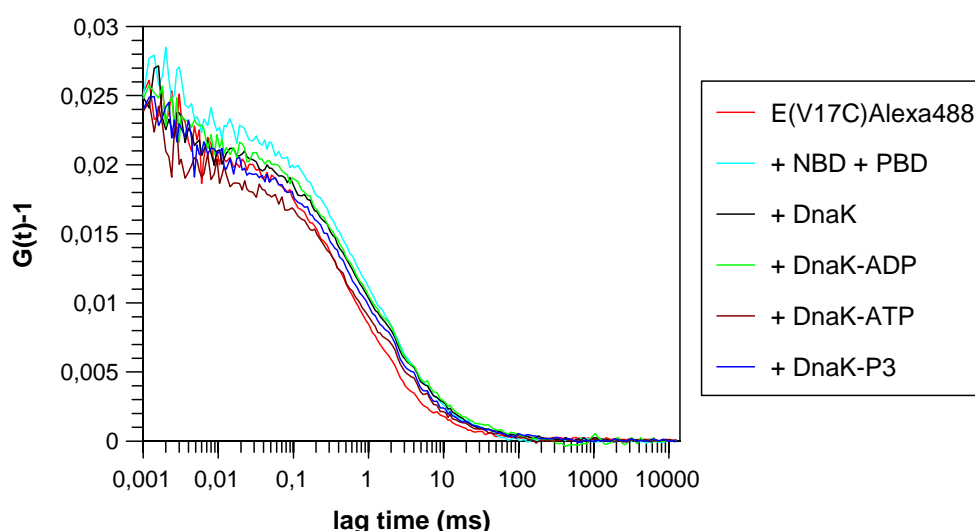


Figure 3.2.23: Autocorrelation curves of 40 nM GrpE(V17C)Alexa488 recorded with free labelled protein (*red line*) and in the presence of 4 μ M DnaK (*black line*), 4 μ M DnaK in a complex with peptide P3 (this peptide is derived from p53 tumor suppressor protein with the sequence FYQLAKTCPV) (*blue line*), 4 μ M DnaK in ADP bound state (*green line*), 4 μ M DnaK in ATP bound state (*dark red line*), mixture of 4 μ M nucleotide binding domain and 4 μ M peptide binding domain (*cyan line*) The measurements were performed in standard fluorescence buffer at 25 °C. Laser power ca. 0.1 mW.

Table 3.2.3: Diffusion time of GrpE(V17C)Alexa488 recorded with free protein and in the presence of the mixture of the nucleotide binding domain (NBD) and the peptide binding domain (PBD) of DnaK, DnaK in different states (nucleotide free, ADP-, ATP- and peptide bound state). To determine diffusion time, autocorrelation curves shown in Fig. 3.2.23 were fitted by a single species model (Eq. 2.4, see Materials and Methods), ignoring triplet state.

Protein	Diffusion time τ_d (ms)
GrpE(V17C)Alexa488	0.583
+ NBD + PBD	0.888
+ DnaK	0.959
+ DnaK-ADP	0.955
+ DnaK-ATP	0.842
+ DnaK-P3	0.867

As compiled in Table 3.2.3, the diffusion time (τ_d) of the free GrpE(V17C)Alexa488 increases to approximately 0.3 ms after addition of two single DnaK's domains and DnaK in different states (nucleotide free, ADP-, ATP- and peptide bound state). For a significant change in the diffusion time, the mass ratio between the labeled protein free in solution and in a complex with non-fluorescent counterpart should be at least eight (Haustein and Schwille, 2003). The change in mass between GrpE(V17C)Alexa488 and the GrpE(V17C)Alexa488-DnaK complex is three. Considering the logarithmic time scale, the quantitative analysis of interaction between these proteins by FCS will be rather difficult. However, the detected difference of about 0.3 ms in τ_d could provide preliminary qualitative information that interaction of GrpE with DnaK is not coupled to the DnaK nucleotide and peptide bound state and GrpE is able to interact with the single nucleotide and peptide binding domains lacking a covalent link.

4. Discussion

4.1. LDH from *S.scrofa* Muscle and LDH from *B.stearothermophilus* as Model Substrates for the DnaK_{Tth}-ClpB_{Tth} System

To get insight into the functional cooperation between components of the DnaK system (DnaK, DnaJ, GrpE) and interaction of the DnaK system with ClpB it was necessary to find a suitable substrate. Molecular chaperones are known to recognize hydrophobic residues and/or unstructured backbone regions of folding intermediates and thereby shield interactive surfaces of non-native polypeptides and prevent aggregation (Rüdiger et al., 1997). The choice of a substrate was based on at least two important criteria: its folding status should be easily monitored by a sensitive spectroscopic assay; it should generate folding intermediates. Whereas some small single-domain proteins have been shown to fold without detectable intermediates (Jackson and Fersht, 1991; Kragelund et al., 1995), many larger, especially oligomeric proteins are known to populate intermediates during their folding process (Jaenicke and Seckler, 1997).

Lactate dehydrogenase from *S.scrofa* (pig) (LDH_{Ssc}) muscle is a tetramer composed of four identical subunits. The structure of the complex between LDH_{Ssc} and its nicotinamide adenine dinucleotide, NADH, coenzyme was solved at 2.2 Å resolution (Dunn et al., 1991). The enzyme Lactate dehydrogenase catalyses NADH-dependent interconversion of pyruvate and lactate. The steady-state assay of LDH activity is based on the spectral properties of NADH. NADH absorbs radiation at 340 nm in reduced form, whilst the oxidized NAD⁺ form does not absorb at this wavelength. A loss of native structure of LDH_{Ssc} as a result of denaturation causes loss of the enzymatic activity which is easily detected with a colorimetric assay.

Before study chaperone assisted reactivation of LDH_{Ssc}, we monitored its inactivation by two of the best known chemical denaturing agents, such as guanidine hydrochloride (GdnHCl)

and urea and denaturation caused by high temperature. It was observed that 500 nM LDH_{Ssc} was almost completely denatured by 2 M GdnHCl, while to get the same level of denaturation 3 M urea was required. Consequently, GdnHCl is 1.5 times more effective than urea in unfolding of LDH_{Ssc}. Because GdnHCl dissociates in aqueous solution producing GdnH⁺ and Cl⁻ ions it is expected to be more efficient than urea (which is not an ionic compound) in masking electrostatic interactions in protein causing unfolding.

Studies of LDH_{Ssc} inactivation by high temperature showed that the co-enzyme NADH stabilizes LDH_{Ssc} against exposure to high temperatures. According to loss of LDH_{Ssc} activity, the maximum denaturation in the absence of NADH was detected at 60 °C, whereas the presence of NADH caused a shift of the maximal denaturation towards higher temperature (70 °C). It is known that ligands stabilise the protein structure (Martinez et al., 1994; Zolkiewski and Ginsburg, 1992). Thermal stability change is obviously related to the energies of the protein-ligand interaction. Application of the Le Chatelier's principle shows that if any ligand specifically binds to the native form of the protein, then this will stabilize the folded state, and unfolding of the protein will become progressively less favorable as ligand concentration increases.

Studies of the chaperone mediated reactivation of urea-denatured LDH_{Ssc} clearly showed that maximal reactivation up to 50% was achieved in the presence of the components of DnaK system (DnaK, DnaJ, GrpE) together with the chaperone ClpB. The maximal reactivation of LDH_{Ssc} assisted by the DnaK system alone was only 34%. Similar results were detected with GdnHCl-denatured LDH_{Ssc}. The single DnaK system gave rise to a recovery of active enzyme up to 12% while reactivation of LDH_{Ssc} assisted by both DnaK system and ClpB was 38% of native control. These data directly demonstrate the importance of cooperative action of the DnaK, DnaJ, GrpE and ClpB machinery for recovery chemically denatured LDH_{Ssc}. The associated action of the DnaK system together with the chaperone ClpB was reported by others. Zolkiewski (1999) showed that the DnaK/DnaJ/GrpE/ClpB system from *E.coli* is able to increase the luciferase reactivation yield up to ~3,000 fold. Using heat-inactivated enzymes (Lactate dehydrogenase, glucose-6-phosphate dehydrogenase and α -glucosidase from *B.stearothermophilus*) Motohashi and co-workers (1999) showed that presence of the ClpB/DnaK/DnaJ/GrpE set from *T.thermophilus* was necessary to achieve a high yield of recovery (~65%). It was suggested that a putative refolding intermediate could be directly transferred between ClpB and DnaK-J-GrpE set via a ClpB-DnaK interface (Motohashi et al.,

1999;Schlee et al., 2004). Therefore the presence of both chaperones in the reactivation period is necessary to yield maximal recovery of the activity of a denatured enzyme.

However, we observed that chaperone assisted reactivation of the heat-denatured LDH_{Ssc} was very weak (3-8% of the native activity). Study of the inactivation of LDH_{Ssc} during different periods showed that even a short period (2 minutes) of the LDH_{Ssc} exposure to 70 °C results in almost complete denaturation of the enzyme. The observed high yield recovery of the LDH_{Ssc} activity after chemical denaturation assisted by chaperones and very weak reactivation after exposure to the high temperature could be explained in terms of different effect of chemical agents and elevated temperature on denaturation. It is conceivable that urea and GdnHCl cause dissociation to dimers and monomers of the tetrameric LDH_{Ssc} with subsequent interaction with both non-polar and polar surfaces of the enzyme resulting in formation of unstructured regions (Jaenicke and Seckler, 1997). These regions are recognized by molecular chaperones which assist refolding into the native tetrameric structure with regain of the catalytic activity.

In contrast to chemical denaturation, elevated temperature acts primarily by disrupting the hydrophobic interactions that make up the stable core of the protein. Hydrophobic patches of different molecules which were hidden in the core may interact with each other in such a way to cause aggregation of the protein. Thus, exposure of the mesophilic LDH_{Ssc} toward elevated temperature stimulates formation of unstable species with exposed hydrophobic surfaces. Such species may tend to assume an alternatively stable conformation in the form of insoluble aggregates that remain inactive at permissive temperature, disaggregation not being possible by chaperones.

To study the ability of the DnaK-ClpB chaperone machinery to mediate reactivation of the thermally inactivated protein we chose the thermophilic Lactate dehydrogenase from *B.stearothermophilus* (LDH_{Bst}) as an alternative to the mesophilic LDH_{Ssc}. The results were remarkable: in the presence of both DnaK system and ClpB chaperone renaturation started immediately and reached 40% of the native activity. Taken together the results obtained give base to propose that quality and size of aggregates formed by the mesophilic eukaryotic LDH and the same enzyme from thermophilic prokaryotic organism are rather different. Based on the nature of the noncovalent interactions that drive aggregate assembly Glover and Tkach (2001) divided aggregates into two groups. In the first group, hydrophobic interactions among heat-perturbed proteins probably lead to the formation of disordered aggregates although

some can form flexible linear chains. In the second group, interactions within the aggregate are primarily governed by hydrogen-bond networks to produce highly ordered self-organizing aggregates. Driven by ATP hydrolysis, the ClpB chaperone is able to disrupt aggregates of small protein or resolubilize heat-shock granules and prion-like structures; the action of the additional chaperone DnaK and its co-chaperones DnaJ and GrpE allows the components of such aggregates, once released, to refold and attain the native conformation (Diamant et al., 2000; Goloubinoff et al., 1999; Schlee et al., 2004). However, the ring-shaped cylinder of ClpB appears able to mediate ATP-dependent disaggregation of “soft” aggregates of up to 600 kDa (Horwich, 2002). Therefore we can assume that as the size of aggregates increases, aggregates become increasingly poorer substrates for the ClpB-DnaK chaperone system. The detailed kinetic studies of LDH (from *S.scrofa* muscle and *B.stearothermophilus*) unfolding, refolding and aggregation will provide ample opportunity to disclose chaperone-assisted refolding of this tetrameric enzyme.

The eukaryotic LDH (LDH from *S.scrofa* muscle) and prokaryotic LDH (LDH from *B.stearothermophilus*) show pairwise sequence identities of 39% and nearly identical three-dimensional structures. However, despite the similarities we observed significant difference in chaperone assisted reactivation of thermally inactivated LDH_{Ssc} and LDH_{Bst}. The rather moderate LDH_{Ssc} reactivation by chaperones (after heat denaturation) in comparison to the *B.stearothermophilus* LDH may have also another possible explanation. Widmann and Christen (2000) monitored refolding of the orthologous eukaryotic and prokaryotic proteins (Aspartate aminotransferase, Malate dehydrogenase, Lactate dehydrogenase). They observed that the rates of refolding of the prokaryotic proteins after denaturation in GdnHCl were faster than those of their orthologous counterpart. In addition, the prokaryotic proteins were refolded with a significantly higher yield. These results prompted Widmann and Christen (2000) to hypothesize that the folding of eukaryotic and prokaryotic enzymes is under different control. The folding of eukaryotic enzymes seems to be under kinetic control and may span long time periods; the rate of equilibration between intermediate conformational states is slow compared to the rate of formation of the final conformational state. Incorrectly folded conformers generated during renaturation cannot shuffle within a physiologically significant time interval. In contrast, the folding of prokaryotic proteins seem to be mainly under thermodynamic control; the conformational isomers generated during refolding apparently exist in rapid equilibrium, and the initial formation of incorrect conformers is corrected by

their conversion to the thermodynamically most stable form and therefore prokaryotic proteins fold faster than their orthologous eukaryotic counterparts.

Taking into account the detected yield of recovery of LDH enzymatic activity mediated by the DnaK-ClpB system (Tab. 4.1) we can conclude that urea-denatured LDH from *S.scrofa* (pig) muscle and heat-inactivated LDH from *B.stearothermophilus* could be suitable model substrates for the DnaK-ClpB chaperone system from *T.thermophilus*.

Table 4.1: Maximal reactivation of chemically and thermally denatured Lactate dehydrogenase from *S.scrofa* (pig) muscle (LDH_{Ssc}) and from *B.stearothermophilus* (LDH_{Bst}) assisted by ClpB_{Th} and the DnaK_{Th} system (DnaK, DnaJ, GrpE) after 5 hours of incubation.

Protein	Maximal reactivation, % of native control
Urea-denatured LDH _{Ssc}	50 %
GdnHCl-denatured LDH _{Ssc}	33 %
Heat-inactivated LDH _{Ssc}	15 %
Heat-inactivated LDH _{Bst}	41 %

4.2. Interaction between DnaK and GrpE

Like all Hsp70 proteins known so far, DnaK is composed of a highly conserved N-terminal nucleotide-binding domain and a less conserved C-terminal peptide-binding domain. Functional cooperation between the ATPase domain and the peptide binding domain of the *E.coli* DnaK has been widely reported in literature. Using HPLC analysis and quantitative double-labeling experiments it was demonstrated that binding of ATP alone, in the absence of hydrolysis, is sufficient to accelerate greatly the dissociation of peptide substrates bound to DnaK_{Eco} (McCarty et al., 1995; Palleros et al., 1991). Theyssen with colleagues (1996) kinetically showed that stimulation of the peptide exchange rate by ATP is 1,000-fold. Thus, it is possible to assume that the nucleotide state of DnaK_{Eco} plays a crucial role in the substrate binding properties of this protein.

The functional coupling between both domains of DnaK from *T.thermophilus* was also shown on the level of nucleotide regulated peptide binding. However, ATP accelerated the dissociation of a peptide from a DnaK_{Th}-peptide complex by only a factor of five (Klostermeier et al., 1999). The increase in the dissociation rate constant (5-fold) in case of *T.thermophilus* DnaK is very low in comparison to a 1,000-fold stimulation of the peptide exchange observed for DnaK from *E.coli*. This leads to a proposal that the nucleotide state of DnaK_{Th} does not play a significant role in substrate binding properties of this thermophilic chaperone. The functional coupling between the nucleotide binding domain and peptide binding domain of DnaK_{Eco} was also detected on the level of peptide stimulated ATPase activity of this protein. A model peptide stimulated the steady state ATPase rate of DnaK_{Eco} by 9-fold (McCarty et al., 1995). Such domain-domain interactions in DnaK_{Eco} provide the intraprotein communication that is necessary to coordinate function. These findings gave base to assume that DnaK_{Eco} alone in the absence of the co-chaperone DnaJ_{Eco} and nucleotide exchange protein GrpE_{Eco} has a physiologically relevant role in prevention of aggregation and promotion of folding.

The nucleotide and peptide bound state of DnaK_{Eco} is regulated not only on the level of the domain-domain interactions but it is also controlled by the nucleotide exchange factor GrpE_{Eco}. To assist the chaperone function of DnaK, GrpE and DnaK have to interact physically. The interaction between GrpE and DnaK from *E.coli* has indeed been verified by using a series of methods like non-denaturing polyacrylamide gel electrophoresis, dynamic light scattering, analytical ultracentrifugation and glycerol gradient centrifugation

(Buchberger et al., 1994a; Schönfeld et al., 1995; Zylicz et al., 1987). The stoichiometry of a stable complex formed by DnaK_{Th} and GrpE_{Th} is 1:2. Using isothermal calorimetric titrations it was detected that the affinity of GrpE to DnaK from *T.thermophilus* is 0.15 μM (Groemping et al., 2001). In this work we analysed the interaction between GrpE_{Th} and DnaK_{Th} using the fluorescence correlation spectroscopy (FCS) technique. We found for the first time that the structural integrity between the nucleotide binding and the peptide binding domain of DnaK_{Th} is likely not necessary for the complex formation between DnaK_{Th} and GrpE_{Th}. In this regard GrpE_{Th} might be viewed as molecular bridge, with the β -sheet domain serving as device for interaction with the nucleotide binding domain and stimulation of nucleotide release, whereas the long α -helical tail is involved in signal transduction from the nucleotide binding domain to the peptide binding domain.

The maximum stimulation of nucleotide exchange by *E.coli* GrpE is 5,000-fold in comparison to a 80,000-fold stimulation by GrpE from *T.thermophilus* (Groemping et al., 2001; Packschies et al., 1997). Using fluorescence spectroscopic techniques Mally and Witt (2001) kinetically showed that GrpE_{Eco} can directly stimulate peptide release. Specifically, the binding of GrpE_{Eco} to a DnaK_{Eco}-peptide complex, increases k_{off} by about 200-fold. The results are consistent with a GrpE_{Eco}-induced conformational change in the C-terminal peptide binding domain of DnaK_{Eco}, which results in a unique low affinity intermediate from which peptide can dissociate. Unfortunately, quantitative data regarding to *T.thermophilus* GrpE stimulated release of a substrate bound to DnaK_{Th} are not available yet. However, based on the published results showing that ATP bound to the ATPase domain of DnaK_{Th} negligibly accelerates peptide release from the DnaK_{Th}-peptide complex in comparison to the nucleotide effect observed for DnaK from *E.coli*, we can propose that the thermophilic GrpE but not nucleotide plays an important role in stimulation of peptide substrate release from the peptide binding domain of DnaK_{Th}.

Using fluorescence correlation spectroscopy measurements we observed that GrpE_{Th} interacts with DnaK_{Th} in the presence of ADP. In details, the diffusion time of free GrpE(V17C)Alexa488 was increased from 0.583 ms to 0.955 ms due to complex formation with DnaK-ADP. This observation is in the line with previously published experiments demonstrating that GrpE_{Th} binds to DnaK-ADP with a K_d of 1.3 μM (Groemping et al., 2001).

Using DSC measurements in this work it could be observed that ADP causes stabilization of DnaK_{Tth}. The formation of a DnaK-ADP complex was detected by a 6.4 °C shift of the thermal transition towards higher temperatures. This observation is in the line with that demonstrated by Palleros and co-workers (1992) that Mg²⁺/ADP increases the thermal stability of DnaK from *E.coli*. This stability change is obviously related to the energies of the protein-ligand interaction (Martinez et al., 1994; Martinez et al., 1995; Zolkiewski and Ginsburg, 1992). In addition, Flaherty and co-workers (1990) solved the crystal structure of a complex of the DnaK_{hsc} ATPase domain with Mg²⁺/ADP. It was shown that the DnaK_{hsc} ATPase domain adopts a closed conformation in ADP bound form. The interface of the DnaK_{hsc} ATPase domain-Mg²⁺/ADP complex includes hydrogen bonds between oxygens of the α and β phosphates of ADP with the hydroxyl of Thr-14, as well as with several amide nitrogens of the peptide backbone. The adenine ring is sandwiched between the aliphatic methylene segments of the side chains of Arg-272 and Arg-342, further stabilizing the bound state of the nucleotide (Flaherty et al., 1994).

In case of the nucleotide exchange factor GrpE(Δ C) lacking the β -sheet domain, ADP does not stabilize its structure. It was observed in this work that the difference in position of the calorimetric peak of GrpE(Δ C) in the presence and absence of Mg²⁺/ADP is negligible, indicating that the α helical part of GrpE (GrpE(Δ C)) does not interact with nucleotide. Reid and Fink (1996) published that GrpE_{Eco} wild type does not bind ADP or ATP. Therefore we can conclude that the nucleotide exchange factor has no affinity to nucleotides either with or without the β -sheet domain. Taken together, the detected interaction between GrpE_{Tth} and DnaK_{Tth} in the ADP bound state and the known ability of the nucleotide exchange factor to stimulate nucleotide exchange as well as taking into account the fact that this protein has no affinity to nucleotides allow us to decide that the nucleotide exchange factor GrpE_{Tth} stimulates nucleotide release from the ATPase domain of DnaK_{Tth} without direct contact with the nucleotide.

In this work it was detected for the first time binding of GrpE_{Tth} to DnaK_{Tth} in the presence of ATP by fluorescence correlation spectroscopy and protein affinity chromatography with C8-coupled ATP-agarose. This is in contrast to the effect of ATP on the *E.coli* DnaK-GrpE complex observed during sedimentation of the two proteins in glycerol gradients (Zylicz et al., 1987). When ATP was added to the gradient, the complex was disrupted, and the two proteins sediment independently. The nucleotide independent interaction between

thermophilic DnaK_{Th} and GrpE_{Th} could extend control of the regulation of the DnaK_{Th} function at each step of the chaperone cycle.

We showed also using fluorescence correlation spectroscopy measurements that GrpE_{Th} interacts with a DnaK_{Th}-peptide complex. Specifically, the diffusion time of free GrpE(V17C)Alexa488 increased from 0.583 to 0.867 ms due to complex formation with DnaK_{Th} with the occupied peptide binding domain. This result is in good agreement with that reported by Schoenfeld and co-workers. (1995). Using gel filtration chromatography they found that the presence of a peptide substrate does not affect GrpE_{Eco}-DnaK_{Eco} complex formation. It is therefore possible that GrpE binds to DnaK-substrate complexes and stimulates dissociation of the bound substrate.

4.3. Structural Features of GrpE, Implications for Functions

The DnaK chaperone activity in protein folding is regulated by ATP-controlled cycles of substrate binding and release. Nucleotide exchange plays a key role in these cycles by triggering substrate release. The GrpE protein functions as an ADP-ATP exchange factor, which replaces ADP with ATP, enhancing release of substrate proteins from DnaK. The maximum stimulation of nucleotide exchange (k_{off}) by the *T.thermophilus* GrpE is 80,000-fold (Groemping *et al.*, 2001). The crystal structure of GrpE with the DnaK adenosine triphosphatase (ATPase) domain (or nucleotide binding domain, NBD) from *E.coli* determined by Harrison *et al.* (1997) provides an explanation for the ability of GrpE to release nucleotide from DnaK. It was found that a dimer of GrpE_{Eco} interacts in an asymmetric fashion with the DnaK ATP-ase domain. There are six areas of contact between GrpE and NBD. The two largest are between the two faces of the proximal β -sheet domain of GrpE and domains IB and IIB of DnaK on each side of the nucleotide binding cleft. The other areas are on separate regions of the GrpE long helix. The interface includes nonpolar, polar and salt bridge interactions. It was observed that the areas of contact situated in the GrpE long helix are only minimally involved in interaction with NBD. Therefore the hydrophobic contacts from the β -strand region of GrpE contribute substantially to the tight contact of the two proteins. Comparison of the crystal structure of GrpE_{Eco}-bound, nucleotide-free ATPase domain of DnaK_{Eco} with that of ADP-bound bovine brain Hsc70 showed that the co-

chaperone GrpE_{Eco} stimulates mechanical opening of the DnaK_{Eco} structure (Harrison et al., 1997). The GrpE-induced movement of domain IIB displaces by 2 to 3 Å three residues in DnaK that hydrogen bond to the adenine and ribose rings of ADP in Hsc70. Mehl and colleagues (2001) kinetically showed that the GrpE_{Eco} mutant containing two helix bundle and the β -sheet domain is able to increase the off-rate of ATP γ S from DnaK_{Eco} and the NH₂-terminal ATPase domain of DnaK_{Eco}. The β -sheet domain of GrpE_{Eco} directly interacts with residues that constitute the hydrophobic patch (Met 259-Val 59) and the upper salt bridge (Glu 264-Arg 56) of DnaK_{Eco}. Brehmer with co-workers (2001) also kinetically showed that mutation of the DnaK site (DnaK-R56A) contacting GrpE results in decrease of nucleotide dissociation rates up to 15 fold. On the other hand, the DnaK_{Th} system in the presence of a C-terminally truncated GrpE_{Th}-protein lacking the β -sheet domain (GrpE(Δ C)) does not support refolding of denatured luciferase (Groemping and Reinstein, 2001). This finding was explained by the missing nucleotide exchange properties of GrpE(Δ C). Taken together, the structural and functional studies on the ability of GrpE to increase the off-rate of nucleotides from the DnaK ATPase domain evidently show the function of GrpE as a “nucleotide exchange factor”. A similar function has been described for the Bag-1 (Bcl2-associated anthanogene 1) protein, the eukaryotic homolog of GrpE. Bag-1 was first identified in the mammalian cytosol by virtue of its interaction with the anti-apoptotic protein Bcl-2 and was shown to promote cell survival (Takayama et al., 1995). Bag proteins such as Bag-1 play roles in the regulation of signal transduction proteins, transcription factors and proteolysis (Brehmer et al., 2001). They contain at least one copy of a roughly 50 amino acid evolutionarily conserved domain, the “Bag” domain that allows them to interact and stimulate nucleotide release from the Hsp70 ATPase domain (Sondermann et al., 2001). The Ras proteins, belonging to the Ras (Rat-Adeno-Sarcoma) superfamily and serving as binary switches in signal transduction pathways are also shown to be activated by guanine nucleotide exchange factors (GEFs) which stimulate the exchange reaction in which bound GDP is replaced by GTP (Lenzen et al., 1998).

An additional function of GrpE_{Th} as a thermosensor that modulates nucleotide exchange rates in a temperature-dependent manner to prevent substrate dissociation at non-permissive conditions was attributed to the globular C-terminal β -sheet domain (Groemping and Reinstein, 2001). Using results of the GrpE_{Th} and GrpE_{Th}(Δ C) unfolding obtained with DSC it was hypothesized that under heat shock conditions, the DnaK-ADP-protein-substrate

complex is stabilized by the reversibly unfolded GrpE_{Tth} β -sheet domain that refolds under permissive conditions.

In spite of the well documented fact that GrpE stimulates nucleotide release the translation of the GrpE-mediated conformational changes in the DnaK ATPase domain to changes in the substrate binding domain is still unclear and presumably must await determination of the structures of full-length molecules. Using fluorescently labelled peptides (P) Mally and Witt (2001) kinetically showed that binding of the *E.coli* GrpE to an ADP-DnaK-P (or DnaK-P) complex increases k_{off} and k_{on} by ~ 200 -fold and ~ 60 -fold, respectively. The results are consistent with a GrpE induced conformational change in the C-terminal peptide binding domain of the DnaK molecule. Therefore it is possible to assume that GrpE is more than just a nucleotide exchange factor; it is also involved in substrate release. Based on the crystal structure of *E.coli* GrpE with the DnaK adenosinetriphosphatase (ATPase) domain it has been suggested that the NH₂-terminal portion of GrpE that contains the long α -helix and the flexible segment interacts with the peptide binding domain of DnaK (Harrison et al., 1997).

In this work we studied the biological relevance of GrpE's_{Tth} long α -helical region composed of about 107 amino acids. Using protein affinity chromatography we observed that the GrpE helix (GrpE(Δ C)) directly interacts with DnaK_{Tth} in the absence of nucleotides. The detected binding assumes a functional implication of the DnaK_{Tth} chaperone cycle. Thus, using radioactive assay that measures the percentage of bound peptide to DnaK_{Eco} Mehl and colleagues (2001) observed that GrpE_{Eco}(1-89) containing only the α -helical tail domain is able to facilitate release of bound peptide from DnaK that may not need interdomain communication within DnaK. We observed also that GrpE(Δ C) binds to DnaK_{Tth} specifically. The binding of the GrpE_{Tth} α -helical part is dependent on the nature of the DnaK_{Tth} bound nucleotide. It was observed that GrpE(Δ C) binds to DnaK both in the absence and presence of ADP. However, in the presence of ATP interaction between these proteins was not detected. ATP binding must, therefore, induce a conformational change in DnaK that abolished binding of the α -helical part of GrpE_{Tth}. It is well-known that no detectable GrpE_{Eco}-DnaK_{Eco} complex formation occurs in the presence of ATP (Zylicz et al., 1987). This is because ATP binding induces a global conformational change in DnaK (Palleros et al., 1991; Schmid et al., 1994). However, using fluorescence correlation measurements and protein affinity chromatography with C8-coupled ATP-agarose we detected an interaction between DnaK_{Tth} and GrpE_{Tth} wild type in the presence of ATP. This observation suggests that even in the presence of ATP the

nucleotide exchange factor GrpE_{Tth} does not lose a contact with DnaK_{Tth} via its β -sheet domain that could be a special feature of the thermophile DnaK chaperone system. The rate limiting step of the overall ATPase cycle of DnaK_{Tth} is the second step of ATP binding, which is a conformational change that is independent of ATP concentration but is accelerated in the presence of GrpE_{Tth}. Therefore, GrpE_{Tth} causes a switch from the ADP state of DnaK_{Tth} that is dominant in the absence of GrpE_{Tth} to the ATP state by accelerating both binding of ATP and release of ADP.

According to DSC measurements performed, complex formation between DnaK and GrpE(Δ C) was not detectable in either absence or presence of ADP. It is very likely that contact areas located at the α -helical part of GrpE are disrupted with temperature increase. This hypothesis was confirmed by experiments with Ni-NTA columns. It was observed that GrpE(Δ C) binds to DnaK_{Chis} after incubation at 30 and 55 °C. However, after incubation of these proteins at 70 °C GrpE(Δ C) was not detected in elution fractions together with DnaK_{Chis}, suggesting that high temperature may cause dissociation of a DnaK_{Chis}-GrpE(Δ C) complex or prevent its formation. It is known that the dissociation constant of a protein-protein complex is a function of temperature. According to the Van't Hoff equation (eq. 4.1) $d \ln K_d/dT > 0$ for a reaction that is endothermic ($\Delta H > 0$):

$$\frac{d \ln K_d}{dT} = \frac{\Delta H}{RT^2} \quad (4.1)$$

A positive slope means that $\ln K_d$, and therefore K_d itself, increases as the temperature rises. *T.thermophilus* whose molecular chaperones were studied in this work usually lives in an environment with a temperature of approximately 75 °C. Using ITC measurements it was previously observed that GrpE_{Tth} wild type interacts with DnaK_{Tth} at 25, 50 and 75 °C (Groemping, 2000). The K_d^{equ} values detected at different temperatures were 0.11 μ M, 0.14 μ M and 0.31 μ M at 25, 50 and 75 °C, respectively. Taken together, the data presented in this work and published by Groemping (2000) clearly show GrpE's β -sheet domain is necessary for the stable interaction with DnaK_{Tth} at elevated temperatures.

In addition to the direct interaction between DnaK and GrpE(Δ C) detected by protein affinity chromatography, the C-terminally truncated nucleotide exchange factor was found to compete with unfolded protein (urea denatured Lactate dehydrogenase from *S.scrofa* muscle) for binding of DnaK. Taking into account that unfolded substrate binds to the peptide binding

domain of DnaK, we could propose that GrpE lacking the C-terminal β -sheet domain also interacts with this DnaK domain or with at least overlapping sites on DnaK where substrate protein binds. Using radioactively labelled peptide Mehl *et al.* (2001) observed that the GrpE_{Eco}(1-89) mutant containing only the α -helical tail is able to decrease the amount of DnaK-bound peptide. Therefore it is possible to assume that the α -helical part of GrpE from *T.thermophilus* can also directly stimulate displacement of bound substrate from DnaK that may not need interdomain communication within DnaK.

However, the region of GrpE's long α helical tail which influences DnaK-peptide interactions is still unknown. Using radioactively labeled carboxymethylated α -lactalbumin, a permanently unfolded model substrate of DnaK, it was observed that the flexible tail region of GrpE_{Eco} including residues 1 to 33 is necessary for dissociation of a complex between DnaK_{Eco} and substrate (Harrison *et al.*, 1997). It was also shown through surface plasmon resonance technique that the GrpE residues 1-33 are necessary for a complex formation between GrpE_{Eco} and single peptide binding domain of DnaK_{Eco}, DnaK_{Eco} (393-507) (Chesnokova *et al.*, 2003).

The effort to map the specific location where GrpE_{Th}'s tail interacts with DnaK_{Th}'s substrate binding domain was unsuccessful. In detail, the shift in position of the emission maximum of the GrpE(N5C)IANBD and GrpE(V17C)IANBD after incubation with an excess of DnaK were 1.5 nm and 2.5 nm respectively without changing fluorescence intensity. These results show that GrpE_{Th} at position 5 and 17 does not directly bind into the substrate binding pocket of DnaK_{Th}. It could be possible however that the flexible region of GrpE_{Th} (residues 1-33) binds outside the substrate-binding pocket of DnaK_{Th} and thus stimulates the release of the bound substrate.

4.4. Regulation of the DnaK_{Th} Chaperone Cycle on the Level of the DnaK_{Th}-GrpE_{Th} Interactions

In this work we monitored interactions between the molecular chaperone DnaK_{Th} and its nucleotide exchange factor GrpE_{Th}. According to data obtained in these studies the mechanism by which GrpE_{Th} controls the DnaK_{Th} function is proposed as follows.

(1) The ADP state is a holding state of DnaK_{Tth} where a substrate protein is locked in the peptide binding pocket of DnaK_{Tth} and therefore binding and release of a substrate is very slow. ADP release is a rate limiting step in the DnaK_{Tth} chaperone cycle. Therefore the ADP state predominates under cellular conditions in *T.thermophilus* in the absence of GrpE_{Tth}.

(2) The refolding of a substrate can only proceed upon release from DnaK. To overcome the rate limiting ADP-bound state and stimulate substrate release, GrpE_{Tth} binds to DnaK_{Tth} by forming direct contacts with the ATPase domain and the peptide binding domain. The GrpE_{Tth} β -sheet domain stimulates opening of the ATPase domain that result in ADP release. The GrpE_{Tth} α -helical tail alters the conformation of the peptide binding domain in such a way as to make this domain open and solvent accessible. The net result of this step is release of ADP and a substrate.

(3) In a GrpE_{Tth}-DnaK_{Tth} complex GrpE_{Tth} contacts with both the ATPase domain and the peptide binding domain of DnaK_{Tth} keeping them in an open conformation. However, substrate binding is not allowed due to interaction of the GrpE_{Tth} α -helical part with the peptide binding domain of DnaK_{Tth}.

(4-5) ATP binding could be a trigger permitting a substrate to be bound by DnaK_{Tth}. However, the second step of ATP binding, which is a conformational change of DnaK_{Tth} is the second rate limiting step in the overall ATPase cycle of DnaK_{Tth}. Therefore the GrpE_{Tth} β -sheet domain keeping the ATPase domain in an open conformation accelerates binding of ATP and thus also overcomes this rate limiting step. We can assume two possible mechanisms permitting substrate to be bound by DnaK_{Tth}: 1) ATP stimulates a hinge bending motion between the ATPase domain and substrate binding domains; 2) the GrpE_{Tth} β -sheet domain recognising the ATP bound state of DnaK_{Tth} carries the signal into the substrate binding domain via the long α -helical tail that stimulates mechanical movement of the substrate binding domain. ATP supports an open conformation of the substrate binding domain making its accessible for a substrate binding.

(6) The final conformational changes in DnaK_{Tth} result in the weakness of the binding between the GrpE_{Tth} β -sheet domain and the ATPase domain of DnaK_{Tth}. Finally, GrpE_{Tth}

releases from a $\text{DnaK}_{\text{Tth}} \cdot \text{GrpE}_{\text{Tth}}$ complex leaving DnaK_{Tth} in ATP state which converts to the ADP state via ATP hydrolysis locking a substrate in a substrate binding pocket.

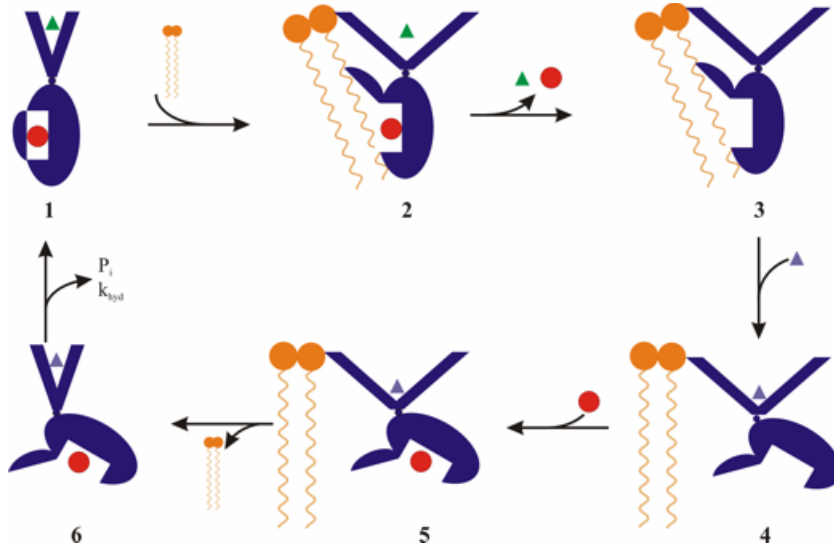
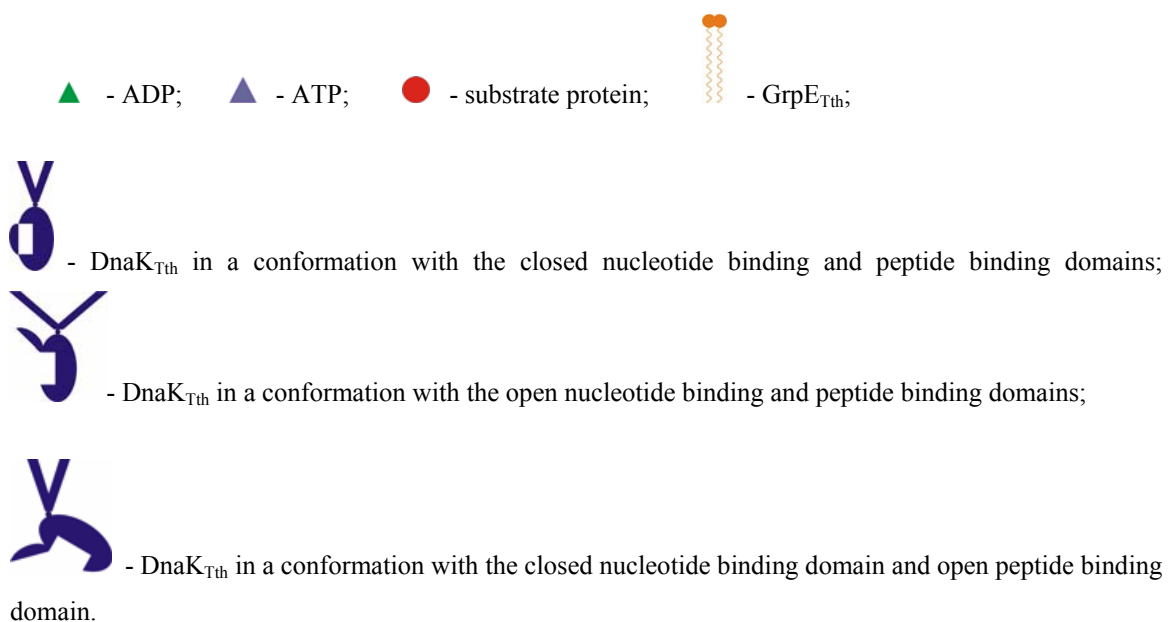


Figure 4.1: Model for the regulated DnaK_{Tth} chaperone cycle on the level of the $\text{DnaK}_{\text{Tth}}\text{-GrpE}_{\text{Tth}}$ interactions. (1) The ADP bound conformation of DnaK_{Tth} is a substrate holding state where the substrate is locked in the substrate binding pocket. (2) GrpE_{Tth} binds to DnaK_{Tth} and stimulates opening of its ATPase and peptide binding domains which allows the release of ADP and substrate. (3) The α -helical domain of GrpE_{Tth} interacting with the peptide binding domain in the nucleotide free state of DnaK_{Tth} does not permit binding of the substrate. (4-5) ATP binding which is controlled by GrpE_{Tth} triggers off conformational changes in DnaK_{Tth} allowing rebinding of the substrate. (6) Conformational changes in DnaK_{Tth} induced by ATP result in release of GrpE_{Tth} .



4.5. Outlook

Our studies have raised important questions regarding the DnaK-ClpB system assisted reactivation of chemically and thermally denatured Lactate dehydrogenase (LDH) as well as functional cooperation between GrpE and DnaK from *T.thermophilus*.

The detailed kinetic studies of LDH (from *S.scrofa* muscle and *B.stearothermophilus*) unfolding and refolding will provide ample opportunity to disclose chaperone-assisted refolding of this tetrameric enzyme. Not only do we need to understand basic intermediates that are possible during the refolding process, but also we need to understand the kinetics of heat induced aggregate formation and characterize the product of aggregation. The process of protein aggregation should be defined and characterized by different methods (DLS, electron microscopy). When we know the quality of aggregates (induced by heat) of the prokaryotic thermophilic LDH and eukaryotic mesophilic LDH, then we will be able to assess if our detected difference in DnaK_{Th}-ClpB_{Th} chaperone system assisted reactivation of the heat denatured LDH from *B.stearothermophilus* and *S.scrofa* muscle correlates with different aggregation states.

The detected interaction between GrpE and DnaK lacking a covalent link between its ATPase domain (residues 1-381) and substrate binding domain (residues 382-615) could be a foundation for further investigation of chaperone activity of the DnaK lacking a covalent structural coupling between its domains. In this way, the enzymatic recovery of urea-denatured Lactate dehydrogenase (LDH) from *S.scrofa* muscle (or heat-denatured LDH from *B.stearothermophilus*) could be monitored in the presence of the DnaK system where DnaK is substituted by the ATPase domain and substrate binding domain.

The detailed binding kinetics of the MABA-ADP, fluorescent analog of ADP, to the single DnaK ATPase domain as well as peptide binding properties of the single peptide binding domain should be investigated to get insight into the biological activity of these domains.

Research into the functional cooperation between thermophile DnaK and GrpE must also include the function of GrpE as a molecular bridge transporting the signal from the ATPase domain to the substrate binding domain. Our understanding of the interdomain communication of DnaK via nucleotide exchange factor GrpE would be greatly advanced from carefully performed FRET studies. The N-terminal part of GrpE and the single peptide binding domain of DnaK should be labeled with different fluorophores forming a FRET pair. Monitoring FRET in a complex comprising labeled GrpE, the ATPase domain of DnaK and the labeled peptide binding domain might reveal an additional possible mechanism for the interdomain communication of DnaK.

In this thesis we reported that the α -helical part of GrpE (GrpE(Δ C)) competes with a substrate for the peptide binding domain of DnaK. Fluorescence measurements with a labeled peptide will help to reveal a further possible ability of GrpE(Δ C) to stimulate peptide release.

Our evidence that the flexible N-terminal part of GrpE at position 5 and 17 does not directly bind into the substrate binding pocket of DnaK could be a basis for study of its regulatory role in substrate release. Future work will involve mapping the specific location where the GrpE's tail interacts with DnaK's substrate binding domain. This site is likely to be situated above position 17. Finally, X-ray crystallography of the GrpE-DnaK complex will help to reveal further the true nature of chaperone-mediated protein folding.

5. Summary

In the living cell, proteins need molecular chaperones to prevent off pathway folding. The molecular chaperone DnaK from *T.thermophilus* belongs to the Hsp70 family. Hsp70 proteins are composed of a highly conserved N-terminal part that comprises the ATPase domain and a less conserved C-terminal peptide binding domain. DnaK cycles between an ADP-bound, high affinity state that tightly binds unfolded substrate and ATP-bound, low affinity state that weakly binds unfolded substrate. GrpE serves as a nucleotide exchange factor, facilitating the release of ADP in exchange for ATP. With the assistance of GrpE, DnaK is re-converted from the ADP-state into the ATP-state. The GrpE protein forms dimers in solution and its structure could be divided into three regions: paired N-terminal α -helices, four helix bundles, and the C-terminal domains.

According to the yield of recovery of enzymatic activity mediated by the DnaK-ClpB system we found that urea-denatured Lactate dehydrogenase (LDH) from *S.scrofa* (pig) muscle and heat-inactivated LDH from *B.stearothermophilus* could be suitable model substrates for the DnaK-ClpB chaperone system from *T.thermophilus*.

Using the fluorescence correlation spectroscopy technique it was observed that GrpE wild type binds to a DnaK-ADP and DnaK-peptide complex. These results lead us to suggest that GrpE plays a role not only in nucleotide exchange but that it is also involved in stimulation of a substrate release. In this thesis we reported for the first time that GrpE wild type interacts with DnaK in the ATP-bound form. It was also observed for the first time that a covalent link between the ATPase and peptide binding domain of DnaK is likely not important for the interaction between DnaK and GrpE.

In this work the contribution of the α -helical part of GrpE (GrpE(Δ C)) to interactions with DnaK was defined. Investigations of the interaction between GrpE(Δ C) and DnaK using Ni-NTA columns and C8-coupled ATP-agarose revealed that the α -helical part of GrpE binds specifically to DnaK. The specificity is related to the nature of nucleotide bound to the

ATPase domain of DnaK. In the presence of ADP GrpE(Δ C) binds to DnaK while in the presence of ATP the interaction between these proteins was not observed. This finding implies that ATP induces a conformational change in DnaK in such a way to abolish binding of the α -helical part of GrpE. Therefore it is possible that ATP determines not only the substrate affinity of DnaK but it also regulates binding of the N-terminal α -helical tail of GrpE. Another explanation of the disruption of GrpE(Δ C)-DnaK interactions in the presence of ATP is based on two observations obtained using the fluorescence correlation spectroscopy technique: (1) the single ATPase domain and peptide binding domain of DnaK lacking a covalent link are able to interact in the presence of GrpE; (2) GrpE wild type interacts with DnaK in the presence of ATP. These findings imply that the GrpE β -sheet domain recognises the ATP-bound state of DnaK followed by signal transduction into the peptide binding domain of DnaK via the GrpE long α -helical tail which stimulates movement of the peptide binding domain away from the GrpE α -helical part.

Using urea-denatured Lactate dehydrogenase from *S.scrofa* muscle as a model substrate bound to DnaK, we found evidence that the α -helical part of GrpE competes with the substrate for the DnaK peptide binding domain. It represents a very good framework for defining the mechanism by which GrpE(Δ C) could possibly stimulate substrate release from DnaK.

Based upon all these observations, a mechanism for regulation of the DnaK_{Tth} chaperone cycle on the level of the DnaK_{Tth}-GrpE_{Tth} interactions was postulated.

6. List of Abbreviations

A	Absorption
AAA	ATPases associated with a variety of cellular activities
ADP	Adenosine 5'-diphosphate
AMP	Adenosine monophosphate
APS	Ammoniumperoxodisulphate
ATP	Adenosine 5'-triphosphate
BSA	Bovine serum albumin
<i>B.stearothermophilus</i> , _{Bst}	<i>Bacillus stearothermophilus</i>
CD	Circular dichroism
Clp	Caseinolytic protease
DEAE	Diethylammoniummethyl-
DMF	Dimethyl formamide
DTT	Dithiothreitol
<i>E.coli</i> , _{Eco}	<i>Escherichia coli</i>
FPLC	Fast Performance Liquid Chromatography
FRET	Fluorescence Resonance Energy Transfer
g	Gram
GdnHCl	Guanidine hydrochloride
HEPES	N-(2-hydroxyethyl)piperazine-N'-(2-ethanesulfonic acid)
HPLC	High Performance Liquid Chromatography
Hsc	Heat shock cognate (protein)
Hsp	Heat shock protein
IPTG	Isopropyl-beta-D-thiogalactopyranoside
ITC	Isothermal Titration Calorimetry
k_{cat}	Catalytic rate constant
K_d	Dissociation constant
kDa	kiloDalton
K_m	Michaelis-Menten constant
KOAc	Potassium acetate
KPi	Potassium phosphate
l	Liter
LDH	Lactate dehydrogenase
ml	Milliliter
ms	Millisecond
NAD^+	Nicotinamide adenine dinucleotide, oxidized form
NADH	Nicotinamide adenine dinucleotide, reduced form
NBD	Nucleotide binding domain
nm	Nanometer
NTA	Nitrilotriacetic acid
OD ₆₀₀	optical density at 600 nm
PAGE	Polyacrylamide-gel electrophoresis
PBD	Peptide binding domain
PCR	Polymerase chain reaction

rpm	Revolutions per minute
<i>S.scrofa</i> , _{Ssc}	<i>Sus scrofa</i>
SDS	Sodium dodecyl sulfate
SFB	Standard fluorescence buffer
<i>T.thermophilus</i> , _{Tth}	<i>Thermus thermophilus</i>
TCA	Trichloroacetic acid
TEMED	N,N,N',N'-tetramethylethylenediamine
T _m	Melting temperature
Tris	Tris(hydroxymethyl)aminomethane
v/v	volume/volume
w/v	weight/volume

7. Literature

Bochtler,M, C Hartmann, H K Song, G P Bourenkov, H D Bartunik, R Huber, 2000, The structures of HsIU and the ATP-dependent protease HsIU-HsIV: *Nature*, v. 403, p. 800-805.

Bonifacino,JS, P Cosson, R D Klausner, 1990, Colocalized transmembrane determinants for ER degradation and subunit assembly explain the intracellular fate of TCR chains: *Cell*, v. 63, p. 503-513.

Bradford,MM, 1976, A rapid and sensitive method for the quantitation of microgram quantities of protein utilizing the principle of protein-dye binding: *Anal.Biochem.*, v. 72, p. 248-254.

Braig,K, Z Otwinowski, R Hegde, D C Boisvert, A Joachimiak, A L Horwich, P B Sigler, 1994, The crystal structure of the bacterial chaperonin GroEL at 2.8 Å [see comments]: *Nature*, v. 371, p. 578-586.

Braig,K, M Simon, F Furuya, J F Hainfeld, A L Horwich, 1993, A polypeptide bound by the chaperonin groEL is localized within a central cavity: *Proc.Natl.Acad.Sci.U.S.A.*, v. 90, p. 3978-3982.

Brehmer,D, S Rüdiger, C S Gassler, D Klostermeier, L Packschies, J Reinstein, M P Mayer, B Bukau, 2001, Tuning of chaperone activity of Hsp70 proteins by modulation of nucleotide exchange: *Nat.Struct.Biol.*, v. 8, p. 427-432.

Buchberger,A, J Reinstein, B Bukau. The DnaK chaperone system. *Inst.Biochem.& Mol.Biol.* 2, 2-14. 1997.

Buchberger,A, H Schröder, M Buttner, A Valencia, B Bukau, 1994a, A conserved loop in the ATPase domain of the DnaK chaperone is essential for stable binding of GrpE: *Nat.Struct.Biol.*, v. 1, p. 95-101.

Buchberger,A, A Valencia, R McMacken, C Sander, B Bukau, 1994b, The chaperone function of DnaK requires the coupling of ATPase activity with substrate binding through residue E171: *EMBO J.*, v. 13, p. 1687-1695.

- Bukau,B, E Deuerling, C Pfund, E A Craig, 2000, Getting newly synthesized proteins into shape: *Cell*, v. 101, p. 119-122.
- Burston,SG, N A Ranson, A R Clarke, 1995, The origins and consequences of asymmetry in the chaperonin reaction cycle: *J.Mol.Biol.*, v. 249, p. 138-152.
- Chen,L, P B Sigler, 1999, The crystal structure of a GroEL/peptide complex: plasticity as a basis for substrate diversity: *Cell*, v. 99, p. 757-768.
- Chen,S, A M Roseman, A S Hunter, S P Wood, S G Burston, N A Ranson, A R Clarke, H R Saibil, 1994, Location of a folding protein and shape changes in GroEL-GroES complexes imaged by cryo-electron microscopy: *Nature*, v. 371, p. 261-264.
- Chen,SS, P C Engel, 1975, Modification of pig M4 lactate dehydrogenase by pyridoxal 5'-phosphate. Demonstration of an essential lysine residue: *Biochem.J.*, v. 149, p. 107-113.
- Chesnokova,LS, S V Slepnev, I I Protasevich, M G Sehorn, C G Brouillette, S N Witt, 2003, Deletion of DnaK's lid strengthens binding to the nucleotide exchange factor, GrpE: a kinetic and thermodynamic analysis: *Biochemistry*, v. 42, p. 9028-9040.
- Chuang,SE, V Burland, G Plunkett, III, D L Daniels, F R Blattner, 1993, Sequence analysis of four new heat-shock genes constituting the hslTS/ibpAB and hslVU operons in *Escherichia coli*: *Gene*, v. 134, p. 1-6.
- Cowan,NJ, S A Lewis, 2001, Type II chaperonins, prefoldin, and the tubulin-specific chaperones: *Adv.Protein Chem.*, v. 59, p. 73-104.
- Diamant,S, A Peres Ben-Zvi, B Bukau, P A Goloubinoff, 2000, Size-Dependent Disaggregation of Stable Protein Aggregates by the DnaK Chaperone Machinery: *J.Biol.Chem.*
- Dunn,CR, H M Wilks, D J Halsall, T Atkinson, A R Clarke, H Muirhead, J J Holbrook, 1991, Design and synthesis of new enzymes based on the lactate dehydrogenase framework: *Philos.Trans.R.Soc.Lond B Biol.Sci.*, v. 332, p. 177-184.
- Ehresmann,B, P Imbault, J H Weil, 1973, Spectrophotometric determination of protein concentration in cell extracts containing tRNA's and rRNA's: *Anal.Biochem.*, v. 54, p. 454-463.
- Ellis,RJ, 1997, Do molecular chaperones have to be proteins?: *Biochem.Biophys.Res.Comm.*, v. 238, p. 687-692.
- Ellis,RJ, 2001a, Macromolecular crowding: an important but neglected aspect of the intracellular environment: *Curr.Opin.Struct.Biol.*, v. 11, p. 114-119.
- Ellis,RJ, 2001b, Molecular chaperones: inside and outside the Anfinsen cage: *Curr.Biol.*, v. 11, p. R1038-R1040.

Engel, A, M K Hayer-Hartl, K N Goldie, G Pfeifer, R Hegerl, S Muller, A C da Silva, W Baumeister, F U Hartl, 1995, Functional significance of symmetrical versus asymmetrical GroEL-GroES chaperonin complexes: *Science*, v. 269, p. 832-836.

Ewalt, KL, J P Hendrick, W A Houry, F U Hartl, 1997, In vivo observation of polypeptide flux through the bacterial chaperonin system: *Cell*, v. 90, p. 491-500.

Flaherty, KM, C DeLuca-Flaherty, D B McKay, 1990, Three-dimensional structure of the ATPase fragment of a 70K heat-shock cognate protein: *Nature*, v. 346, p. 623-628.

Flaherty, KM, S M Wilbanks, C DeLuca-Flaherty, D B McKay, 1994, Structural basis of the 70-kilodalton heat shock cognate protein ATP hydrolytic activity. II. Structure of the active site with ADP or ATP bound to wild type and mutant ATPase fragment: *J.Biol.Chem.*, v. 269, p. 12899-12907.

Frydman, J, E Nimmesgern, H Erdjument-Bromage, J S Wall, P Tempst, F U Hartl, 1992, Function in protein folding of TRiC, a cytosolic ring complex containing TCP-1 and structurally related subunits: *EMBO J.*, v. 11, p. 4767-4778.

Gallie, DR, D Fortner, J Peng, D Puthoff, 2002, ATP-dependent hexameric assembly of the heat shock protein Hsp101 involves multiple interaction domains and a functional C-proximal nucleotide-binding domain: *J.Biol.Chem.*, v. 277, p. 39617-39626.

Glover, JR, S Lindquist, 1998, Hsp104, Hsp70, and Hsp40: a novel chaperone system that rescues previously aggregated proteins: *Cell*, v. 94, p. 73-82.

Goloubinoff, P, A Mogk, A P Zvi, T Tomoyasu, B Bukau, 1999, Sequential mechanism of solubilization and refolding of stable protein aggregates by a bichaperone network: *Proc.Natl.Acad.Sci.U.S.A.*, v. 96, p. 13732-13737.

Gottesman, S, W P Clark, V Crecy-Lagard, M R Maurizi, 1993, ClpX, an alternative subunit for the ATP-dependent Clp protease of *Escherichia coli*. Sequence and in vivo activities: *J.Biol.Chem.*, v. 268, p. 22618-22626.

Gottesman, S, W P Clark, M R Maurizi, 1990, The ATP-dependent Clp protease of *Escherichia coli*. Sequence of *clpA* and identification of a Clp-specific substrate: *J.Biol.Chem.*, v. 265, p. 7886-7893.

Greene, MK, K Maskos, S J Landry, 1998, Role of the J-domain in the cooperation of Hsp40 with Hsp70: *Proc.Natl.Acad.Sci.U.S.A.*, v. 95, p. 6108-6113.

Groemping, Y. Kinetische und funktionelle Untersuchungen des DnaK-Systems aus *Thermus thermophilus* und heterogener Komplexe aus *T. thermophilus* und *E.coli*. 2000.

Groemping, Y, D Klostermeier, C Herrmann, T Veit, R Seidel, J Reinstein, 2001, Regulation of ATPase and chaperone cycle of DnaK from *Thermus thermophilus* by the nucleotide exchange factor GrpE: *J.Mol.Biol.*, v. 305, p. 1173-1183.

- Groemping,Y, J Reinstein, 2001, Folding properties of the nucleotide exchange factor GrpE from *Thermus thermophilus*: GrpE is a thermosensor that mediates heat shock response: *J.Mol.Biol.*, v. 314, p. 167-178.
- Guo,F, M R Maurizi, L Esser, D Xia, 2002, Crystal structure of ClpA, an Hsp100 chaperone and regulator of ClpAP protease: *J.Biol.Chem.*, v. 277, p. 46743-46752.
- Harrison,CJ, M Hayer-Hartl, M Di Liberto, F Hartl, J Kuriyan, 1997, Crystal structure of the nucleotide exchange factor GrpE bound to the ATPase domain of the molecular chaperone DnaK: *Science*, v. 276, p. 431-435.
- Hartl,FU, 1996, Molecular chaperones in cellular protein folding: *Nature*, v. 381, p. 571-579.
- Hartl,FU, M Hayer-Hartl, 2002, Molecular chaperones in the cytosol: from nascent chain to folded protein: *Science*, v. 295, p. 1852-1858.
- Haugland,RP, 1996, Eugene, OR, Molecular Probes, Inc.
- Haustein,E, P Schwille, 2003, Ultrasensitive investigations of biological systems by fluorescence correlation spectroscopy: *Methods*, v. 29, p. 153-166.
- Hesterkamp,T, B Bukau, 1998, Role of the DnaK and HscA homologs of Hsp70 chaperones in protein folding in *E.coli*: *EMBO J.*, v. 17, p. 4818-4828.
- Holmes,KC, C Sander, A Valencia, 1993, A new ATP-binding fold in actin, hexokinase and Hsc70: *Trends Cell Biol.*, v. 3, p. 60-65.
- Horovitz,A, Y Fridmann, G Kafri, O Yifrach, 2001, Review: allostery in chaperonins: *J.Struct.Biol.*, v. 135, p. 104-114.
- Horwich,A, 2002, Protein aggregation in disease: a role for folding intermediates forming specific multimeric interactions: *J.Clin.Invest*, v. 110, p. 1221-1232.
- Horwich,AL, J S Weissman, 1997, Deadly conformations--protein misfolding in prion disease: *Cell*, v. 89, p. 499-510.
- Houry,WA, D Frishman, C Eckerskorn, F Lottspeich, F U Hartl, 1999, Identification of in vivo substrates of the chaperonin GroEL: *Nature*, v. 402, p. 147-154.
- Hunt,JF, A J Weaver, S J Landry, L Gierasch, J Deisenhofer, 1996, The crystal structure of the GroES co-chaperonin at 2.8 Å resolution: *Nature*, v. 379, p. 37-45.
- Hwang,BJ, K M Woo, A L Goldberg, C H Chung, 1988, Protease Ti, a new ATP-dependent protease in *Escherichia coli*, contains protein-activated ATPase and proteolytic functions in distinct subunits: *J.Biol.Chem.*, v. 263, p. 8727-8734.
- Jackson,SE, A R Fersht, 1991, Folding of chymotrypsin inhibitor 2. 1. Evidence for a two-state transition: *Biochemistry*, v. 30, p. 10428-10435.

- Jaenicke,R, 1998, Protein self-organization in vitro and in vivo: partitioning between physical biochemistry and cell biology: *Biol.Chem.*, v. 379, p. 237-243.
- Jaenicke,R, R Seckler, 1997, Protein misassembly in vitro: *Advances in Protein Chemistry*, Vol 50, v. 50, p. 1-&.
- Jordan,R, R McMacken, 1995, Modulation of the ATPase activity of the molecular chaperone DnaK by peptides and the DnaJ and GrpE heat shock proteins: *J.Biol.Chem.*, v. 270, p. 4563-4569.
- Karzai,AW, R McMacken, 1996, A bipartite signaling mechanism involved in DnaJ-mediated activation of the Escherichia coli DnaK protein: *J.Biol.Chem.*, v. 271, p. 11236-11246.
- Kinjo,AR, S Takada, 2002, Effects of macromolecular crowding on protein folding and aggregation studied by density functional theory: dynamics: *Phys.Rev.E.Stat.Nonlin.Soft.Matter Phys.*, v. 66, p. 051902.
- Klostermeier,D, R Seidel, J Reinstein, 1998, Functional properties of the molecular chaperone DnaK from *Thermus thermophilus*: *J.Mol.Biol.*, v. 279, p. 841-853.
- Klostermeier,D, R Seidel, J Reinstein, 1999, The functional cycle and regulation of the *Thermus thermophilus* DnaK chaperone system: *J.Mol.Biol.*, v. 287, p. 511-525.
- Kobayashi,Y, G Sobue, 2001, Protective effect of chaperones on polyglutamine diseases: *Brain Res.Bull.*, v. 56, p. 165-168.
- Kragelund,BB, C V Robinson, J Knudsen, C M Dobson, F M Poulsen, 1995, Folding of a four-helix bundle: studies of acyl-coenzyme A binding protein: *Biochemistry*, v. 34, p. 7217-7224.
- Laemmli,UK, 1970, Cleavage of structural proteins during the assembly of the head of bacteriophage T4: *Nature*, v. 227, p. 680-685.
- Langer,T, C Lu, H Echols, J Flanagan, M K Hayer, F U Hartl, 1992a, Successive action of DnaK, DnaJ and GroEL along the pathway of chaperone-mediated protein folding: *Nature*, v. 356, p. 683-689.
- Langer,T, G Pfeifer, J Martin, W Baumeister, F U Hartl, 1992b, Chaperonin-mediated protein folding: GroES binds to one end of the GroEL cylinder, which accommodates the protein substrate within its central cavity: *EMBO J.*, v. 11, p. 4757-4765.
- Laufen,T, M P Mayer, C Beisel, D Klostermeier, A Mogk, J Reinstein, B Bukau, 1999, Mechanism of regulation of Hsp70 chaperones by DnaJ cochaperones: *PNAS*, v. 96, p. 5452-5457.
- Laufen,T, U Zuber, A Buchberger, B Bukau. DnaJ Proteins. *Molecular Chaperones in Proteins 1*, 241-274. 1997.

- Lenzen,C, R H Cool, H Prinz, J Kuhlmann, A Wittinghofer, 1998, Kinetic analysis by fluorescence of the interaction between Ras and the catalytic domain of the guanine nucleotide exchange factor Cdc25Mm: *Biochemistry*, v. 37, p. 7420-7430.
- Liberek,K, J Marszalek, D Ang, C Georgopoulos, M Zylicz, 1991, Escherichia coli DnaJ and GrpE heat shock proteins jointly stimulate ATPase activity of DnaK: *Proc.Natl.Acad.Sci.U.S.A.*, v. 88, p. 2874-2878.
- Makarov,AA, I I Protasevich, V M Lobachov, M P Kirpichnikov, G I Yakovlev, R M Gilli, C M Briand, R W Hartley, 1994, Thermostability of the barnase-barstar complex: *FEBS Lett.*, v. 354, p. 251-254.
- Mally,A, S N Witt, 2001, GrpE accelerates peptide binding and release from the high affinity state of DnaK: *Nat.Struct.Biol.*, v. 8, p. 254-257.
- Martin,J, M Mayhew, T Langer, F U Hartl, 1993, The reaction cycle of GroEL and GroES in chaperonin-assisted protein folding: *Nature*, v. 366, p. 228-233.
- Martinez,JC, M el Harrous, V V Filimonov, P L Mateo, A R Fersht, 1994, A calorimetric study of the thermal stability of barnase and its interaction with 3'GMP: *Biochemistry*, v. 33, p. 3919-3926.
- Martinez,JC, V V Filimonov, P L Mateo, G Schreiber, A R Fersht, 1995, A calorimetric study of the thermal stability of barstar and its interaction with barnase: *Biochemistry*, v. 34, p. 5224-5233.
- Maurizi,MR, 1992, Proteases and protein degradation in Escherichia coli: *Experientia*, v. 48, p. 178-201.
- Mayhew,M, A C da Silva, J Martin, H Erdjument-Bromage, P Tempst, F U Hartl, 1996, Protein folding in the central cavity of the GroEL-GroES chaperonin complex: *Nature*, v. 379, p. 420-426.
- McCarty,JS, A Buchberger, J Reinstein, B Bukau, 1995, The Role of ATP in the Functional Cycle of the DnaK Chaperone System: *J.Mol.Biol.*, v. 249, p. 126-137.
- Mehl,AF, L D Heskett, K M Neal, 2001, A GrpE mutant containing the NH(2)-terminal "tail" region is able to displace bound polypeptide substrate from DnaK: *Biochem.Biophys.Res.Commun.*, v. 282, p. 562-569.
- Mogk,A, T Tomoyasu, P Goloubinoff, S Rudiger, D Roder, H Langen, B Bukau, 1999, Identification of thermolabile Escherichia coli proteins: prevention and reversion of aggregation by DnaK and ClpB: *EMBO J.*, v. 18, p. 6934-6949.
- Motohashi,K, Y Watanabe, M Yohda, M Yoshida, 1999, Heat-inactivated proteins are rescued by the DnaK-J-GrpE set and ClpB chaperones: *Proc.Natl.Acad.Sci.U.S.A.*, v. 96, p. 7184-7189.

Neuwald,AF, L Aravind, J L Spouge, E V Koonin, 1999, AAA+: A class of chaperone-like ATPases associated with the assembly, operation, and disassembly of protein complexes: *Genome Res.*, v. 9, p. 27-43.

Nikolaeva,OP, V N Orlov, I V Dedova, V A Drachev, D I Levitsky, 1996, Interaction of myosin subfragment 1 with F-actin studied by differential scanning calorimetry: *Biochem.Mol.Biol.Int.*, v. 40, p. 653-661.

Packschies,L, H Theyssen, A Buchberger, B Bukau, R S Goody, J Reinstein, 1997, GrpE accelerates nucleotide exchange of the molecular chaperone DnaK with an associative displacement mechanism: *Biochemistry*, v. 36, p. 3417-3422.

Palleros,DR, K L Reid, J S McCarty, G C Walker, A L Fink, 1992, DnaK, hsp73, and their molten globules. Two different ways heat shock proteins respond to heat: *J.Biol.Chem.*, v. 267, p. 5279-5285.

Palleros,DR, W J Welch, A L Fink, 1991, Interaction of hsp70 with unfolded proteins: effects of temperature and nucleotides on the kinetics of binding: *Proc.Natl.Acad.Sci.U.S.A.*, v. 88, p. 5719-5723.

Patel,S, M Latterich, 1998, The AAA team: related ATPases with diverse functions: *Trends Cell Biol.*, v. 8, p. 65-71.

Peitsch,MC, 1996, ProMod and Swiss-Model: Internet-based tools for automated comparative protein modelling: *Biochem.Soc.Trans.*, v. 24, p. 274-279.

Pellecchia,M, T Szyperski, D Wall, C Georgopoulos, K Wuthrich, 1996, NMR structure of the J-domain and the Gly/Phe-rich region of the Escherichia coli DnaJ chaperone: *J.Mol.Biol.*, v. 260, p. 236-250.

Pramanik,A, R Rigler, 2001, Ligand-receptor interactions in the membrane of cultured cells monitored by fluorescence correlation spectroscopy: *Biol.Chem.*, v. 382, p. 371-378.

Reid,KL, A L Fink, 1996, Physical interactions between members of the DnaK chaperone machinery: characterization of the DnaK.GrpE complex: *Cell Stress.Chaperones.*, v. 1, p. 127-137.

Richardson,A, S J Landry, C Georgopoulos, 1998, The ins and outs of a molecular chaperone machine: *Trends Biochem.Sci.*, v. 23, p. 138-143.

Rohrwild,M, G Pfeifer, U Santarius, S A Muller, H C Huang, A Engel, W Baumeister, A L Goldberg, 1997, The ATP-dependent HslVU protease from Escherichia coli is a four-ring structure resembling the proteasome: *Nat.Struct.Biol.*, v. 4, p. 133-139.

Rüdiger,S, A Buchberger, B Bukau, 1997, Interaction of Hsp70 chaperones with substrates: *Nat.Struct.Biol.*, v. 4, p. 342-349.

Rüdiger,S, L Germeroth, J Schneider-Mergener, B Bukau, 1997, Substrate specificity of the DnaK chaperone determined by screening cellulose-bound peptide libraries: *EMBO J.*, v. 16, p. 1501-1507.

Russell,R, K A Wali, A F Mehl, R McMacken, 1999, DnaJ dramatically stimulates ATP hydrolysis by DnaK: insight into targeting of Hsp70 proteins to polypeptide substrates: *Biochemistry*, v. 38, p. 4165-4176.

Saibil,H, Z Dong, S Wood, M A auf der, 1991, Binding of chaperonins: *Nature*, v. 353, p. 25-26.

Schär,HP, H Zuber, 1979, Structure and function of L-lactate dehydrogenases from thermophilic and mesophilic bacteria. I) Isolation and characterization of lactate dehydrogenases from thermophilic and mesophilic bacilli: *Hoppe Seylers.Z.Physiol Chem.*, v. 360, p. 795-807.

Schirmer,EC, J R Glover, M A Singer, S Lindquist, 1996, HSP100/Clp proteins: a common mechanism explains diverse functions: *Trends Biochem.Sci.*, v. 21, p. 289-296.

Schlee,S, P Beinker, A Akhrymuk, J Reinstein, 2004, A chaperone network for the resolubilization of protein aggregates: direct interaction of ClpB and DnaK: *J.Mol.Biol.*, v. 336, p. 275-285.

Schmid,D, A Baici, H Gehring, P Christen, 1994, Kinetics of Molecular Chaperone Action: *Science*, v. 263, p. 971-973.

Schönfeld,HJ, D Schmidt, H Schröder, B Bukau, 1995, The DnaK chaperone system of *Escherichia coli*: quaternary structures and interactions of the DnaK and GrpE components: *J.Biol.Chem.*, v. 270, p. 2183-2189.

Schröder,H, T Langer, F U Hartl, B Bukau, 1993, DnaK, DnaJ and GrpE form a cellular chaperone machinery capable of repairing heat-induced protein damage: *EMBO J.*, v. 12, p. 4137-4144.

Sherman,MY, A L Goldberg, 1996, Involvement of molecular chaperones in intracellular protein breakdown: *EXS*, v. 77, p. 57-78.

Shore,JD, D E Day, A M Francis-Chmura, I Verhamme, J Kvassman, D A Lawrence, D Ginsburg, 1995, A fluorescent probe study of plasminogen activator inhibitor-1. Evidence for reactive center loop insertion and its role in the inhibitory mechanism: *J.Biol.Chem.*, v. 270, p. 5395-5398.

Sigler,PB, Z Xu, H S Rye, S G Burston, W A Fenton, A L Horwich, 1998, Structure and function in GroEL-mediated protein folding: *Annu.Rev.Biochem.*, v. 67, p. 581-608.

Sondermann,H, C Scheufler, C Schneider, J Höhfeld, F U Hartl, I Moarefi, 2001, Structure of a Bag/Hsc70 complex: convergent functional evolution of Hsp70 nucleotide exchange factors: *Science*, v. 291, p. 1553-1557.

Squires,CL, S Pedersen, B M Ross, C Squires, 1991, ClpB is the *Escherichia coli* heat shock protein F84.1: *J.Bacteriol.*, v. 173, p. 4254-4262.

Sriram,M, J Osipiuk, B Freeman, R Morimoto, A Joachimiak, 1997, Human Hsp70 molecular chaperone binds two calcium ions within the ATPase domain: *Structure.*, v. 5, p. 403-414.

Stevens, TL, J H Blum, S P Foy, L Matsuuchi, A L DeFranco, 1994, A mutation of the mu transmembrane that disrupts endoplasmic reticulum retention. Effects on association with accessory proteins and signal transduction: *J.Immunol.*, v. 152, p. 4397-4406.

Studier, FW, B A Moffatt, 1986, Use of bacteriophage T7 RNA polymerase to direct selective high-level expression of cloned genes: *J.Mol.Biol.*, v. 189, p. 113-130.

Szabo, A, T Langer, H Schröder, J Flanagan, B Bukau, F U Hartl, 1994, The ATP hydrolysis-dependent reaction cycle of the Escherichia coli Hsp70 system DnaK, DnaJ, and GrpE: *Proc.Natl.Acad.Sci.U.S.A.*, v. 91, p. 10345-10349.

Takayama, S, T Sato, S Krajewski, K Kochel, S Irie, J A Millan, J C Reed, 1995, Cloning and functional analysis of BAG-1: a novel Bcl-2-binding protein with anti-cell death activity: *Cell*, v. 80, p. 279-284.

Teter, SA, W A Houry, D Ang, T Tradler, D Rockabrand, G Fischer, P Blum, C Georgopoulos, F U Hartl, 1999, Polypeptide flux through bacterial Hsp70: DnaK cooperates with trigger factor in chaperoning nascent chains: *Cell*, v. 97, p. 755-765.

Turnell, WG, J T Finch, 1992, Binding of the dye congo red to the amyloid protein pig insulin reveals a novel homology amongst amyloid-forming peptide sequences: *J.Mol.Biol.*, v. 227, p. 1205-1223.

Volkin, DB, A M Klibanov, 1987, Thermal destruction processes in proteins involving cystine residues: *J.Biol.Chem.*, v. 262, p. 2945-2950.

Volkin, DB, A M Klibanov, 1992, Alterations in the structure of proteins that cause their irreversible inactivation: *Dev.Biol.Stand.*, v. 74, p. 73-80.

Volkin, DB, H Mach, C R Middaugh, 1997, Degradative covalent reactions important to protein stability: *Mol.Biotechnol.*, v. 8, p. 105-122.

Wall, D, M Zylicz, C Georgopoulos, 1994, The NH₂-terminal 108 amino acids of the Escherichia coli DnaJ protein stimulate the ATPase activity of DnaK and are sufficient for lambda replication: *J.Biol.Chem.*, v. 269, p. 5446-5451.

Webb, HM, L W Ruddock, R J Marchant, K Jonas, P Klappa, 2001, Interaction of the periplasmic peptidylprolyl cis-trans isomerase SurA with model peptides. The N-terminal region of SurA is essential and sufficient for peptide binding: *J.Biol.Chem.*, v. 276, p. 45622-45627.

Weber, F, F Keppel, C Georgopoulos, M K Hayer-Hartl, F U Hartl, 1998, The oligomeric structure of GroEL/GroES is required for biologically significant chaperonin function in protein folding: *Nat.Struct.Biol.*, v. 5, p. 977-985.

Weissman, JS, H S Rye, W A Fenton, J M Beechem, A L Horwich, 1996, Characterization of the active intermediate of a GroEL-GroES-mediated protein folding reaction: *Cell*, v. 84, p. 481-490.

- Wickner,S, M R Maurizi, 1999, Here's the hook: similar substrate binding sites in the chaperone domains of Clp and Lon: *Proc.Natl.Acad.Sci.U.S.A*, v. 96, p. 8318-8320.
- Wild,J, E Altman, T Yura, C A Gross, 1992, DnaK and DnaJ heat shock proteins participate in protein export in *Escherichia coli*: *Genes Dev.*, v. 6, p. 1165-1172.
- Woo,KM, K I Kim, A L Goldberg, D B Ha, C H Chung, 1992, The heat-shock protein ClpB in *Escherichia coli* is a protein-activated ATPase: *J.Biol.Chem.*, v. 267, p. 20429-20434.
- Xu,Z, A L Horwich, P B Sigler, 1997, The crystal structure of the asymmetric GroEL-GroES-(ADP)₇ chaperonin complex [see comments]: *Nature*, v. 388, p. 741-750.
- Yifrach,O, A Horovitz, 1994, Two lines of allosteric communication in the oligomeric chaperonin GroEL are revealed by the single mutation Arg196-->Ala: *J.Mol.Biol.*, v. 243, p. 397-401.
- Zhu,X, X Zhao, W F Burkholder, A Gragerov, C M Ogata, M E Gottesman, W A Hendrickson, 1996, Structural analysis of substrate binding by the molecular chaperone DnaK: *Science*, v. 272, p. 1606-1614.
- Zimmerman,SB, S O Trach, 1991, Estimation of macromolecule concentrations and excluded volume effects for the cytoplasm of *Escherichia coli*: *J.Mol.Biol.*, v. 222, p. 599-620.
- Zolkiewski,M, A Ginsburg, 1992, Thermodynamic effects of active-site ligands on the reversible, partial unfolding of dodecameric glutamine synthetase from *Escherichia coli*: calorimetric studies: *Biochemistry*, v. 31, p. 11991-12000.
- Zylicz,M, D Ang, C Georgopoulos, 1987, The *grpE* protein of *Escherichia coli*. Purification and properties: *J.Biol.Chem.*, v. 262, p. 17437-17442.
- Zylicz,M, D Ang, K Liberek, C Georgopoulos, 1989, Initiation of lambda DNA replication with purified host- and bacteriophage-encoded proteins: the role of the *dnaK*, *dnaJ* and *grpE* heat shock proteins: *EMBO J.*, v. 8, p. 1601-1608.

Acknowledgment

Many people have contributed to my education through their guidance and support throughout my Ph.D. program years.

I would like to thank Prof. Dr. Roger S. Goody for giving me opportunity to work at Max Planck Institute of Molecular Physiology in Dortmund and for access to all laboratories and facilities.

I especially want to thank my thesis advisor, PD Dr. Jochen Reinstein, who accepted me into his laboratory and supported my scientific endeavors.

I am also grateful indebted to PD Dr. Ilme Schlichting, who gave me a chance to finish writing of my Ph.D. thesis.

I would like to thank Dr. Sandra Schlee, Dr. Philipp Beinker, Dr. Yvonne Grömping, Georgeta Dumitru, Simone Popp, Petra Herde and Elizabeth Hartmann who were notable friends and colleagues freely offering me their advice, both scientifically and personally.

I thank Dr. Ralf Seidel for providing with plasmids.

I owe a lot of thanks to Dr. Roman Fedorov, Dr. Tatjana Domratscheva, Dr. Elena Rostkova, Dr. Peter Bayer, Dr. Elena Bayer for their scientific and also emotional support.

Many thanks go to Dr. Herbert Opitz, Dr. Branko Kolaric for their help with fluorescence correlation spectroscopy measurements.

It is my pleasure to acknowledge to Prof. Dr. Rolf Kinne, Dr. Jutta Roetter and all other members of the International Max Planck Research School in Chemical Biology (IMRS)

for organizing teaching scientific courses which helped to increase my scientific knowledge. I would like to thank also my colleagues from the IMPRS for their friendship.

My apologies to the others who I have not mentioned by name, I am indebted to them for the many ways they helped me.

I am especially appreciative of my parents who always shared in my joy of learning and supported me. Finally, I would like to thank my husband Victor for his understanding and patience.